A STUDY OF THE REACTION MECHANISM OF (d p) REACTIONS ON ^{12}C AND ^{9}Be AT BOMBARDING ENERGIES BELOW 2MeV

by

BENI MADHAW BAHAL

DEPARTMENT OF PHYSICS

INDIAN INSTITUTE OF TECHNOLOGY KANPUR

FEBRUARY 1975

TO

MY PARENTS

STATEMENT

I hereby declare that the work presented in this thesis is the result of investigations carried out by me in the Department of Physics, Indian Institute of Technology, Kanpur, India under the supervision of Professor V.K. Deshpande.

In keeping with the general practice of reporting scientific observations, due acknowledgement has been made wherever the work described is based on the findings of other investigators.

B M. Bahal

B. M. Bahal

CERTIFICATE

Certified that the work presented in this thesis entitled " A Study of Reaction Mechanism of (d,p) Reactions on ^{12}C and ^{9}Be at Bombarding Energies below 2 MeV" has been carried out by Mr. B.M. Bahal under my supervision and the same has not been submitted elsewhere for a degree.

V.K. Deshpande

(V.K. Deshpande)
Professor
Department of Physics,
Indian Institute of Technology, Kanpur

ACKNOWLEDGEMENTS

I thank Professor V.K Deshpande for his continued guidance and help in carrying out this work.

I wish to thank Dr. N.K Ganguli, BARC, for his interest in my work and for permitting me to use the DWUCK program and computer facilies at BARC. I also wish to thank Dinesh and Pal of BARC for their active support in the computational part of this work. I thank Dinesh and Paranjape for their hospitality during my stay at BARC.

My thanks are due to Dr. G.K. Mehta and the staff of the Van de Graaff laboratory for their help with the accelerator system and to Sri P N. Dubey and Sri J. Sharma of the Physics Workshop for their help in the construction of the scattering chamber and evaporating system.

I am grateful to my friends Prabhakara and Bagwan for help rendered during experimental work, to Ramesh, Krish, Prakash and Brijesh for help in the checking of the thesis manuscript. To Tejasvi, Kamal, Singhvi, Vijay, Surendra and Kapoor my sincere thanks.

Financial assistance of CSIR and Physics Department, I.I.T., Kanpur is acknowledged.

B.M. Bahal

TABLE OF CONTENTS

.....

LIST OF TABLES

LIST OF FIGURES

Figure Page

Figure

....

SYNOPSIS

In this work angular distributions and excitation curves of (d,p) reaction on ^{12}C and ^{9}Be have been obtained at the sub-coulomb bombarding energy in the range of 500 to 1800 KeV using the 2 MeV Van-de-Graaff accelerator at I I.T., Kanpur. Strong resonances were observed in the case of ^{12}C and comparatively weaker resonances in the case of ^{9}Be in the excitation curves. The angular distributions in both cases,however, showed a peak at about 35^{o}_{CM} typical of direct stripping mode. At resonant energies the main effect was in the enhancement of the backward peak. Some data on both these reactions was previously available. However, the analysis was done either in terms of compound nucleus process alone or the stripping mode alone. In the case of compound nucleus mechanism, it was necessary to assume contribution from rather high partial waves, and in the case of stripping mechanism, it was necessary to assume optical model parameters of DWBA calculations which were not consistent with those used at higher energies where the angular distributions show better stripping patterns. It was, therefore, decided to analyse the data in terms of coherent contribution of the reasonant and non-resonant amplitudes and then compare the non-resonant cross-section with the DWBA calculations with optical model parameters consistent with those

used at higher energies For a proper consideration of the interference effects it was necessary to take the data at required energies and angles, although some data was available from previous work

The amplitude was assumed to be of the form

$$A = A^{Resonant} + A^{Non\text{-}resonant}$$

in the vicinity of resonance peak Where $A^{Resonant}$ included contribution from the main peak and one or two neighbouring peaks It was assumed that the energy dependence of the resonant amplitudes was given by Breit-Wigner term, with phases of the neighbours relative to the main resonance The direct amplitude was considered relatively insensitive to energy over the region of the resonance and was assumed to be at the most linearly dependent on it with the undetermined phase relative to the main resonance This assumption about the total amplitude leads to an expression for the total cross-section with a term corresponding to the non-resonant cross-section, and others depending upon energy in the specified way The experimental cross-section in the neighbourhood of resonances in the excitation curve was then subjected to a least squares fit using the expression for cross-section with strengths of various terms resonant energies and widths, as parameters The least squares fit provides a value of the non-resonant cross-section at each energy of the excitation curve obtained at each angle

It is then possible to reconstruct the angular distribution due to the non-resonant process alone

These extracted non-resonant angular distributions were compared with a DWBA calculations of the stripping process made with a program DWUCK available at the Bhabha Atomic Research Centre It was found that there were satisfactory agreement with the shape and absolute cross-section between the two

It is, therefore concluded that while the contributions of various processes in determining the cross-section are to be determined by coupled channel calculations the simpler model of adding resonant and non-resonant amplitudes suggested by physical considerations in the classical limit seems to yield satisfactory results With this approach the contribution of the direct reaction in the case of ^{12}C was found to be about 20%, and that in the case of ^{9}Be about 90% In view of this, the assignment of spins and parities made previously by neglecting the non-resonant part needs to be re-examined An attempt to fit the extracted direct cross-section with Coulomb distortions alone did not provide satisfactory fits inspite of the low bombarding energy Nuclear distortion is therefore, found important even at these energies The finite range and non-local corrections in the DWBA calculations did not produce any major change in the shape However, the absolute cross-section reduced by about 10% with these corrections applied to the zero range approximation

CHAPTER I

INTRODUCTION

The striking feature that was noted in the early stages of nuclear reaction work was the appearance of narrow resonances in the cross-section as a function of bombarding energy. This led to the suggestion of the compound-nucleus mode of nuclear reactions by N Bohr,[1] with compound-nucleus life time of the order of 10^{-14} - 10^{-18} sec which was much larger than the typical transit time of the bombarding particle across the nuclear diameter The theory of nuclear reactions on the basis of compound-nucleus formation mechanism was subsequently developed by many authors[2] and was successfully applied to determine the properties of many compound nucleus levels

In the case of nuclear reactions proceeding via compound nucleus formation mechanism it is expected that excitation function will show resonances whose shapes are given by the Breit Wigner formula [2e] Since the formation and decay of the compound-nucleus are independent of each other the same reaction products

would be obtained even if a particular level of the compound-nucleus is formed by two different initial channels The angular distribution of the reaction products proceeding through a single level is expected to be symmetric about 90° in the centre of mass system Since the shape of the angular distribution is characteristic of the partial waves in the outgoing channel, it is possible to make an inference about the spin of the compound-nucleus level If at relevant excitation energy two or more levels of the compound nucleus of different parities contribute, the angular distributions are not expected to be symmetric and the shape of the angular distribution is expected to vary noticeably with the bombarding energy The width and the density of the compound-nucleus level are expected to increase with excitation energy and when a large number of levels contribute it is expected that, due to essentially random phase of contribution the angular distribution would again be symmetric and weakly dependent on angle

Even before the suggestion of compound-nucleus process by Bohr[1], Oppenheimer and Phillips[3] had proposed a radically different model to account for the higher probability of (d,p) reactions as compared to (d, n) reactions They pointed out that at the low bombarding energy which was used at that time, the proton in the deuteron would not cross the Coulomb-barrier of the target while the neutron would get close enough to get captured. It was thus possible to explain the preferential proton

emission which is just the opposite of the predictions of compound-nucleus theory The full implication of this model was not clear at that time since at very low deuteron energies the angular distributions were isotropic as only s-wave interactions took place In the fifties, (d p) and (d, n) reactions were studied at higher energies and they were found to be equally probable, showing that Coulomb force plays the secondary role However, the most interesting feature was the angular distribution The cross-section peaked either in the forward direction or at some small angle and decreased to small values at backward angles These features were independent of bombarding energies, and peak position depended upon the target used These features were explained first by Serber[4] and later more accurately by Butler [5] The explanations were based on the single step model of the reaction in which the deuteron is stripped of one of its nucleons, due to the low binding energy of the deuteron, during the close passage of the captured nucleon relative to the tafget nucleus The other nucleon can still have a relatively large impact parameter in view of the large deuteron radius In the stripping process therefore the deuteron as a whole and the target do not combine to form a compound nucleus Butler showed that the angular distribution is essentially of the form of the square of the spherical Bessel function [6] $J_l(QR)$ of order l , where l is the orbital angular momentum transfered to the target nucleus by the captured nucleon Q is the linear momentum

transferred and R is the nuclear radius The study of deuteron stripping reactions therefore provided a new technique of nuclear spectroscopy to study the properties of the low lying levels of the residual nucleus, while the reactions proceeding through compound nucleus mechanisms led to the study of highly excited levels of the compound nucleus The inverse (p, d) and (n, d) reactions are called the pick-up reactions in which the incident nucleon picksup an appropriate peripheral nucleon to form the emergent deuteron without forming the compound nucleus The Bulter theory is directly applicable to such reactions and the peak position in the angular distribution now depends upon the angular momentum of the picked nucleon in the target nucleus The pick-up reactions thus provide information about the ground state of the target nucleus

In a rearrangement collision the amplitude of the reaction $\alpha \rightarrow \beta$ is given by[7]

$$A_{\alpha\beta} = \int \phi_{\beta}^{(-)*} \, e^{-i\bar{K}_{\beta} \, \bar{r}_{\beta}} \, V_{\beta} \, \Psi \, d\tau \qquad (1\ 1)$$

where ϕ_{β} is the internal wave function of the reaction products in channel β, V_{β} the final state interaction and, Ψ the total wave function In the (d,p) reaction $V_{\beta} = V_{pn} + V_{pN}$ where V_{pn} is the proton-neutron interaction and V_{pN} is the sum of the interactions of the proton with the nucleons of the target In the pure stripping model it is assumed that the interaction

V_{pN} can be neglected. The Butler treatment[8a] and the other alternative treatments[8b] that appeared soon afterwards are essentially equivalent to making a plane wave Born approximation (PWBA) in which the total wave function Ψ is replaced by plane wave $e^{i\bar{K}_\alpha \cdot \bar{r}_\alpha}$ in the incident channel. The method used by Butler[8a] involves wave function matching at the nuclear boundary and it leads to same result as the PWBA with the difference that the radial integral for amplitude is cut-off at the nuclear radius R and does not extend to the origin.

In spite of the success of the PWBA theory for deuteron stripping reactions, the theory does not yield a particularly detailed account of the angular distributions For medium and heavy nuclei the agreement between the PWBA theory and the experimental angular distributions is poor.[9] Even for light nuclei there are cases in which the assignment of the orbital angular momentum is ambiguous.[10] Further, PWBA gives a value of the absolute cross-section which is several times the measured cross-section.

The exact expression (1.1) for the amplitude of the reaction can also be put in the form

$$A_{\alpha\beta} = \int \chi_\beta^{(-)*}(\bar{r}_\beta)\, \phi_\beta^* \quad (V_\beta - \bar{V}_\beta)\, \Psi \, d\tau \qquad \ldots(1.2)$$

where $\bar{V}_\beta$ is a model potential and $\chi_\beta(\bar{r}_\beta)$, represents the relative motion in the model potential. The PWBA is improved upon by using the Distorted Wave Born approximation (DWBA) theory

The total wave function Ψ in expression (1.2) is replaced not by the plane unscattered wave but by the scattered wave $\chi_\alpha(\vec{r}_\alpha)$ in the incident channel. The scattering state wave function is generated from the optical model, where the optical model parameters are determined from the available scattering data in the incident channel. The model potential $\bar{V}_\beta$ is chosen equal to the optical potential which gives correct scattering in channel β. Thus $\chi_\beta(\vec{r}_\beta)$ is the scattering-state wave function in channel β. This wave function is generated from the optical model potentials which determine the optical model parameters for a given system. As mentioned before, for the (d, p) reaction $V_\beta = V_{pn} + V_{pN}$, therefore,

$$V_\beta - \bar{V}_\beta = V_{pn} + (V_{pN} - \bar{V}_\beta) \qquad \ldots(1.3)$$

It is assumed that $\bar{V}_\beta$ is a close approximation of V_{pN}, which is the total interaction the proton experiences due to the nucleons in the target nucleus. Thus in the DWBA theory the plane wave is replaced by the distorted wave, which is a better approximation to the total wave function and instead of neglecting the interaction of the outgoing nucleon with the target, it is assumed that V_{pN} is equal to the optical interaction to a good approximation.

The optical model potential, which is in general required in DWBA treatment, includes both Coulomb and nuclear interactions.

The inclusion of nuclear interaction in both the incoming and outgoing channel represents a departure from the pure stripping mechanism as envisaged originally by Butler. It implies that the deuteron as a whole does experience nuclear potential. Similarly the outgoing proton does not entirely pass through the region exterior to the nucleus. However, the optical potential $\bar{V}_\beta$ is adjusted to give the correct energy-averaged scattering amplitude and does not reproduce the fluctuations in the elastic channels.[12] The potential $\bar{V}_\beta$ is not identical with V_{pN}. DWBA treatment, therefore, does not take into account the possible compound nucleus formation and subsequent contribution to the reaction leading to narrow resonances in the cross-section. DWBA, however, provides a more accurate description of the dynamical behaviour of the incoming deuteron and outgoing proton and by doing this provides a sounder basis for using proton-neutron interaction as the operator for the matrix element in the amplitude (1.2).

Generally speaking DWBA calculations require extensive use of computers. Several computer programmes for such calculations are now available.[13] Many programmes use a zero-range approximation for the neutron-proton interaction since it reduces the dimensionality of integral (1.2). Calculations which take into account the finite-range of V_{pn} are lengthier. Programmes which include such finite range correction as well as the spin-orbit term in the optical potential are also

available. Computations are also made with non-local potentials. There is usually a provision to use a cut-off radius in integral (1.2) as an option. The DWBA calculations usually give a much more satisfactory account in the entire range of angular distribution as compared to PWBA calculations. Further, the absolute cross-sections predicted on the basis of DWBA calculations are in far better agreement with the experimental results.

For bombarding energies which are lower than the Coulomb barrier the (d,p) cross-sections are expected to be small and the Coulomb distortion is expected to be the predominant effect.[14] Secondly, the relative contribution to the reaction due to compound nucleus formation is expected to be larger This is due to the fact that the relative strength of the low partial waves in the incident wave increases as energy is decreased and the compound nucleus formation is more probable with such low partial waves with correspondingly low centrifugal barrier On the other hand, when compound nucleus is formed at high bombarding energy it is highly excited and therefore has several open channels. The fractional contribution of the decaying compound nucleus in the outgoing proton channel is therefore reduced. At low bombarding energies, therefore, it is expected that the cross-section would be low, distortion effects will be primarily due to Coulomb field and the compound-nucleus process will make a significant contribution to (d,p) reaction.

The Q value of (d,p) reaction is an important consideration particularly at low-bombarding energies.[15a] When the Q value of the reaction is large the momentum of the outgoing proton is large. To have this large momentum it is expected that the proton is close to the neutron in the deuteron when the neutron is stripped. Therefore, such protons pass close to the nuclear region and experience marked nuclear distortion. It is expected, therefore, that in the high Q reaction the plane wave approximation will be poor. This has been observed for several cases.[15b,c] The (d,p) reaction on ^{12}C and ^{9}Be have been studied at bombarding energies in range 0.8 - 2.0 MeV. In these reactions Q values are high. Therefore, both compound-nucleus effects and high distortion effects in (d,p) reactions are expected.

When both compound-nucleus and direct amplitudes are present, it is expected that they will add coherently. While the duration of a direct event should be of the order of 10^{-21} seconds and that of the compound-nucleus some 10^{4} times greater; the duration of the wave packet which is incident from the accelerator is of the order of 10^{-10} seconds. The difference in delay between the direct and compound-nucleus mechanism is therefore insignificant. The well known experimental evidence of the existence of interference is that between the potential scattering and resonant scattering of neutrons. The time

intervals involved in direct interactions are the same as those involved in potential scattering. When the interfering amplitudes are few in number the interference effects will be noticeable in the cross-section measurements. When the number of interfering amplitudes is large the interference terms may tend to cancel.

In the presence of an isolated resonance in the (d,p) reaction one may assume the presence of two amplitudes $q^{Resonant}$ and $q^{Non\text{-}Resonant}$ adding coherently.[16] If the resonance is not well isolated one may have to add the amplitudes due to neighbouring resonances. In the statistical region where a large number of resonances contribute, this approach is not possible. In the analysis of excitation function in the presence of one or more resonances, the resonant amplitudes may be assumed to vary according to the Breit-Wigner formula[2e] while the Non-Resonant (NR) amplitude may be assumed essentially constant over the width of the resonance. It is then possible to extract the NR cross-section from the experimental excitation curves by fitting them with the algebraic function written down on the basis of above assumptions. The extracted NR cross-section can then be analysed on the basis of DWBA.

In the present work we have studied deuteron induced reaction at low bombarding energies on light targets with the 2 MeV Van de Graaff accelerator facility available at the Indian

Institute of Technology, Kanpur. ^{12}C and ^{9}Be were used as targets Previous data on carbon-12 (d,p) reaction in this energy range have been published in 1960[17a] which showed presence of resonances and the data was anlysed by the authors in the frame-work of compound-nucleus process alone, although the angular distributions did retain some feature of the main stripping peak which shows up more prominently at 4 MeV.[16,18] A preliminary calculation of pure stripping at this bombarding energy showed that the stripping cross-section may not be negligible. It was, therefore, decided to study the contribution of the direct mode relative to the compound-nucleus mode, by considering coherent addition of amplitudes. For this, it was necessary to check previous data and to take additional data to study the interference effects. Some data on (d,p) reaction on ^{9}Be in this energy range was also available[19] which was analysed by the authors in terms of compound-nucleus process alone or the direct reaction process[20] alone using optical parameters not consistent with those used at higher energies.

In the present work it was found that in $^{12}C(d,p)$ reaction the direct mechanism makes about 20% contribution as compared to the figure of less than 2% mentioned in the earlier work[17b] The extracted NR cross-sections show strong distortions as expected in relatively high Q value reactions. The extracted cross-section can not be fitted by pure Coulomb distortions, Reasonably good fits are obtained with optical

potentials with parameters consistent with those used at higher energies In the case of beryllium-9 the compound-nucleus contribution is found to be small. The extracted cross-sections can again be fitted reasonably well with optical model parameters consistent with those used at higher energies.

CHAPTER II

NUCLEAR REACTIONS

Introduction

In a nuclear reaction a target nucleus 'A' with n_A number of nuclei is bombarded with a projectile 'a' consisting of n_a number of nuclei and the reaction products are detected in the asymptotic region. The reaction

$$a + A \longrightarrow B + b \qquad \ldots(2\ 1)$$

is described by denoting the initial and final channels by α and β respectively. Besides the identification of initial and final products other relevant quantum numbers are denoted collectively by symbols i and j respectively, so that the reaction is represented by $(\alpha, i) \rightarrow (\beta, j)$ when necessary.

The total system thus consists of $n_A + n_a = N$ particles with the Hamiltonian H and a wave function Ψ. In practice the state is a non-stationary state, to be represented by collision of wave packets, but it is generally represented[21] as a

stationary state satisfying

$$H \Psi = E \Psi \qquad \ldots (2.2)$$

The stationary state wave-function Ψ can be expanded in terms of a suitable basis such as independent particle model (IPM) states of N particles. It may be noted that for sufficiently high excitation energies,the finite well IPM provides both bound and unbound states. The excitation energy can either be distributed over many excited single particle bound states or it may be in the form of one or few particles excited into the single particle continuum. The bound states of IPM therefore provides a discrete spectrum in the same region where the unbound states provide continuum. The unbound states represent the flux of particles in the asymptotic region. In nuclear reactions the energy of the total system is sufficiently high to provide unbound components at least in the initial channel. The wave-function Ψ could then be written in the form

$$\Psi = \Psi_{bound} + \Psi_{unbound} \qquad .. (2.3)$$

where Ψ_{bound} is a summation over the bound basis states and $\Psi_{unbound}$ is a summation over unbound basis states. $\Psi_{unbound}$ is often expressed as

$$\Psi_{unbound} = \sum_{\beta} \Phi_{\beta} \xi_{\beta} (\bar{r}_{\beta}) \qquad ..(2.4)$$

where Φ_β is the product $\phi_b\phi_B$ of the internal wave functions of clusters b and P and $\xi_\beta(\bar{r}_\beta)$ describes their relative motion. While this description of $\Psi_{unbound}$ could be used for large values of $\bar{r}_\beta$, it is sometimes used for small values of the order of nuclear radius as a model wave function. It is assumed that in the asymptotic region where the bound states do not contribute the total wave function has the form

$$\Psi_\alpha^+ \longrightarrow \Phi_\alpha e^{i\bar{K}_\alpha \cdot \bar{r}_\alpha} - \sum_\beta \frac{\mu_\beta}{2\pi\hbar^2} \Phi_\beta A_{\alpha\beta}(K_\alpha, K_\beta) \frac{e^{iK_\beta r_\beta}}{r_\beta} \quad .. (2.5)$$

This expression describes an incident plane wave in channel α and outgoing spherical waves in various channels β. Since only the unbound states contribute in the asymptotic region, the expansion (2.4) must have the asymptotic form (2.5). The quantity $A_{\alpha\beta}(\bar{K}_\alpha, \bar{K}_\beta)$ is called the amplitude of the reaction $\alpha \rightarrow \beta$ and the cross-section is proportional to the square of this amplitude. Measurement of cross-section therefore provides a sampling of the unbound component of the total wave-function.

Ψ_{bound} and $\Psi_{unbound}$, however, are two components of the total wave function and these are directly coupled with each other through the Schrödinger Eq. (2.2). Thus, if we introduce projection operators P and Q with the property

$$P\Psi = \Psi_{unbound}, \quad Q\Psi = \Psi_{bound} \qquad ...(2.6)$$

the Schrödinger equation directly leads to the coupled equations:

$$(E-H_{PP})\ \Psi_{unbound} = H_{PQ}\ \Psi_{bound}$$

$$(E-H_{QQ})\ \Psi_{bound} = H_{QP}\ \Psi_{unbound} \qquad \ldots(2.7)$$

where

$$H_{PP} \equiv PHP \qquad H_{QQ} \equiv QHQ$$

$$H_{PQ} \equiv PHQ \qquad H_{QP} \equiv QHP \qquad \ldots(2.8)$$

Ψ_{bound} is a superposition of bound IPM states and the strength of such components are expected to vary sensitively with the system energy leading in turn to energy sensitivity of Ψ_{bound}. Due to the coupling of $\Psi_{unbound}$ with Ψ_{bound}, this energy sensitivity will also appear in $\Psi_{unbound}$ and therefore in the reaction amplitude. If the bound component of the total wave-function could be neglected, then the $\Psi_{unbound}$ is expected to be relatively energy insensitive since they represent continuum states of the system.

In the nuclear reaction theory exact calculations are at present not attempted and it becomes necessary to use approximations and models. In the direct reaction theories the bound component of wave function is not considered explicitly. The form (2.4) for the unbound wave function is usually used as the total model wave function in the entire region including the nuclear interior. The model potential V_β which determines

$\xi_\beta(\bar{r}_\beta)$ is empirically determined to fit the observed data in the corresponding scattering channel alone. It is in general not possible to find model optical potentials which will reproduce narrow fluctuations typical of a system with many degrees of freedom.

The approach of the compound nucleus theory is to assume that, while $\Psi_{unbound}$ is the dominant term of Ψ in the region starting just outside the nuclear volume, Ψ_{bound} is the dominant term inside the nuclear volume. The coupling between the two is then taken into account by the physical requirement of matching the two wave functions at the nuclear surface. The fluctuations can then be understood in terms of rapidly changing boundary conditions as determined by Ψ_{bound}. An assumption of smooth behaviour of the logarithmic derivative on the nuclear surface then leads to Breit-Wigner formula for the resonance The resonance is attributed to a predominant excitation of a bound state component.

Both the treatments involve approximations to the actual problem, and introduction of models within these approximations. The support for introduction of such simplification however, is provided by the experimental data which in different suitable circumstances correspond to good approximations to the two different treatments. Further, the physical considerations at least in the classical limit lend support to the introduction of these simplifications.

In a semiclassical approach the nuclear reaction can be considered in terms of the development of rearrangement collision in time. Thus, when a deuteron is incident on the target there is a possibility of the neutron being captured and the proton released. Alternately, both the nucleons may enter the target, form a compound assembly where they excite one, few or many nucleons and eventually a proton is released again. The life time of the compound state may be expected to be small if fewer nucleons get excited by the incoming deuteron while that of a state which is complicated may be expected to be relatively long. One would therefore expect resonances with varying widths on the basis of uncertainty principle. In the event that the probability of the simplest process, where the proton does not enter the nucleus at all, is large compared to others, a treatment purely on the basis of direct reactions might give satisfactory results. In general, however, both processes will contribute to the observed proton yield. This is the basis for adding the amplitudes as calculated on the basis of two respective mechanisms. In general the two amplitudes have to be added coherently when the wave-packet representing the incident particle is much longer than the expected time delay caused by the direct and compound nucleus reaction mechanisms. A resonance of width ΔE_R is observed with the beam of energy resolution ΔE_B, when ΔE_B is smaller than ΔE_R.

The corresponding uncertainty Δt_B in the arrival of the beam particle is larger than the time delay Δt_R which is of the order of nuclear life time. Hence the dimension of the beam packet is large compared to the distortion produced at its edges by the finite life time of the compound nucleus. It is expected therefore that the compound-nucleus amplitude will add coherently and produce interference effects The experimental evidence of this situation is provided by elastic scattering experiments where one finds interference effects between potential and resonant scattering in the excitation curve.

Direct Reactions

In the direct reaction theory the Hamiltonian of the system is considered in the form[11]

$$H = H_a + H_A + T_{aA} + V_{aA} \qquad \ldots(2.9a)$$

$$= H_\alpha + T_\alpha + V_\alpha \qquad \ldots(2.9b)$$

$$= H_\beta + T_\beta + V_\beta \qquad \ldots(2.9c)$$

where H_α is the sum of the internal Hamiltonians of the two clusters a and A, T_α the relative kinetic energy of the two clusters and V_α is the sum of the potential energies of all particles in the cluster a due to each particle in cluster A. The form (2.9) of the Hamiltonian is not suitable for consideration of bound wave functions but is suitable for the

consideration of unbound wave functions. Let Φ_β be the eigen function of H_β so that,

$$H_\beta \Phi_\beta = \varepsilon_\beta \Phi_\beta \qquad \ldots(2.10)$$

The Schrödinger equation for the total wave function is

$$H \psi^{(+)} = E \psi^{(+)} \qquad \ldots(2.11)$$

taking the scalar product with Φ_β we have

$$(\Phi_\beta, H \psi^{(+)}) = E (\Phi_\beta, \psi^{(+)}) \qquad \ldots(2.12)$$

where the integration is only over the internal variables of Φ_β Substituting Eq. (2.9c) for H into (2 12) we get

$$(T_\beta + \varepsilon_\beta - E) (\Phi_\beta, \psi^{(+)}) = -(\Phi_\beta, V_\beta \psi^{(+)}) \qquad \ldots(2.13)$$

Since the scalar product $(\Phi_\beta \psi^{(+)})$ involves integration over only the internal variables of Φ_β, it defines a function of $\bar{r}_\beta$, which is denoted by

$$(\Phi_\beta, \psi^{(+)}) \equiv \xi_\beta (\bar{r}_\beta)$$

Therefore, we have

$$(T_\beta + \varepsilon_\beta - E) \xi_\beta = -(\Phi_\beta, V_\beta \psi^{(+)}) \qquad \ldots(2.14)$$

This equation has solution

$$\xi_\beta(\bar{r}_\beta) = e^{i\bar{K}_\alpha \cdot \bar{r}_\alpha} \delta_{\alpha\beta} - \frac{\mu_\beta}{2\pi\hbar^2} \int e^{\frac{iK_\beta(\bar{r}_\beta - \bar{r}'_\beta)}{|\bar{r}_\beta - \bar{r}'_\beta|}} (\Phi_\beta, V_\beta \psi^{(+)}) d\bar{r}'_\beta \qquad \ldots(2.15)$$

where we have

$$E - \varepsilon_\beta = \frac{(\hbar K_\beta)^2}{2\mu_\beta}$$

Taking the asymptotic term of eqn (2 15), the amplitude

$$A_{\alpha\beta}(\bar{K}_\alpha, \bar{K}_\beta) = -\frac{\mu_\beta}{2\pi\hbar^2}\left(\Phi_\beta e^{i\bar{K}_\beta \cdot \bar{r}_\beta}, V_\beta \Psi^{(+)}\right) \quad \ldots(2.16)$$

The formula represented by Eq (2.16) is exact. It can be recast into a different form which is useful for the discussion of applications We add the term $\bar{V}_\beta (\Phi_\beta, \Psi^{(+)})$ to both sides of Eq. (2.13), where $\bar{V}_\beta$ is an arbitrary function of r_β . This leads to the relation

$$(T_\beta + \bar{V}_\beta + \varepsilon_\beta - E)\,\xi_\beta = -(\Phi_\beta, (V_\beta - \bar{V}_\beta)\Psi^{(+)}) \quad \ldots(2.17)$$

The solution of this eqn. is obtained by using the Green's function technique as above. This leads to the following expression for the amplitude

$$A_{\alpha\beta}(\bar{K}_\alpha, \bar{K}_\beta) = -\frac{\mu_\beta}{2\pi\hbar^2}\left(\Phi_\beta \chi_\beta^{(-)}, (V_\beta - \bar{V}_\beta)\Psi^{(+)}\right) \quad \ldots(2.18)$$

where $\chi_\beta^{(-)}$ is a solution of the homogeneous Eq.

$$(T_\beta + \bar{V}_\beta + \varepsilon_\beta - E)\chi_\beta = 0 \quad \ldots(2.19)$$

Both forms given by Eq. (2.17) and (2.19) are equivalent. For applying either of the two forms a knowledge of the total

wavefunction $\Psi^{(+)}$ is needed. In the direct reaction theory the bound state component of $\Psi^{(+)}$ is neglected From amongst the unbound components often only the component in the incident scattering channel is retained. Use of more than one unbound component leads to a more complicated coupled channel calculation. The calculation further requires the use of the channel potential V_β. Simplifying assumptions are usually made for calculations.

In the Plane Wave Born Approximation (PWBA) the total wave function $\Psi^{(+)}$ is replaced only by the incident plane wave $\Phi_\alpha e^{i\vec{K}_\alpha \vec{r}_\alpha}$ in the incident channel α The scattered part of the incident wave is therefore further omitted. In the case of (d,p) reactions the approximation to V_β is made as follows. We have

$$V_\beta = V_{pn} + V_{pN}$$

where V_{pn} is the proton neutron interaction and V_{pN} is the total interaction of the outgoing proton with all the nucleons of the target. In the pure stripping mechanism model of Butler it is assumed that the proton does not enter the nucleus at all. It is therefore assumed that the contribution due to the interaction V_{pN} could be neglected in evaluating the integral (2.16). In this approximation the amplitude becomes

$$A_{\alpha\beta} = -\frac{\mu_\beta}{2\pi\hbar^2}\int \Phi^*_\beta\, e^{-i\bar{k}_\beta\cdot\bar{r}_\beta}\, V_{np}\, \Phi_\alpha e^{i\bar{k}_\alpha\cdot\bar{r}_\alpha} d\tau$$

$$= -\frac{\mu_\beta}{2\pi\hbar^2}\int \langle\phi_B|\phi_A\rangle\, e^{-i\bar{k}_p\cdot\bar{r}_p}\, V_{np}\, \phi_d\, e^{i\bar{k}_d\cdot\bar{r}_d}\, d\bar{r}_n d\bar{r}_p \qquad \ldots(2.20)$$

where ϕ_p and ϕ_d are expressed in terms of the proton and the deuteron coordinates respectively. The integration in the scalar product $\langle\phi_B|\phi_A\rangle$ is over the internal coordinates of the target nucleus A and it has the form

$$\langle\phi_B|\phi_A\rangle = s\,\eta_l(\bar{r}_{nN}) \qquad \ldots(2\ 20a)$$

where s is essentially the coefficient of fractional parentage and $\eta_l(\bar{r}_{nN})$ is a normalised function of the neutron coordinate typical of the angular momentum l carried by the neutron bound to the target N

Further the interaction V_{np} in Eq. (2.20) can be written in terms of deuteron binding energy by writing the Schrodinger equation for the deuteron. Finally, changing the variables from $\bar{r}_n$, $\bar{r}_p$ to the relative coordinates $\bar{r}_{pn}$ and $\bar{r}_{nN}$, we get

$$A = s\,(\epsilon_d + q^2/2\mu_{pn})\frac{\mu_{pN}}{\hbar^2 2\pi}\{\int d\bar{r}_{np}\, \phi_d(\bar{r}_{np})\, e^{-i\bar{q}\cdot\bar{r}_{np}}\}$$

$$\times \quad \{d\bar{r}_{nN}\, \eta^*_l(\bar{r}_{nN})\, e^{i\bar{Q}\cdot\bar{r}_{nN}}\}$$

$$\ldots(2.21)$$

where $\bar{q}$ and $\bar{Q}$ are essentially the change of momenta of the proton and the nucleus with some scale factors. In order to evaluate the integrals in (2.21) the exponential factors are expanded in terms of spherical Bessel functions as follows

$$e^{i\bar{q}.\bar{r}} = 4\pi \sum_{\lambda\,\mu} i^{\lambda} j_{\lambda}(qr) Y^{\lambda}_{\mu}(\Omega_r) Y^{\lambda}_{\mu}(\Omega_q) \qquad \ldots(2.22)$$

Since ϕ_d involves spherical harmonics of order zero and η_l that of order l, the integration over angles leads to the appearance of Bessel functions j_o and j_1 respectively. For the evaluation of integral over $\bar{r}_{nN}$ often a cut off radius R of the order of nuclear radius is used. The angular dependence of the amplitude is then primarily given by

$$A \sim j_1 (QR) \qquad \ldots(2.23)$$

The angular distribution of the proton is therefore determined by the value of l and the momentum transfer Q, which depends upon the angle of emission. The radius R is usually used as a parameter within limits. The Bessel function has an oscillatory behaviour with rapid damping. The main peak of $|j_1(QR)|^2$ is compared with the experimental main peak in (d,p) reactions. The peak position in many (d,p) reactions is predicted to a good approximation by this theory but not in all cases. The agreement away from the peak is however

not found satisfactory. For prediction of absolute cross-sections estimate of the coefficient s is obtained from structure consideration and using this the predicted cross-section is found to be higher than the observed cross-section by a large factor

In the Distorted Wave Born Approximation (DWBA) the total wave function $\Psi^{(+)}$ is replaced by the incident channel wave function including the scattered part. To obtain this incident channel wave-function , scattering data in the incident channel is used. The parameters of the optical model potential are first determined using scattering data and these are then used to calculate the incident channel wave-function. In the expression (2.18) for the amplitude, the function $\bar{V}_\beta$ is any arbitrary function of the channel radius $\bar{r}_\beta$ and the function χ_β is then an eigen function of the two body problem with the potential $\bar{V}_\beta$. In the DWBA the function $\bar{V}_\beta$ is chosen equal to optical model potential in channel β which leads to the observed scattering data in the channel β. For the (d,p) reactions we then have

$$(V_\beta - \bar{V}_\beta) = V_{pn} + V_{pN} - V_{opt} \qquad \ldots(2.24)$$

It is then assumed that the last two terms cancel each other to a good approximation, so that the remaining interaction is then V_{pn}.

The interaction V_{pN} is the sum of all interactions that the individual nucleons of the target exert on the outgoing proton. It is not clear that this sum can be represented by a function of the channel radius alone. Such reduction of a many body interaction to an equivalent two body interaction is an approximation. However, the reduction of the operator $(V_\beta - \bar{V}_\beta)$ in (2.18) to V_{pn} by a proper choice of $\bar{V}_\beta$ is a much better approximation than neglecting V_{pN} as is done in the PWBA. Thus the DWBA method involves a better approximation to $\psi^{(+)}$ as well as to the operator in the matrix element. The amplitude in Eq. (2.20) is then given by

$$A_{\alpha\beta} = - \frac{\mu_\beta}{2\pi\hbar^2} \int \Phi_\beta \; \chi_\beta^{(-)*} V_{pn} \; \Phi_\alpha \; \chi_\alpha^{(+)} \; d\tau \qquad \ldots(2.25)$$

where the functions χ_β are the solutions of

$$\{\frac{\hbar^2 k^2}{2\mu_\beta} - T - \bar{V}_\beta\} \chi_\beta = 0 \qquad \ldots(2.26)$$

with the asymptotic forms,

$$\chi^{(+)} \longrightarrow e^{i\bar{k}.\bar{r}} + f(\theta,\phi) \; \frac{e^{ikr}}{r}$$

$$\chi^{(-)} \longrightarrow e^{i\bar{k}.\bar{r}} + f^*(\pi-\theta, \pi+\phi) \; \frac{e^{-ikr}}{r} \qquad \ldots(2.27)$$

The optical potentials $\bar{V}_\beta$ are of the form,

$$\bar{V}_\beta = U_C + U_N$$

where U_C is the Coulomb potential in the channel and U_{II} is the optical potential. This potential is of the form

$$U_M = W_R + iW_I$$

and various forms for the real and the imaginary part are commonly used.

The amplitude (2.25) can be written in the form

$$A_{\alpha\beta} = -J \frac{\mu_\beta}{2\pi\hbar^2} \int d\bar{r}_\alpha \int d\bar{r}_\beta \; \chi_\beta^{(-)*} \langle\beta| V_{pn} |\alpha\rangle \; \chi_\alpha^{(+)} \qquad \ldots(2.28)$$

where J is the Jacobian of transformation to the relative co-ordinates, and $\langle\beta | V_{pn} | \alpha\rangle$ includes integration over the internal co-ordirates of the target.

$$\langle\beta | V_{pn} | \alpha\rangle = \langle \phi_B | V_{pn} | \phi_A \phi_a \rangle$$

$$= \langle \phi_B | \phi_A \rangle \; V_{pn} \; \phi_a$$

$$= s \; \eta(\bar{r}_{nN}) V_{pn} \; \phi_a(\bar{r}_{np})$$

This factor, which depends upon $\bar{r}_{nN}$ and $\bar{r}_{np}$ can be expressed in terms of the channel radii $\bar{r}_\alpha$ and $\bar{r}_\beta$. The integral (2.28) is then a six dimensional integral Often the interaction V_{pn} is assumed to be of zero range and is replaced by a delta function $D_o \, \delta(r_{np})$. This effectively leads to the

simplification,

$$\bar{r}_{nN} = \bar{r}_{\alpha} = \frac{M_B}{M_A} \bar{r}_{\beta}$$

So that the integral (2 28) reduces to three dimensions

In evaluating the integral (2.28), the matrix element $\langle \beta | V_{pn} | \alpha \rangle$ is exparded into a series of multipoles each of which corresponds to transfer to the target nucleus, a definite angular momentum $\bar{j}$ composed of an orbital part $\bar{l}$ and a spin part $\bar{S}$. We have then

$$\bar{j} = \bar{l} + \bar{S} = \bar{J}_B - \bar{J}_A$$

and in the absence of the spin-flip, we have

$$\bar{S} = \bar{S}_a - \bar{S}_b$$

Often only one value of j, l and S is important or allowed in a transition. The distorted waves χ are also expanded in terms of partial waves,

$$\chi = \frac{4\pi}{kr} \sum_{LM} Y_M^L(\hat{r}) \, Y_M^{L^*}(\hat{k}) \, i^L \chi_L$$

we then have

$$\bar{l} = \bar{L}_{\alpha} - \bar{L}_{\beta}$$

The cross-section, which is proportional to the square of the

amplitude, can then be written in the form[22]

$$\frac{d\sigma}{d\Omega} = \frac{2J_B+1}{2J_A+1} \sum_{lsJ} \frac{|B_{lsJ}|^2}{1.0x10^4} \frac{\sigma_{DW}^{lsJ}}{(2J+1)} \qquad \ldots(2.29a)$$

where

$$\sigma_{DW}^{lsJ} = \frac{4\pi}{E_a E_b} \frac{k_a}{k_b} \left|\frac{M_B}{M_A}\right|^2 \frac{1.0x10^4}{2S_a+1} (2l+1) \sum_{mm_a m_b} |S_{lsJ}^{mm_a m_b}|^2$$

$$\ldots(2.29b)$$

where B_{lsJ} is the measure of strength and is proportional to the spectroscopic factor s_{lsJ}. The quantity $S_{lsJ}^{mm_a m_b}$ is given by

$$S_{lsJ}^{mm_a m_b} = \sum_{J_a J_b L_a L_b} 1^{L_a - L_b - l} (L_a s_a o\ m_a | J_a m_a)\ (L_b s_b o\ m_b | J_b m_b)$$

$$(J_b J\ m_a - mm\ |\ J_a m_a)(2L_b+1)(L_a l o o |\ L_a o) \sqrt{(2s_a+1)(2J+1)}$$

$$\sqrt{(2J_b+1)(2L_a+1)} \begin{bmatrix} L_b & s_b & J_b \\ l & s & J \\ L_a & s_a & J_a \end{bmatrix} d^{J_b}_{m_b m_a - m}(\hat{k}_b)$$

$$\left(\frac{M_A}{M_B} \int dr_a\ \chi_{L_b}\left(k_b \frac{M_A}{M_B} r_a\right) f_{lsJ}(r_a)\ \chi_{L_a}(k_a r_a)\right)$$

$$\ldots(2.30)$$

where $m = m_B - m_A + m_b - m_a$ and $d^{J_b}_{m_b m_a - m}(\hat{k}_b)$ is the rotational matrix. The symbol (|) represents the Clebsch-Gordan coefficients and $f_{lsJ}(r_a)$ is the form factor depending upon the

choice of the neutron bound state wave function and $|B_{lsj}|^2$ is proportional to the interaction strength D_o^2 and the spectroscopic factor s_{lsj}.

In the case of (d,p) reaction the formula (2.29b) reduces to

$$\frac{d\sigma}{d\Omega} = 1.53 \frac{2J_B+1}{2J_A+1} \sum_{lsj} \frac{s_{lsj}\ \sigma_{DW}^{lsj}}{(2j+1)} \qquad \ldots(2.31).$$

where Hulthen function[23] has been assumed for the deuteron wave function. Normally only one value of lsj is required and therefore (2.31) simplifies to the form

$$\frac{d\sigma}{d\Omega} = 1.53 \frac{2J_B+1}{2J_A+1} \frac{s_{lsj}\ \sigma_{DW}^{lsj}}{(2j+1)}$$

Compound Nucleus Reactions

A discussion of formation of compound nucleus would really need the consideration of the time development of the non-stationary state produced in nuclear reactions. The state at $t = -\infty$ develops into a bound state at the instant of compound nucleus formation which subsequently decays providing flux in unbound channel in an exponential manner. In the compound nucleus model it is assumed that the Ψ_{bound} component of the stationary state wave function predominates within

the nuclear volume to provide the boundary conditions at the nuclear surface and the stationary unbound wave functions predominate just outside the nuclear volume. The coupling between the two is provided by the boundary conditions. The compound nucleus has a definite spin J_c and parity π_c so that we have

$$\bar{l}_\alpha + \bar{S}_a + \bar{J}_A = \bar{J}_c = \bar{l}_\beta + \bar{S}_b + \bar{J}_B$$

$$\pi_a \pi_A (-1)^{l_\alpha} = \pi_B \pi_b (-1)^{l_\beta} = \pi_c \qquad \ldots(2.31a)$$

It is usual to introduce channel spins $\bar{S}_\alpha$, $\bar{S}_\beta$ such that

$$\bar{S}_\alpha = \bar{S}_a + \bar{J}_A \qquad \bar{S}_\beta = \bar{S}_b + \bar{J}_B \qquad \ldots(2.31b)$$

As a consequence of restrictions (2.31) the values of angular momenta in the channels α and β are restricted by

$$l_\alpha = (J_c + S_\alpha) \ldots |J_c - S_\alpha|$$

$$l_\beta = (J_c + S_\beta) \ldots |J_c - S_\beta| \qquad \ldots(2.32)$$

Further, because of parity conservation the permitted values of l_α and l_β are either all odd or all even. The angular dependence of the amplitude $A_{\alpha\beta}$ in channel β therefore, has the form

$$A_{\alpha\beta} = \sum_{\substack{l \\ m}}^{l_{max}} {}_{l(\text{even or odd})} a_m^l \, Y_m^l \qquad \ldots(2.33)$$

The cross-section is proportional to the square of the amplitude and therefore has terms which are of even order. The dependence on the azimuthal angle vanishes after summation over the magnetic quantum numbers and the cross-section can be expressed in the form

$$\frac{d\sigma}{d\Omega} \propto \sum_{L_{even}}^{L_{max}} A_L \, P_L(\cos\theta) \qquad \ldots(2.34)$$

after expansion in terms of Legendre polynomials. The angular distribution, therefore, are symmetric about 90° in the centre of mass coordinates. If more than one level of the compound nucleus of different parities contribute the summation (2.33) will be over even as well as odd values of l and the angular distribution will then no longer be symmetric about 90° CM. In the case of contribution from two or more levels of the compound nucleus the angular distribution changes rapidly with the bombarding energy, since the relative contribution from different levels changes.

The angular dependence of the amplitude $A_{s\, m_s\, s'\, m_{s'}}$ from initial channel $s\ m_s$ to final channel $s'\ m_{s'}$ is given by (Blatt and Biedenharn)[2a]

$$q_{s\, m_s\, s'\, m_{s'}} = -\sum \sqrt{\pi}\,(2l+1)^{\frac{1}{2}}\,(l\ s\ o\ m_s | J_c\ m_c) \times (l's'\ m_l, m_{s'} | J_c m_c)\, i^{l'-l}\, U^{J_c}_{ls\ l's'}\, Y^{l'}_{m_{l'}}(\theta,\phi) \qquad \ldots(2.35)$$

where $A_{s\ m_s\ s'\ m_{s'}}$ is related to amplitude $q_{s\ m_s\ s'\ m_{s'}}$ by the relation

$$|A_{s\ m_s\ s'\ m_{s'}}|^2 = \frac{\mu_\alpha\ \mu_\beta k_\alpha\ k_\beta}{(2\pi\hbar^2)^2}\ |q_{s\ m_s\ s'\ m_{s'}}|^2$$

Eq.2.35 is the detailed form of (2.33). The summation is over all quantum numbers except s, m_s, s', $m_{s'}$. The quantity U is the partial reduced amplitude which is independent of angle but depends upon the system energy. If a single level of the compound nucleus is excited, there is no summation over J_c. If a statistically large number of levels contribute it is expected that the interference terms due to their randomness may cancel and the cross-section will be relatively insensitive to θ. Also, angular distribution will be approximately symmetric about 90° in centre of mass system. The total cross-section is obtained by summing over the final channel spins and averaging over the initial channel spins in case of unpolarized beam.

The calculation of the quantity U is to be carried out as a problem of nuclear structure in the region of high excitation energy. This leads to the prediction of the position, angular momentum, parity and other properties of the levels of the compound nucleus. The compound-nucleus model developed

so far does not attempt to calculate these from first principles. However, assuming that these levels exist, their effect on the nuclear reaction process can be predicted with some simplifying assumptions. If at excitation energy E_n such a level exists, the probability of finding the incident particle a within the nuclear volume is expected to be high, since at this energy a bound state is predominantly excited. The condition of high probability within the nuclear volume is satisfied when the slope of the radial wave function $rR_l(r)$ of the unbound state is zero at the nuclear surface. The energy at which a level of the compound nucleus is formed, is therefore also the energy at which the logarithmic derivative f_l at the nuclear surface is zero. The general quantum mechanical theory of scattering in the presence of absorption shows that the cross-section for scattering and for compound nucleus formation peak for this boundary condition. It is therefore possible to understand appearance of resonances in terms of levels of compound nucleus by introducing boundary conditions at the nuclear surface. The behaviour of cross-section in the neighbourhood of resonance is found to be of typical dispersive type as given by the Breit-Wigner formula. This feature is a consequence of the fact that the logarithmic derivative varies reasonably smoothly with energy in the neighbourhood of its value zero. In that case it can be expanded in power series,

about the resonant energy and the retention of the linear term alone directly leads to Breit-Wigner formula which is of the form[24]

$$U \sim \frac{U_o}{(E-E_n)+ i\Delta} \qquad \ldots(2.36)$$

The cross-section is proportional to U^2 and for the shape of the resonance the parameter Δ is found to be equal to $\Gamma/2$, where Γ is the full width of the resonance at half maximum. According to uncertainty principle the width is proportional to the rate of decay of the compound nucleus. The rate of decay can be further divided into partial rates of decay into various specific channels. We can thus define partial widths Γ_β, Γ_α etc corresponding to these partial rates such that $\Gamma = \sum_\beta \Gamma_\beta$ The energy dependence of the quantity U of Eq. (2.35) is

$$U^{J_c}_{ls\ l's'} = \frac{\sqrt{\Gamma_{nls}\ \Gamma_{nl's'}}}{(E-E_n) + \frac{i\Gamma_n}{2}} \qquad \ldots(2.37)$$

Substituting Eq (2.37) in (2.35), summing over all quantum numbers, the amplitude q has the form

$$q = \sum_n \frac{q_n}{\{(E-E_n) + \frac{i\Gamma_n}{2}\}} \qquad \ldots(2.38)$$

where n represents different resonance energies, q_n represents dependence on parameters other than energy and the phase factor is included in q_n.

Contribution of Direct and Compound Nucleus Reactions

As mentioned earlier the actual problem of finding the asymptotic behaviour of the total wave function, which includes the bound and unbound parts with the coupling between the two, is treated in terms of models The amplitude is assumed to be made of a resonant part and non-resonant part. This has basis in terms of semi-classical consideration and is applicable when reasonably resolved Breit-Wigner type of resonances are found riding over general background in the measured cross-section. This is particularly applicable in the case of reactions like the (d,p) reactions on light targets where well recognized stripping patterns of angular distributions are observed at a bombarding energy of about 4-5 MeV while at bombarding energy of about 2-MeV the stripping patterns appear in a somewhat distorted form and resonances appear in the excitation curves.

In such cases it is possible to assume that the amplitude q is given by

$$q(E,\theta) = \sum_n \frac{q_n(\theta)}{\{(E-E_n)+\frac{i\Gamma_n}{2}\}} + q^{NR}(\theta) \qquad \ldots(2.39)$$

where the non-resonant amplitude q^{NR} may be considered to be energy insensitive in magnitude and phase over the width of the resonance, though it may depend upon θ The phase of the resonant part of the amplitude varies with energy as determined by Breit-Wigner formula. Due to this energy dependence it is possible to empirically separate the non-resonant part of the cross-section from the resonant part by analysing the experimental excitation curve data at each angle It is then possible to reconstruct the angular distributions of the non-resonant mechanism alone and compare these with the available predictions of the direct reaction theory.

CHAPTER III

EXPERIMENT

Accelerator

The present work was done with a two-Mev Van-de-Graaff accelerator available at the Indian Institute of Technology, Kanpur. It is a standard two-Mev machine of High Voltage Engineering Corporation, Burlington, Mass., U.S.A

The accelerator was purchased without the gas drying system which was designed and assembled locally. The system provides a fresh charge of nitrogen and carbon dioxide mixture with a dew point of $-60^{\circ}F$ in about ten hours which is then transported to the pressure tank at 350 psi to provide insulation of the high voltage dome. A water chilling plant was similarly locally assembled.

The ion source is a standard radio frequency source which is at present used with hydrogen and deuterium as source gases. The ions are focussed and accelerated down the beam tube to provide total currents upto about 150 μamperes with an

energy resolution of about 10 KeV. The analysing and switching magnet for beam handling was under construction while this work was in progress. Therefore, a laboratory magnet providing about 10 kilo-gauss of magnetic field was used to separate the molecular beam from the atomic beam.

The voltage on the dome was measured by means of a generating voltmeter (GVM) fixed inside the pressure tank. It consists of a rotor which alternately shields and reveals a stator to the electric field produced by the charge of the dome. An AC signal is therefore generated on the stator which is amplified, rectified and measured. The output DC signal is proportional to dome voltage. The absolute calibration of the beam energy was done by locating the $^{7}Li(p,n)$ threshold expected at 1.88 MeV and the $^{27}Al(p,\gamma)$ resonance expected at 0.992 MeV. The neutrons were detected with a BF_3 counter embedded in paraffin and γ-rays were detected with a NaI crystal of dimension 5"x4" mounted on photomultiplier. The final dome voltage was read on a digital voltmeter. The average fluctuation in the dome voltage during the period of data collection was $\pm$3KeV.

Target Chamber

A scattering chamber with a diameter of 10" was designed for charged particle experiments and is shown in Figure 1. A system of two slits was used to collimate the beam to a narrow

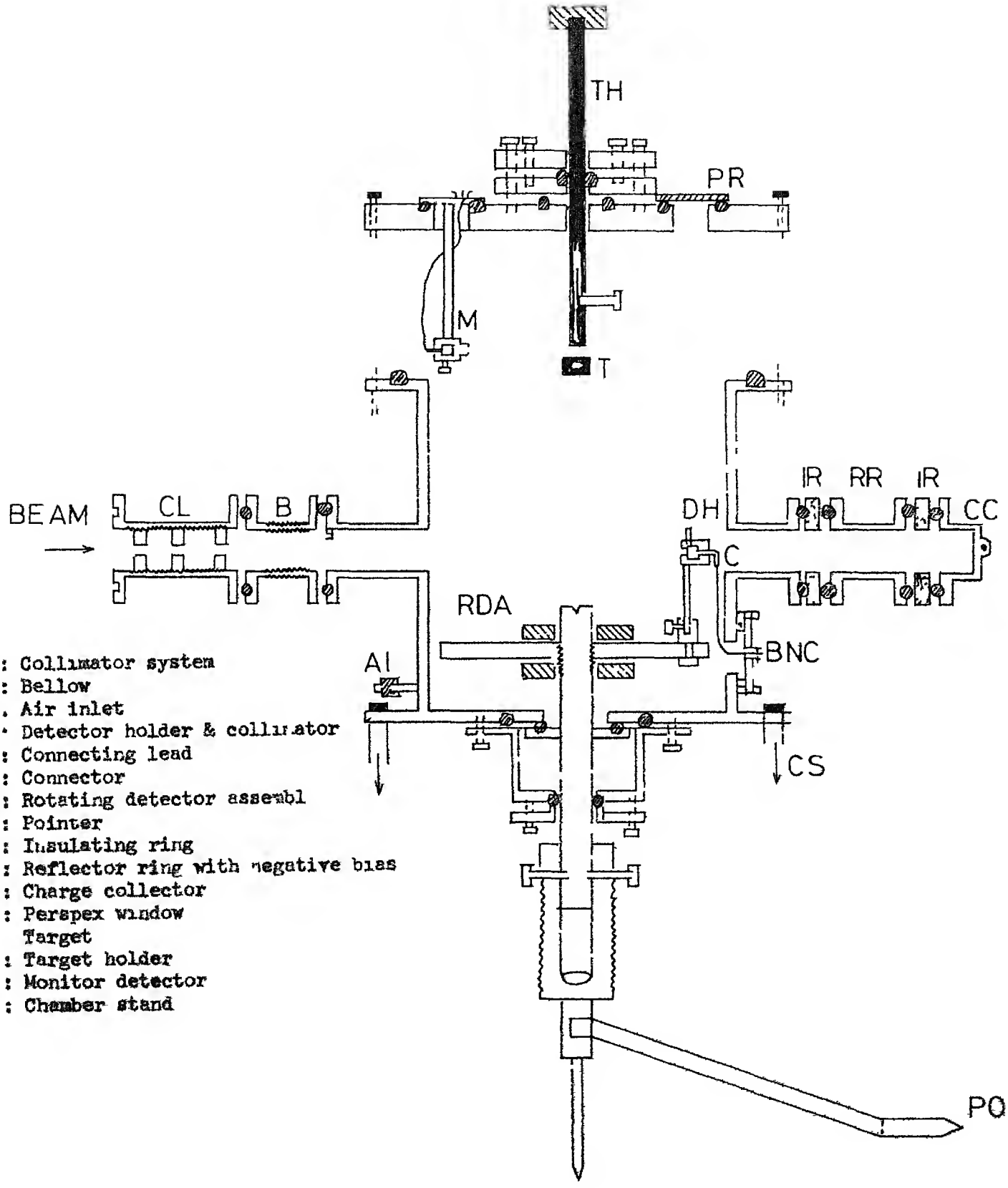

CL : Collimator system
B : Bellow
AI . Air inlet
DH : Detector holder & collimator
C : Connecting lead
BNC : Connector
RDA : Rotating detector assembl
PO : Pointer
IR : Insulating ring
RR : Reflector ring with negative bias
CC : Charge collector
PR : Perspex window
T Target
TH : Target holder
M : Monitor detector
CS : Chamber stand

Fig 1

spot of two millimeters in diameter and a third slit with a larger aperture was placed nearer the target as an anti-scattering baffle. The target was mounted on a brass holder which could be raised, lowered or rotated without breaking the vacuum by adjusting the clamps on the top of the scattering chamber The centering of the target could be ensured by visual checks of the fluorescence through the perspex window provided for the purpose. The scattering chamber had the provision of holding a number of solid state detectors at any desirable radial distance from the target and their angular position could be read and varied without breaking the vacuum with a knob at the bottom of the chamber. Arrangement for a monitoring detector at a fixed angle was also made. An electrically isulated Faraday cup was provided to collect the transmitted beam. This is fitted with a secondary electron suppressing ring which was kept at -150 volts to prevent leakage of charge through secondary electron emission from the Faraday cup. The output of the Faraday cup was fed to an Elcor current integrator which measures the current as well as the integrated charge. The chamber was provided with an evacuating port and a vacuum of 10^{-6} mm was maintained using the evacuating system of the machine.

Detector

For the detection of charged particles surface barrier solid state detectors were used. They had a depletion layer sufficiently thick to stop 6 MeV protons and 24 MeV alpha particles. These were obtained from the Oak Ridge Technical Corporation (ORTEC), Oak Ridge, Tenn , U.S.A and some were obtained from the Bhabha Atomic Research Centre, Trombay, Bombay. Some detectors made in this laboratory were also used for preliminary studies. The detector signals were fed to ORTEC model 101 and 102 low noise preamplifiers and model 201 and 202 ORTEC amplifiers The output of the amplifier was analysed using a 512-channel multi-channel analyzer (MCA) purchased from Nuclear Data Corporation. The resolution of the detection system was checked with the ^{241}Am alpha source and was found to be 0.8% for the 5.48 MeV alpha particles. It was improved to 0.7% when only the central portion of the detectors was used with a detector collimation system. A slight effect of degradation of resolution, due to neutron irradiation, was observed during the course of (d,p) experiment. The MCA itself was calibrated using a linear pulser provided in the ORTEC amplifier system

Target

The targets of ^{12}C and ^{9}Be were made by vacuum evaporation technique. The system was assembled in this laboratory

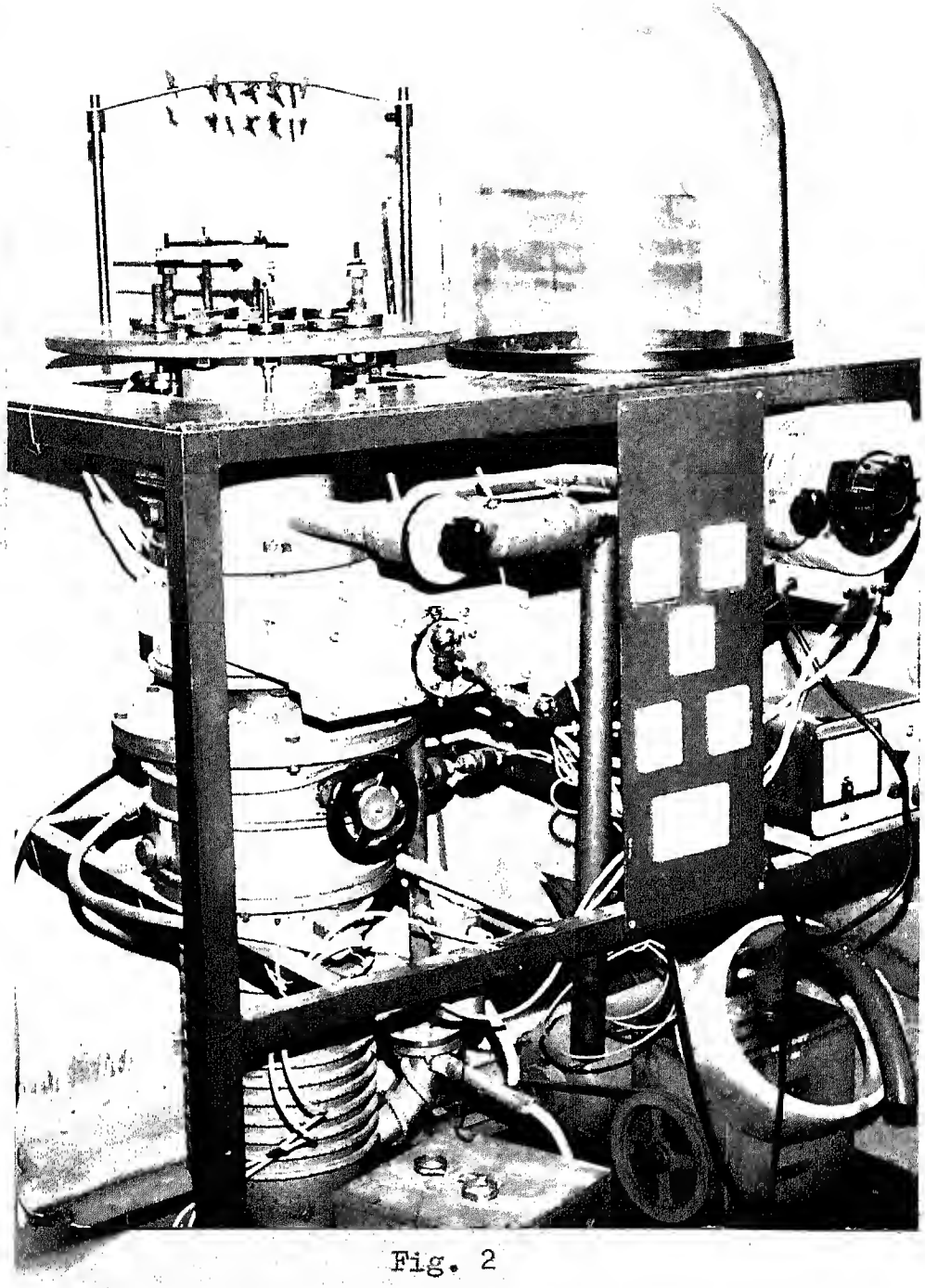

Fig. 2

and is shown in Figure 2. The electrode system couplings and the liquid nitrogen trap were fabricated locally. It was possible to obtain a vacuum of 10^{-6} mm in the evaporation dome and a current of about hundred amperes could be used for evaporation of the material.

For the preparation of carbon targets, two carbon electrodes (99.9% purity) were fitted to the live posts. The tip of one was tapered and that of the other was a plane surface. The tips were brought in touch with a rotary seal arrangement to strike an arc. A tantalum boat was fitted to two other live posts and a small quantity of sodium chloride was placed in the boat. Glass slides etched with hydrofluoric acid and cleaned with acetone were held at about 15 cm above the boat for deposition. A clean glass dome was placed above the whole system and the dome was evacuated. The sodium chloride was first evaporated by passing current through the boat and the glass slides were thus coated with thin-layer of sodium chloride. An arc was then struck between the carbon electrodes which led to the deposition of a carbon film over the sodium chloride film. The slides were then removed and slowly immersed in distilled water which dissolved sodium chloride. The carbon films floating on the surface of water were then picked up on rectangular brass mounts with circular holes in them.

For preparing the beryllium targets carbon films were first prepared as backing and the glass slides were replaced by these mounted films for evaporation of beryllium. Beryllium (99.99% purity) was evaporated using tungstun filament instead of a tantalum boat, since beryllium forms an amalgum with tantalum. The berylbum targets with carbon backing were used in the experiment and the additional peaks in the reaction spectrum arising out of beryllium reactions could be easily detected since the carbon peaks were already studied. The beryllium peaks of interest were well separated from the carbon peaks due to the difference in the Q values. Attempts to prepare a self supporting beryllium film did not succeed since the beryllium flaked-off when attempt was made to peel off the film from the glass slides.

The relative measurement of the thickness of the carbon targets used was obtained from their respective yields of (d,p_o) reaction. The absolute thickness was found by weighing a relatively thick film in a microbalance and also by studying the energy loss of 1.90 MeV protons by studying the shift in the threshold of ^{7}Li (p,n) reaction as shown in Figure 3. The two methods gave consistent results to within 10%. The carbon targets used had a thickness between 3-16 KeV for 1.9 MeV protons. In the case of beryllium target, the thickness of the backing carbon film was first determined and that of beryllium film

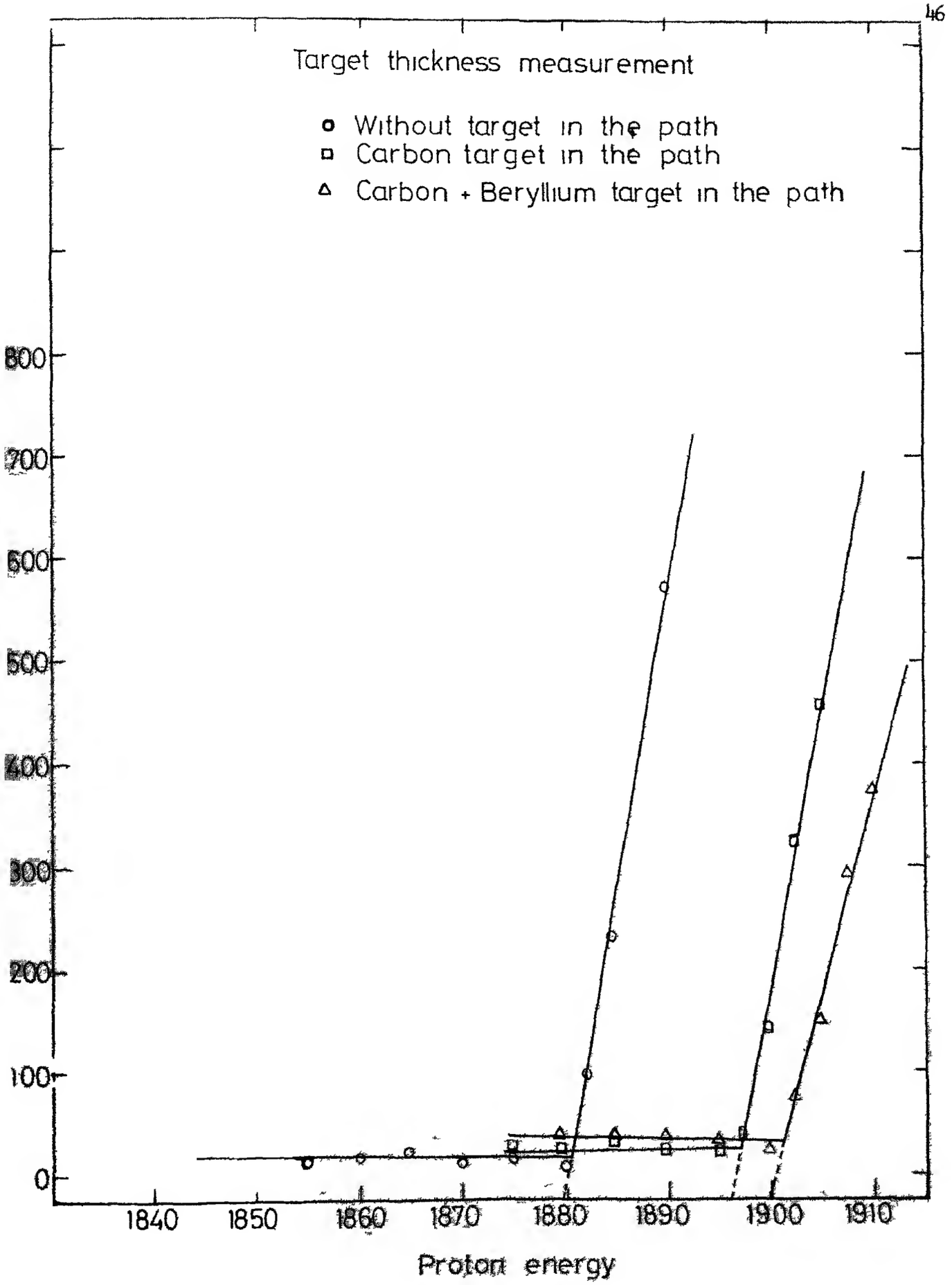
Target thickness measurement
o Without target in the path
□ Carbon target in the path
△ Carbon + Beryllium target in the path
800
700
600
500
400
300
200
100
0
1840
1850
1860
1870
1880
1890
1900
1910
Proton energy

Fig-3

was obtained by measuring the energy loss through the two films together. Beryllium targets used had a thickness of 3 to 7 KeV for 1.9 MeV protons. To improve an overall accuracy, thick-target thickness was determined.

Measurements

For alignment of the beam, the Faraday cup was replaced by a pyrex disc and the position of the scattering chamber was adjusted to ensure that the beam spot was at the centre of the pyrex disc. The target was then lowered and the passage of the beam through its centre was ensured by checking visually the bright spot on the target appearing due to beam bombardment. The pyrex disc was then replaced by the Faraday cup. The zero degree position for the detector was checked by observing the yield of the protons scattered from carbon 12 at the same positive and negative angles for several angular positions.

A typical spectrum at 1600 KeV deuteron energy and $\theta_{lab} = 113^{o}$ for beryllium on carbon backing is shown in Figure 4. All resolved peaks in the spectrum could be identified from the known Q values for the respective reactions For reaction angles smaller than 70^{o} lab, the elastic scattering cross-section increased rapidly as compared to reaction cross-sections. This increased the dead time of the equipment to an undesirable extent. Therefore, a nickel film was placed in front of the

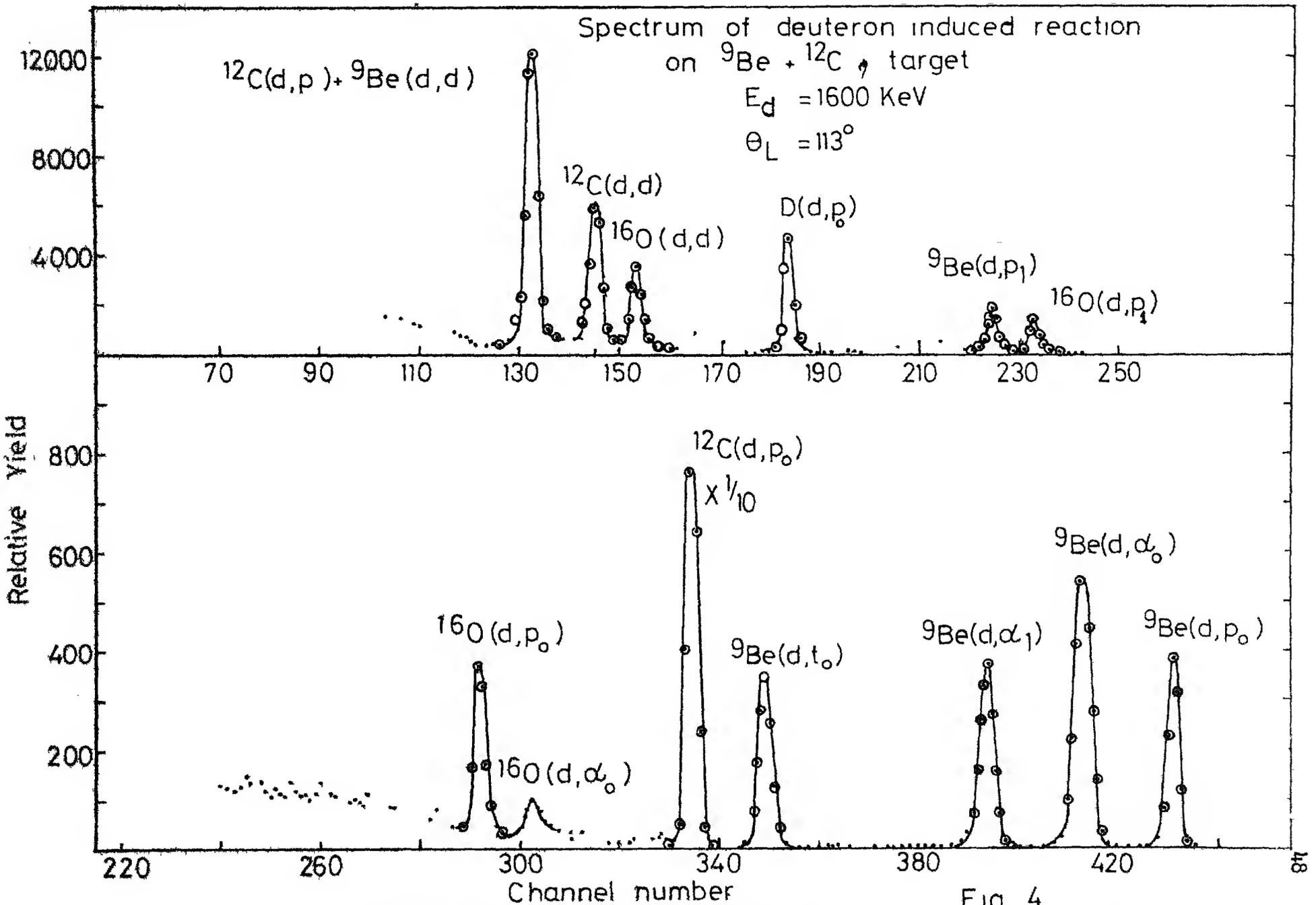
Spectrum of deuteron induced reaction
on ^{9}Be + ^{12}C target
E_d = 1600 KeV
θ_L = 113°
$^{12}C(d,p)$ + $^{9}Be(d,d)$
$^{12}C(d,d)$
$^{16}O(d,d)$
$D(d,p_0)$
$^{9}Be(d,p_1)$
$^{16}O(d,p_1)$
$^{12}C(d,p_0)$
X 1/10
$^{16}O(d,p_0)$
$^{16}O(d,\alpha_0)$
$^{9}Be(d,t_0)$
$^{9}Be(d,\alpha_1)$
$^{9}Be(d,\alpha_0)$
$^{9}Be(d,p_0)$
Relative Yield
Channel number
12000
8000
4000
800
600
400
200
70
90
110
130
150
170
190
210
230
250
220
260
300
340
380
420

Fig 4

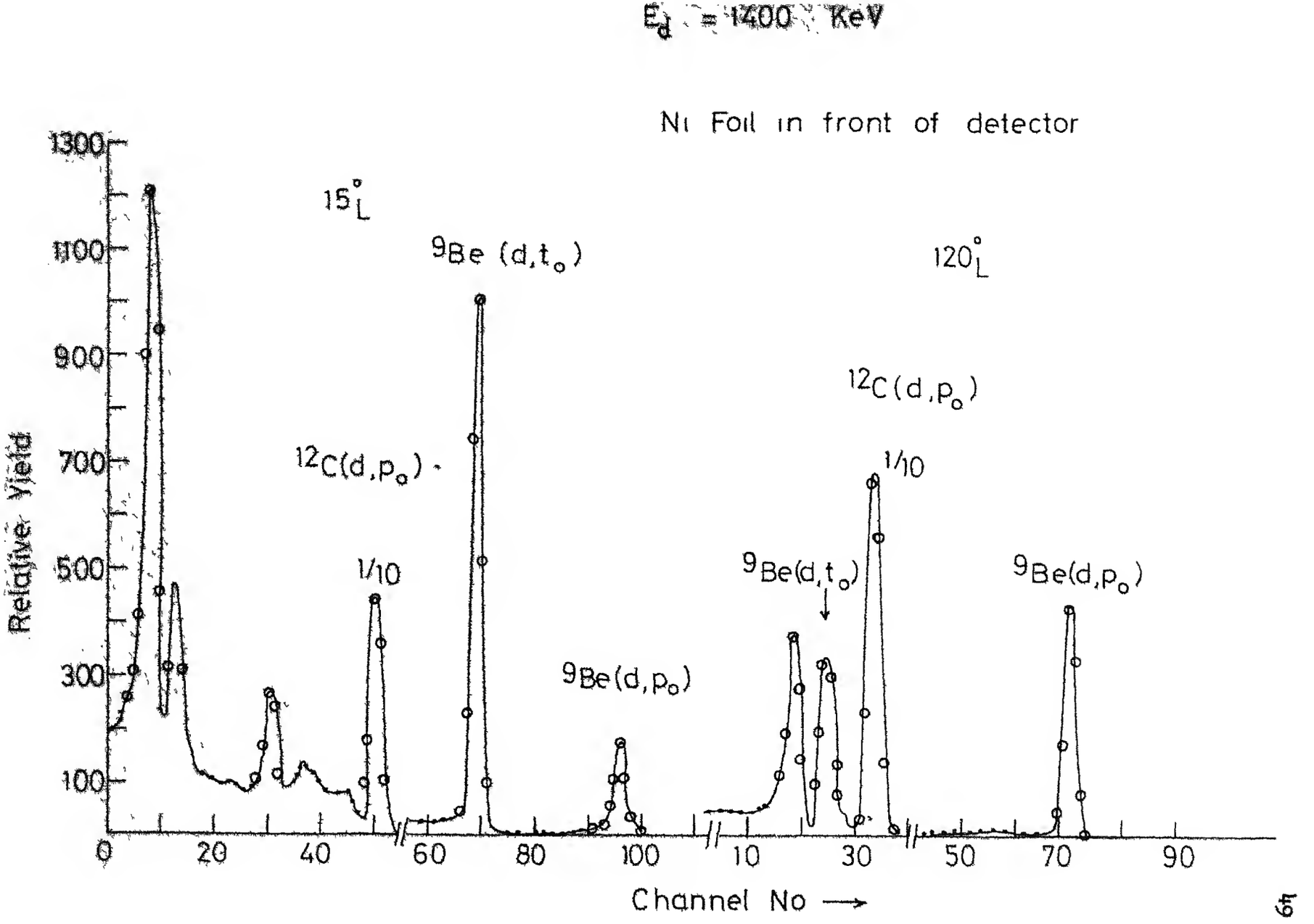
E_d = 1400 KeV
Ni Foil in front of detector
15° L
^{9}Be (d,t$_o$)
120° L
^{12}C(d,p$_o$)
^{12}C(d,p$_o$)
1/10
1/10
^{9}Be(d,t$_o$)
^{9}Be(d,p$_o$)
^{9}Be(d,p$_o$)
Relative Yield
1300
1100
900
700
500
300
100
0
20
40
60
80
100
10
30
50
70
90
Channel No →

Fig 5

detector to just stop the elastically scattered deuterons but not the energetic protons from (d,p) reactions. With nickel foil in front of the detector, data upto 15^{o}Lab. could be taken in the forward direction. A typical spectrum with nickel foil in front of the detector is shown in Figure 5. To identify peaks in this case, loss of energy in Ni foil for each reaction product had to be calculated separately.

The excitation function for $^{12}C(d,p_o)$ reaction was obtained at nine laboratory angles in steps of 10 KeV in the deuteron energy range of 800 to 1850 KeV, shown in Figures 6-9. The excitation curve for $^{12}C(d,d)$ channel, in the same range, is shown in Figure 10. Further, for consistency check, angular distributions in the angular range 15^{o} to 160^{o} laboratory angles in steps of 10^{o} were taken at seventeen values of bombarding energy in the range 800 to 1800 KeV. These are shown in Figures 11 to 13. In the low energy range of 500-800KeV no resonances were observed. Excitation curve in this range at the three laboratory angles and angular distributions at two bombarding energies are shown in Figures 10 and 14.

On ^{9}Be target data on (d,p_o), (d,t), (d,d_o) and (d,α_1) could be obtained. Since these reactions have a higher Q value than the $^{12}C(d,p_o)$ reaction, the corresponding peaks could be studied inspite of carbon backing at most of the angles. In the energy range of 800 to 1800 KeV excitation functions for $^{9}Be(d,p_o)$ reactions were taken at nine angles. These are

shown in Figures 6, 15 and 16. For consistency check angular distribution in the angular range 15^{o} to 160^{o} laboratory angles in steps of 10^{o} were taken at eighteen values of bombarding energy in the range 500 to 2000 KeV as shown in Figures 17 to 20. In addition, excitation functions for ^{9}Be (d,p_1) reaction in the range 800 to 1800 KeV and excitation function for ^{9}Be (d,α_o) in the same bombarding energy range are shown in Figures 21 and 22. Excitation curve for ^{9}Be (d,t_o) in the range 800-1800 KeV is shown in Figure 23.

It is estimated that the cross-sections have been measured with an energy resolution of 0.5%. The relative error in the cross-sections is about 2% and the error in absolute cross-section is about 12% in carbon and 15% for beryllium. In the present analysis the accuracy in relative cross-section is of primary importance.

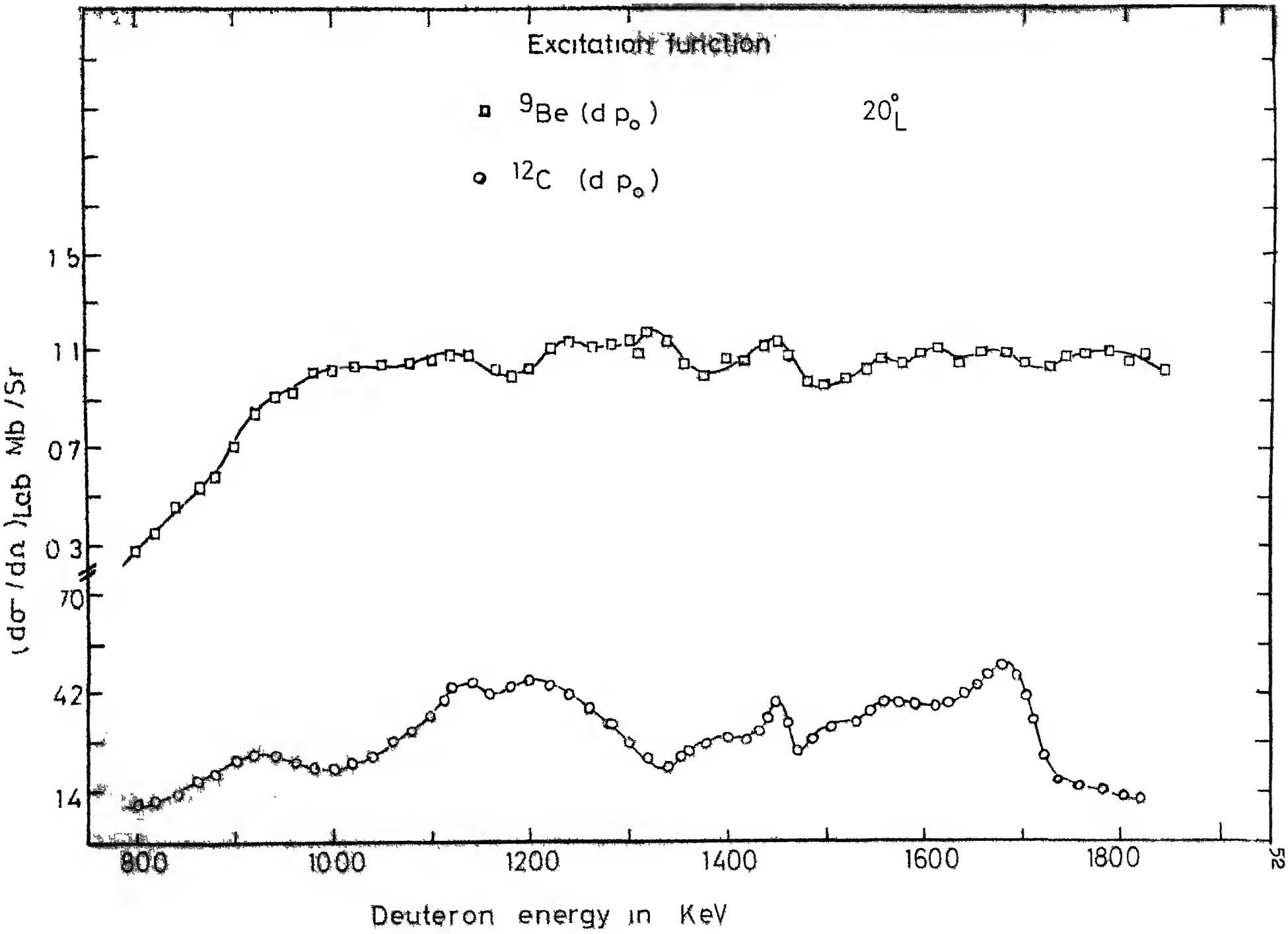
Excitation function
^{9}Be (d p_o)
^{12}C (d p_o)
20° L
1 5
1 1
0 7
0 3
70
42
14
(dσ / dΩ) Lab Mb / Sr
800
1000
1200
1400
1600
1800
52
Deuteron energy in KeV

Fig 6

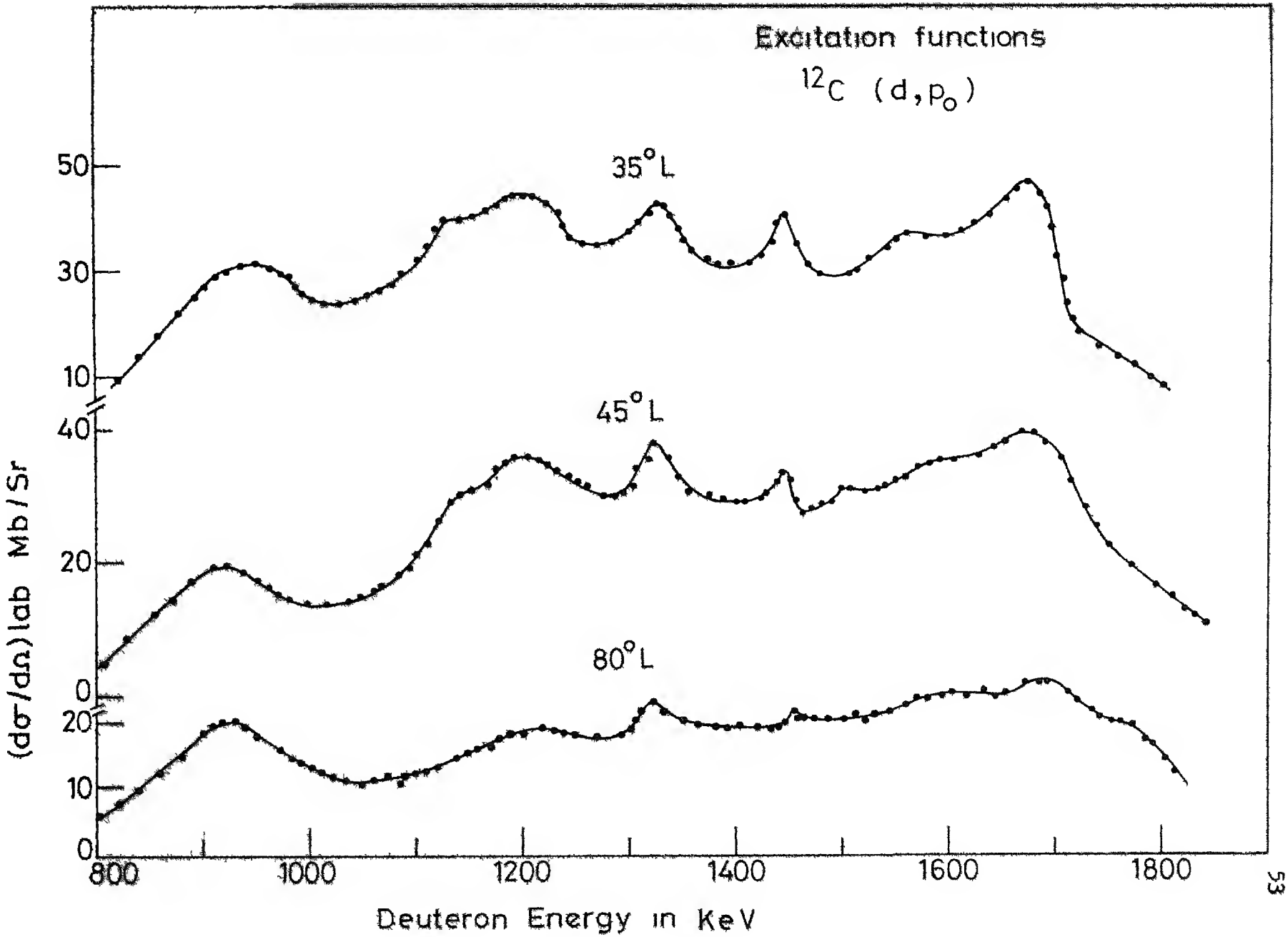
Excitation functions
^{12}C (d, p_o)
35° L
45° L
80° L
50
30
10
40
20
0
20
10
0
800
1000
1200
1400
1600
1800
(dσ/dΩ) lab Mb/Sr
Deuteron Energy in KeV

Fig 7

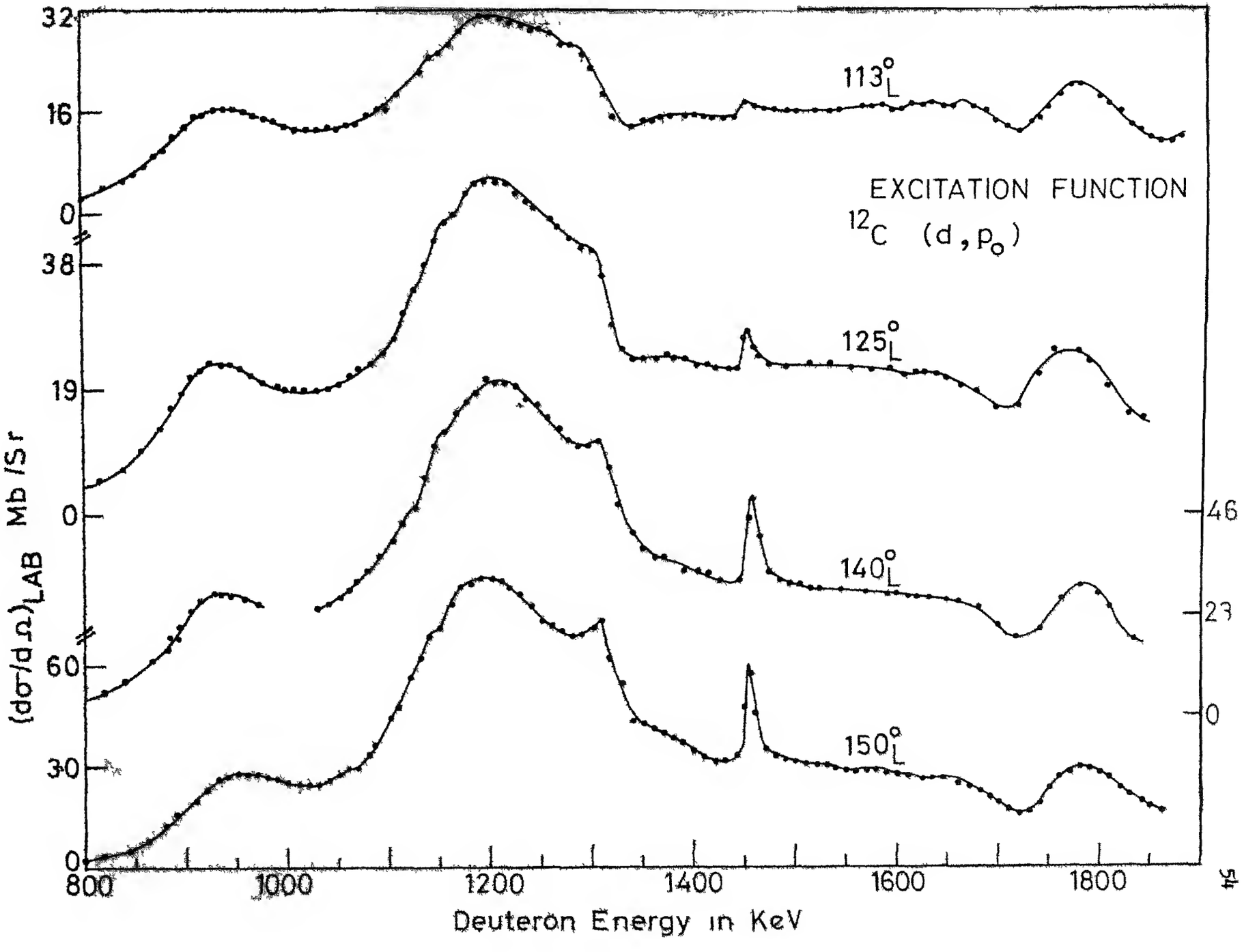
EXCITATION FUNCTION
^{12}C (d, P_o)
113°L
125°L
140°L
150°L
32
16
0
38
19
0
60
30
0
46
23
0
800
1000
1200
1400
1600
1800
Deuteron Energy in KeV
$(d\sigma/d\Omega)_{LAB}$ Mb /Sr

Fig_8

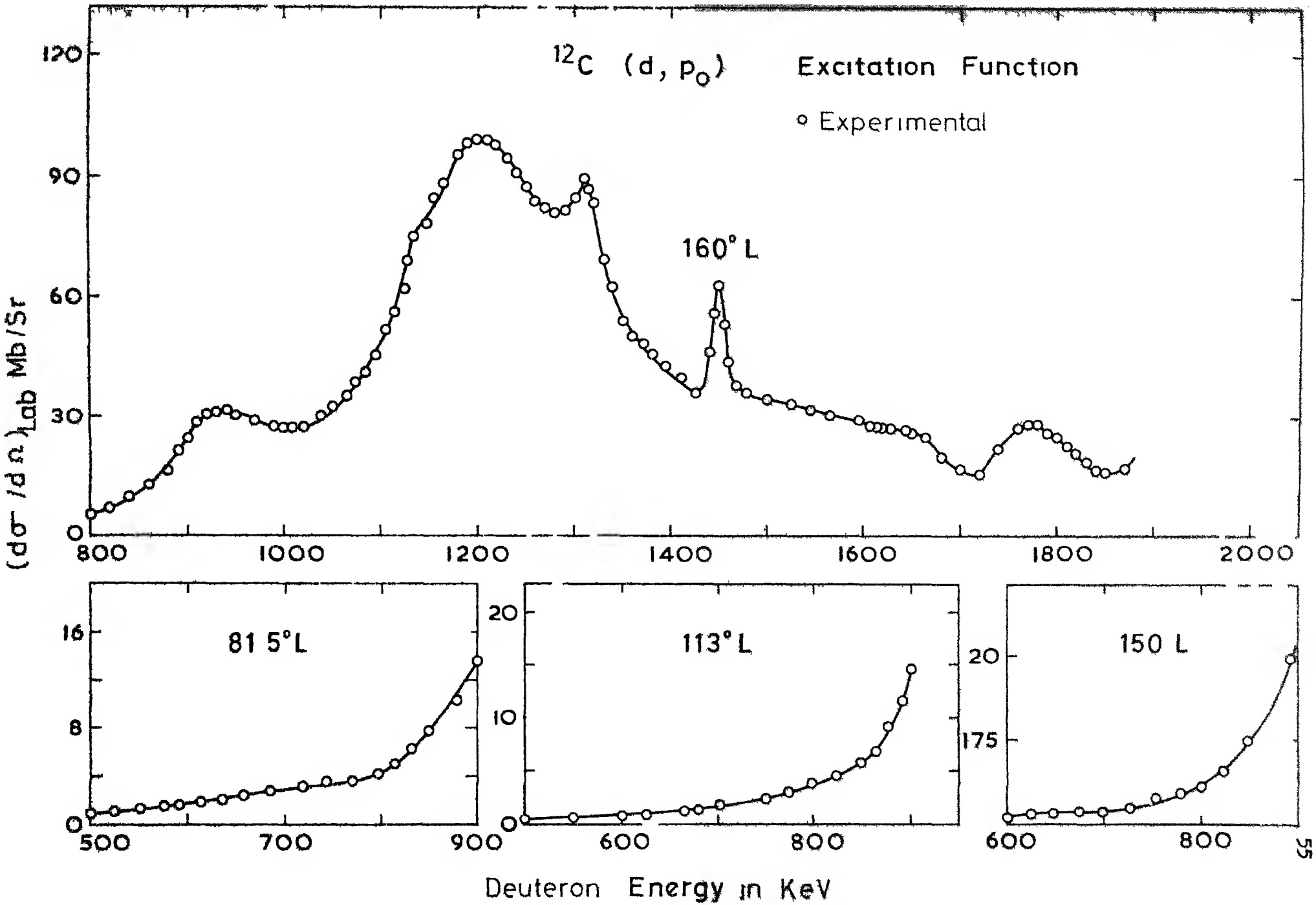
^{12}C (d, p_0) Excitation Function
° Experimental
160° L
81 5°L
113° L
150 L
$(d\sigma/d\Omega)_{Lab}$ Mb/Sr
Deuteron Energy in KeV

Fig 9

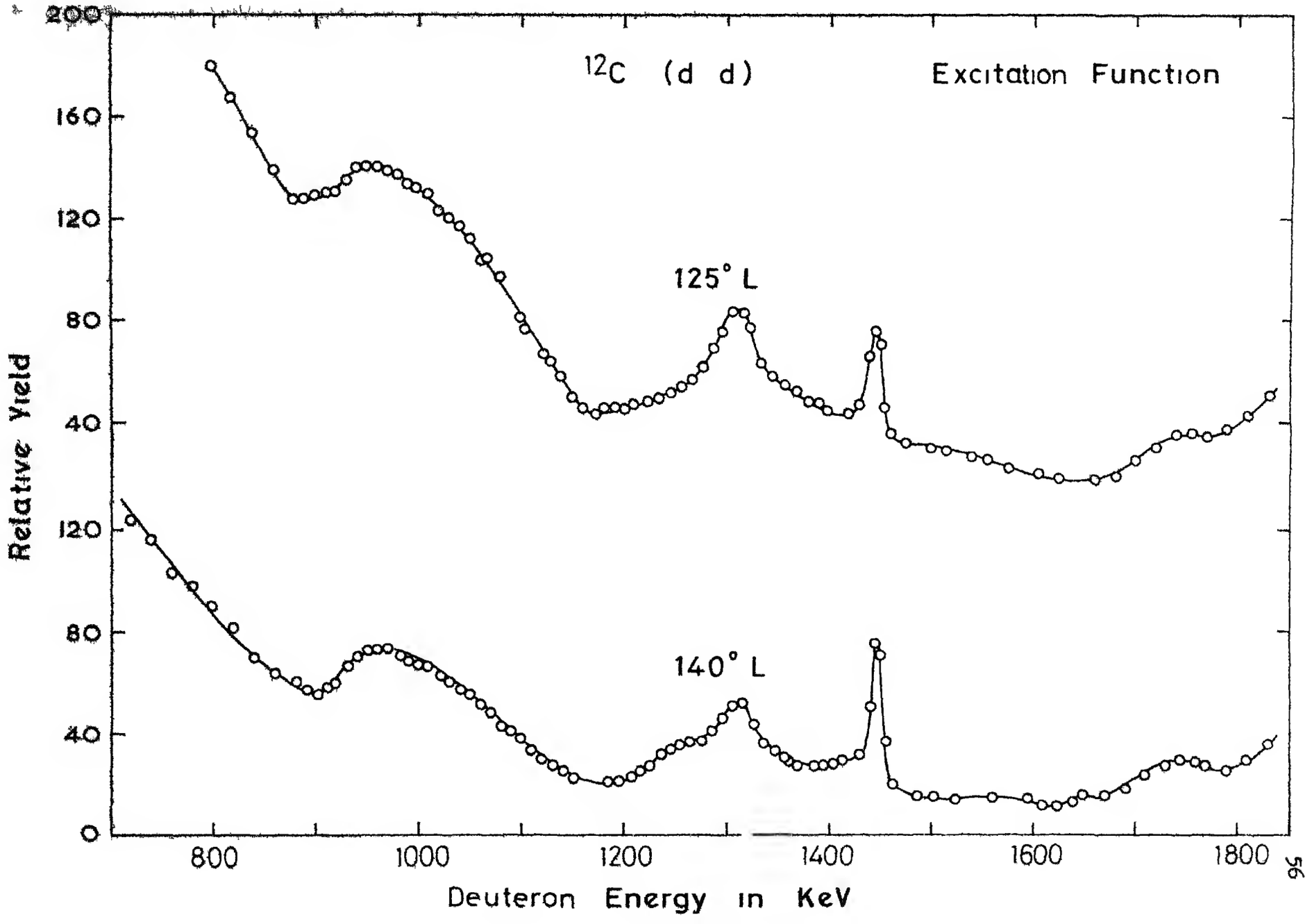
^{12}C (d d) Excitation Function
125° L
140° L
Relative Yield
200
160
120
80
40
120
80
40
0
800
1000
1200
1400
1600
1800
Deuteron Energy in KeV

Fig 10

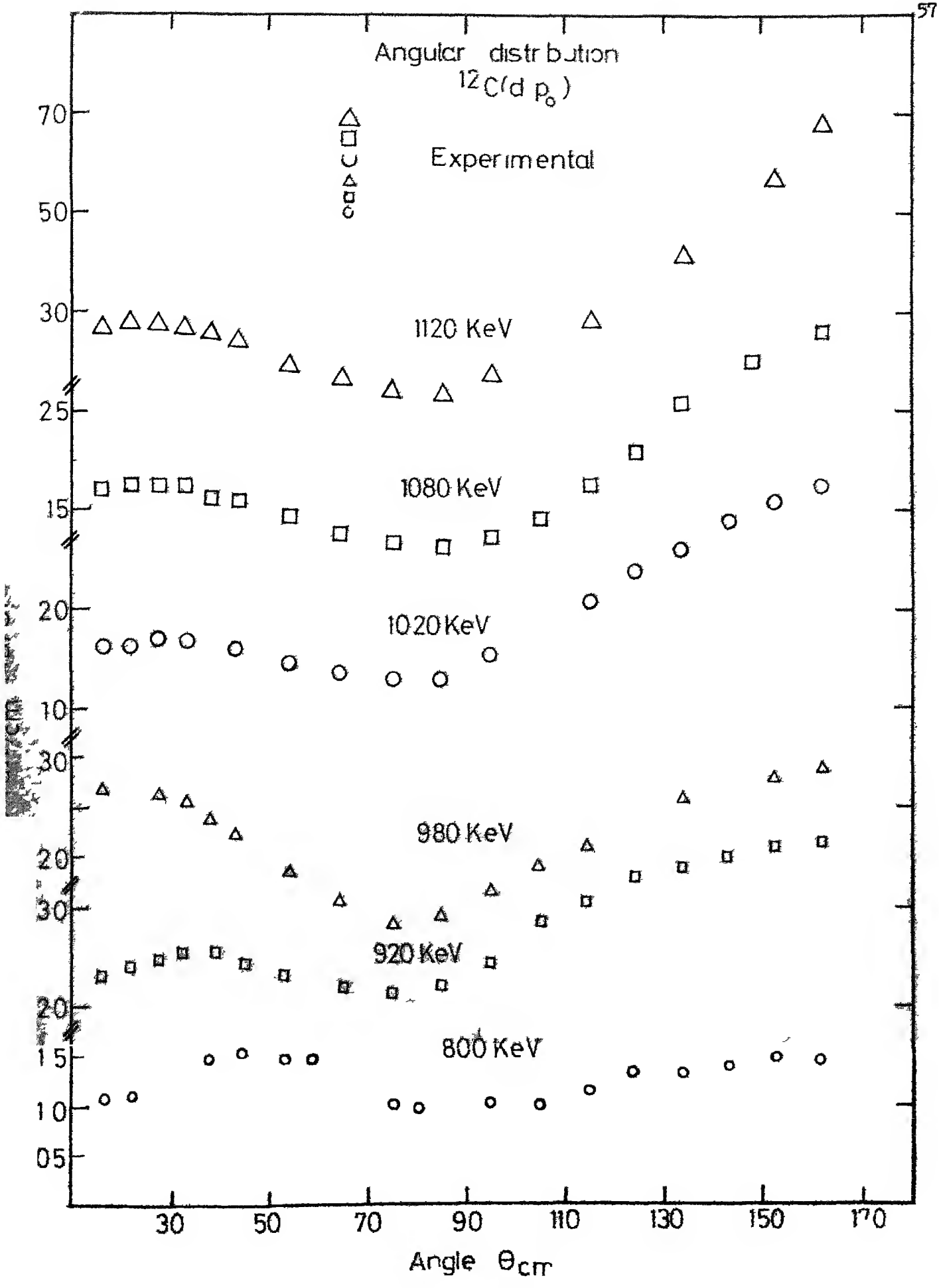
Angular distribution
12C(d p0)
Experimental
1120 KeV
1080 KeV
1020 KeV
980 KeV
920 KeV
800 KeV
70
50
30
25
15
20
10
05
30
50
70
90
110
130
150
170
Angle θcm

Fig 11

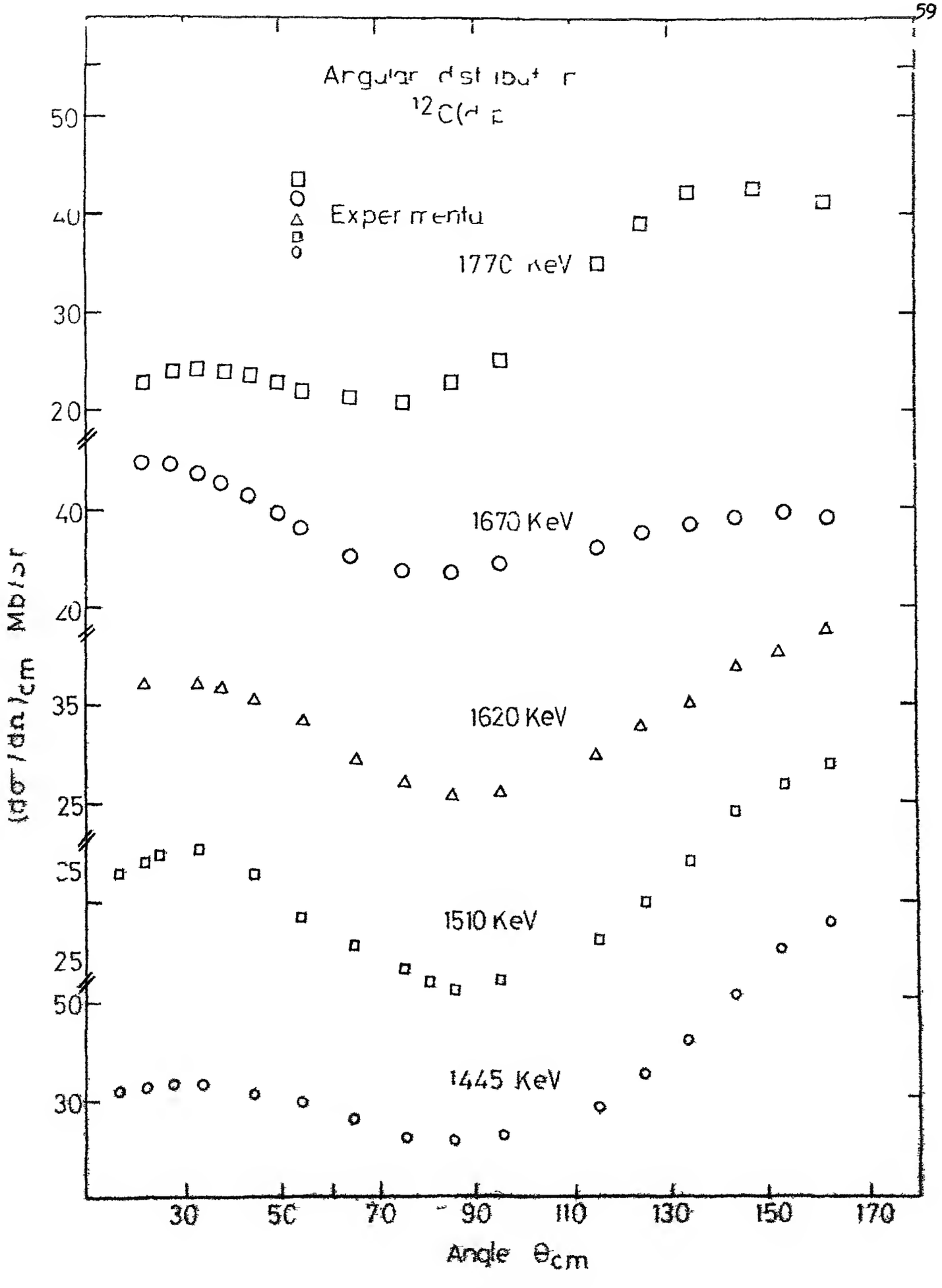
Angular distribution
$^{12}C(d,\alpha)$
Experimental
1770 KeV
1670 KeV
1620 KeV
1510 KeV
1445 KeV
$(d\sigma/d\Omega)_{cm}$ Mb/sr
Angle θ_{cm}
50
40
30
20
40
40
35
25
25
50
30
30
50
70
90
110
130
150
170

Fig 13

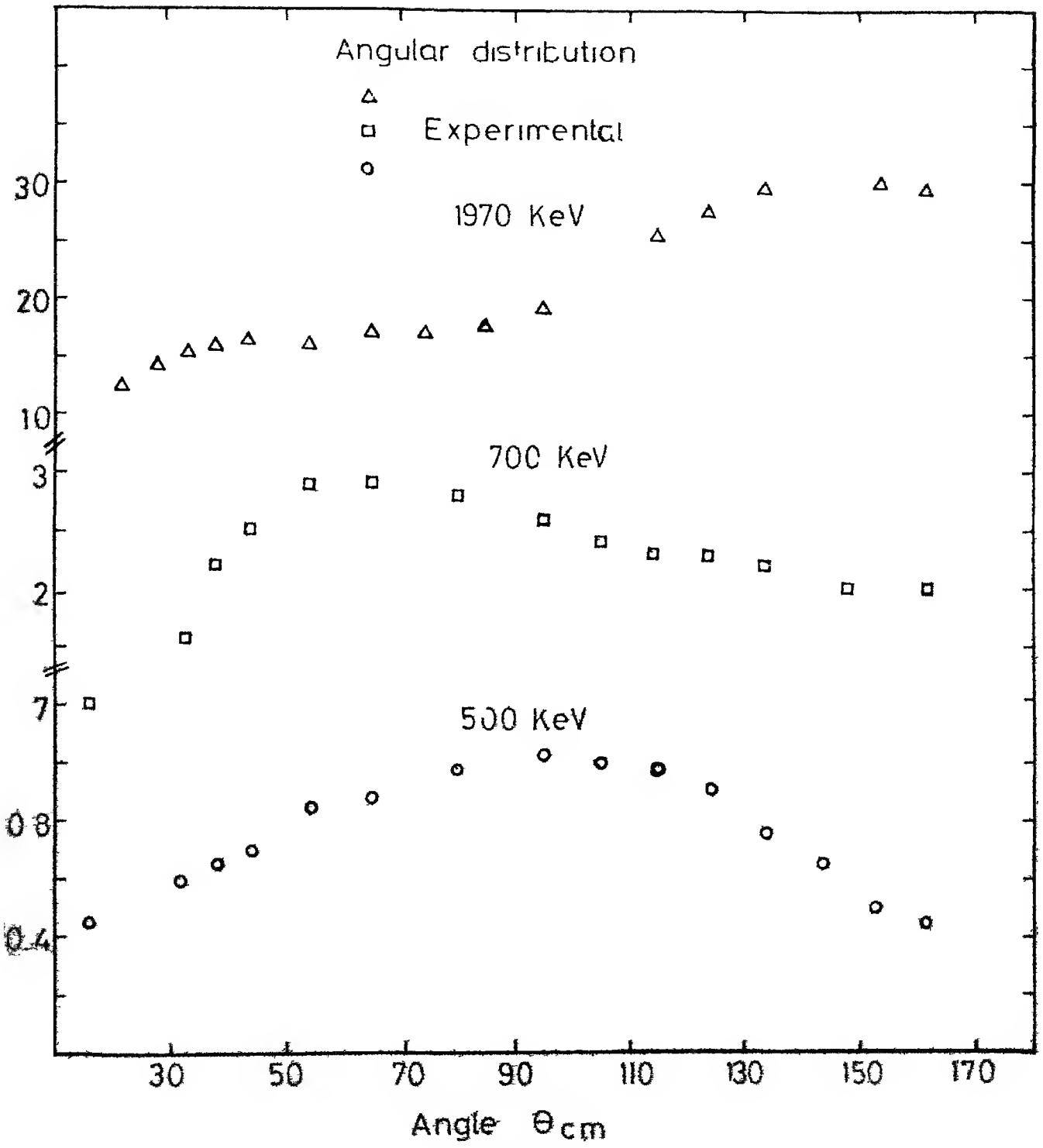
Angular distribution
Experimental
1970 KeV
700 KeV
500 KeV
30
20
10
3
2
7
0.8
0.4
30
50
70
90
110
130
150
170
Angle θcm

Fig 14

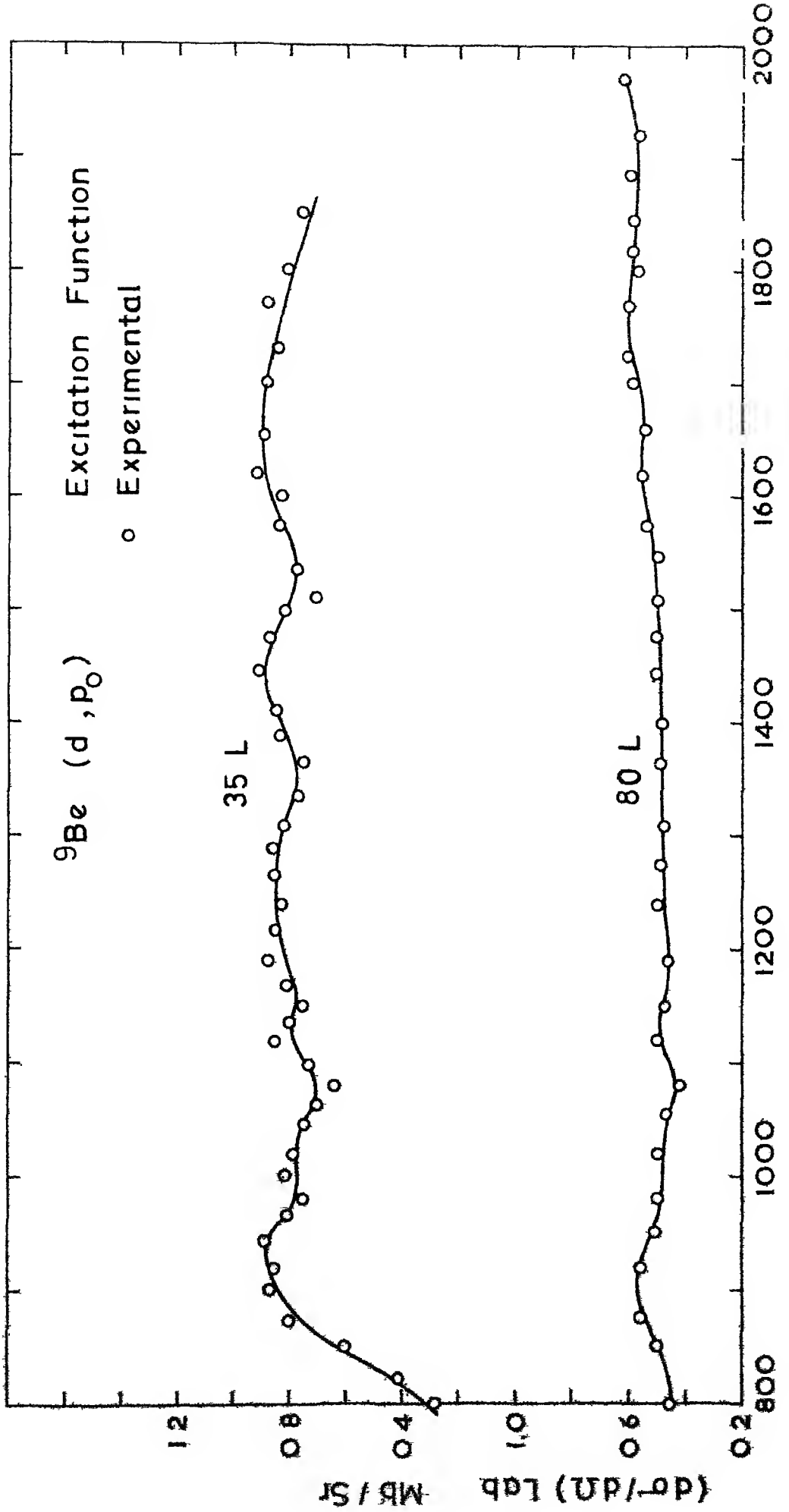
Excitation Function
o Experimental
^{9}Be (d, p_0)
35 L
80 L
(dσ/dΩ) Lab MB / Sr
Deuteron Energy in KeV
800
1000
1200
1400
1600
1800
2000
0.2
0.6
1.0
0.4
0.8
1.2

Fig 15

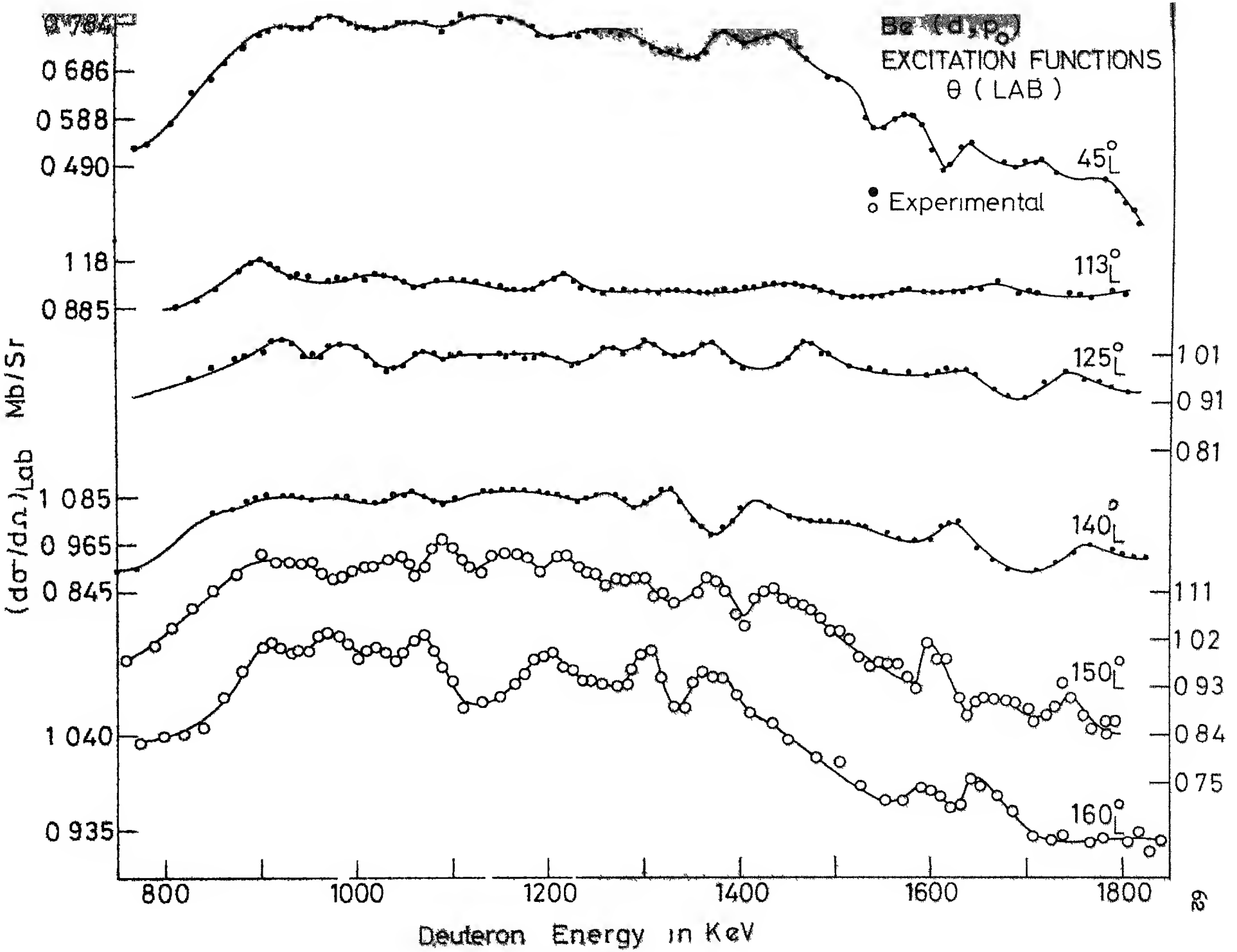
Be (d,p0)
EXCITATION FUNCTIONS
θ (LAB)
Experimental
45°L
113°L
125°L
140°L
150°L
160°L
0 784
0 686
0 588
0 490
1 18
0 885
1 085
0 965
0 845
1 040
0 935
1 01
0 91
0 81
1 11
1 02
0 93
0 84
0 75
(dσ/dΩ)Lab Mb/Sr
800
1000
1200
1400
1600
1800
Deuteron Energy in KeV

Fig 16

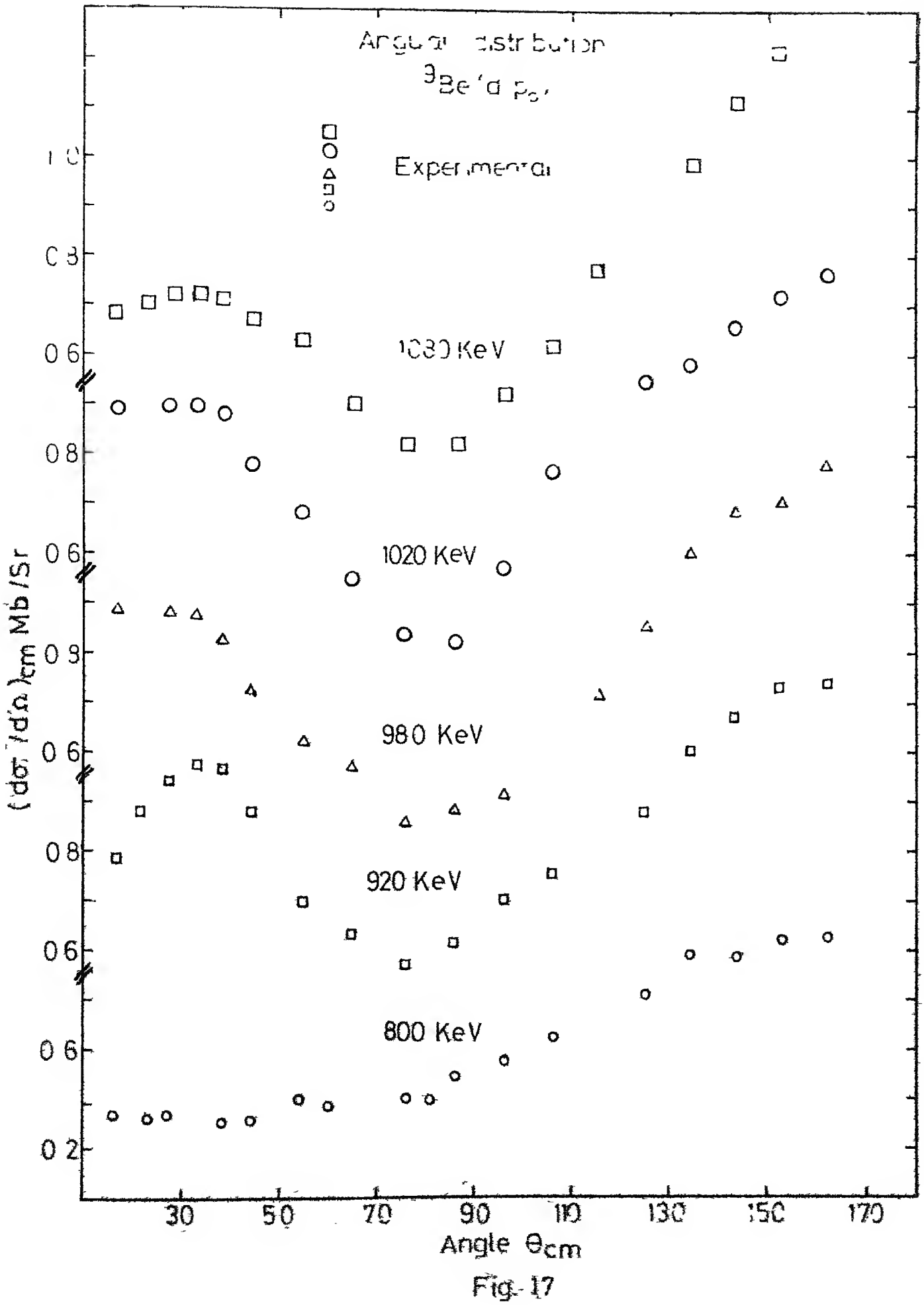
Angular distribution
9Be(d,p0)
Experimental
1080 KeV
1020 KeV
980 KeV
920 KeV
800 KeV
(dσ/dΩ)cm Mb/Sr
Angle θcm
30
50
70
90
110
130
150
170

Fig-17

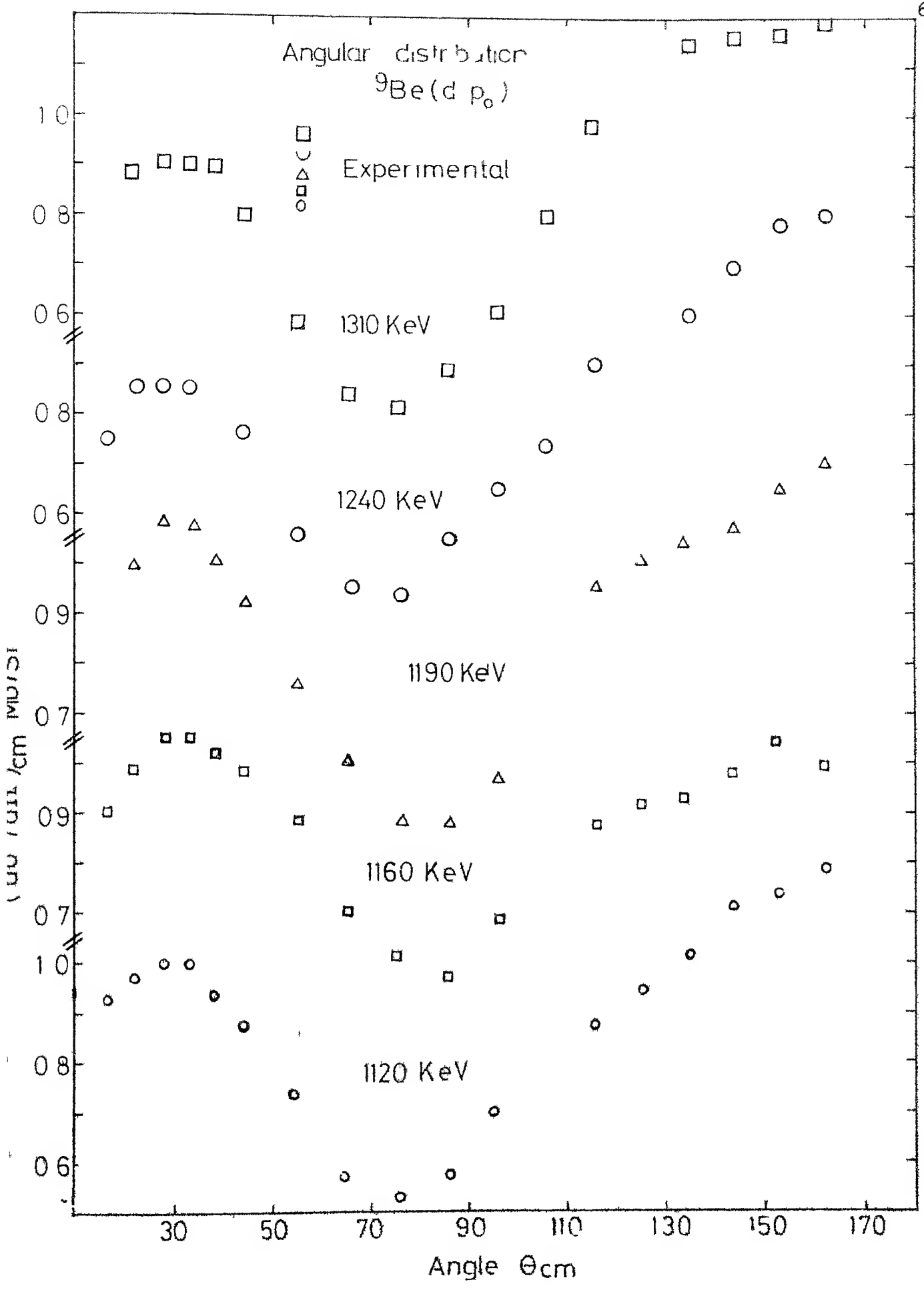
Angular distribution
$^{9}Be(d\ p_0)$
Experimental
1310 KeV
1240 KeV
1190 KeV
1160 KeV
1120 KeV
1.0
0.8
0.6
0.8
0.6
0.9
0.7
0.9
0.7
1.0
0.8
0.6
30
50
70
90
110
130
150
170
Angle Θcm

Fig 18

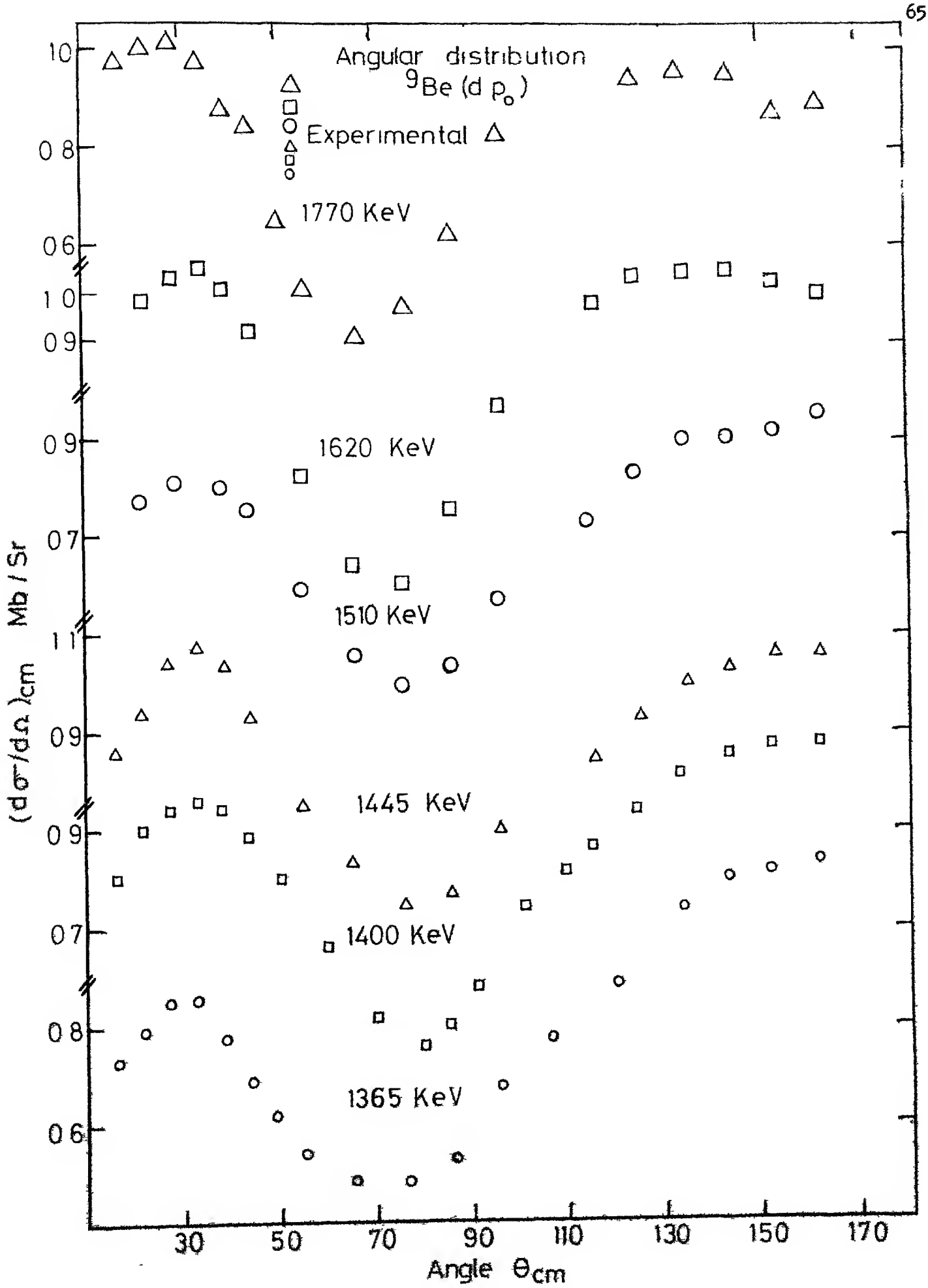
Angular distribution
^{9}Be (d p_o)
Experimental
1770 KeV
1620 KeV
1510 KeV
1445 KeV
1400 KeV
1365 KeV
$(d\sigma/d\Omega)_{cm}$ Mb / Sr
Angle θ_{cm}
10
0 8
0 6
1 0
0 9
0 9
0 7
1 1
0 9
0 9
0 7
0 8
0 6
30
50
70
90
110
130
150
170

Fig 19

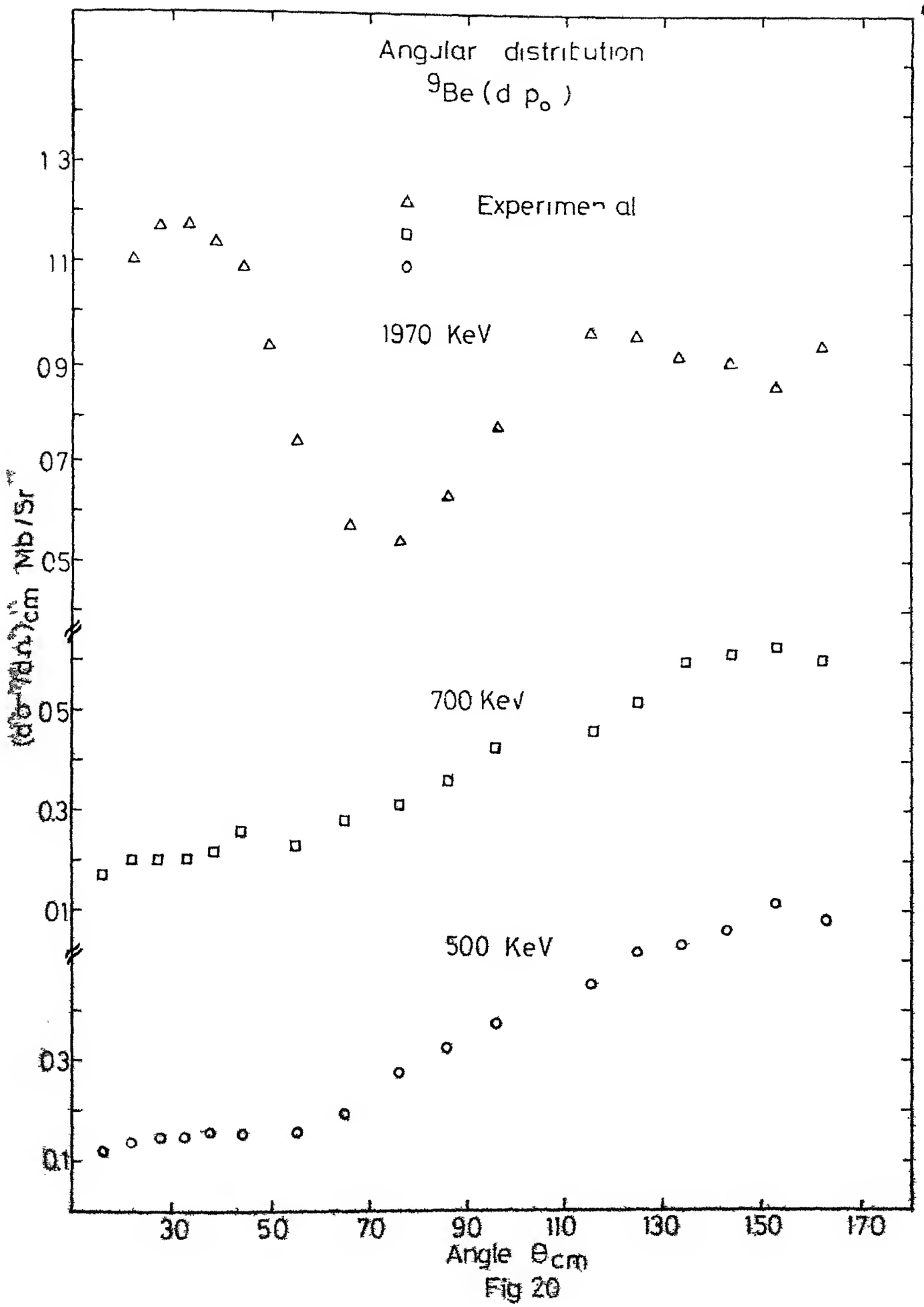
Angular distribution
$^{9}Be(d\ p_o)$
Experimental
1970 KeV
700 KeV
500 KeV
1.3
1.1
0.9
0.7
0.5
0.5
0.3
0.1
0.3
0.1
(dσ/dΩ)cm Mb/Sr
30
50
70
90
110
130
150
170
Angle θ_{cm}

Fig 20

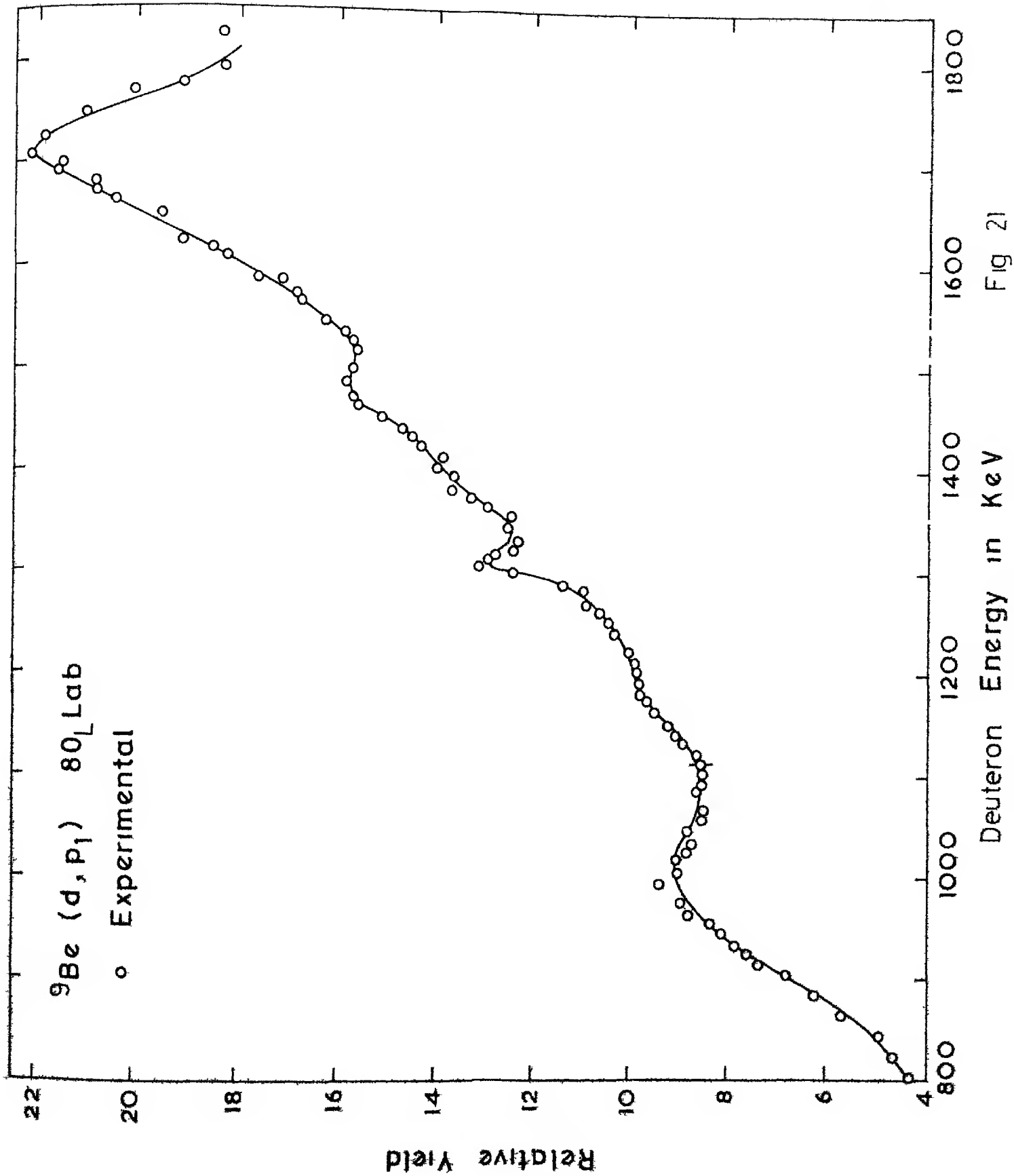
$^{9}Be\ (d, p_1)\ 80_L$ Lab
o Experimental
Relative Yield
Deuteron Energy in KeV
800
1000
1200
1400
1600
1800
4
6
8
10
12
14
16
18
20
22

Fig 21

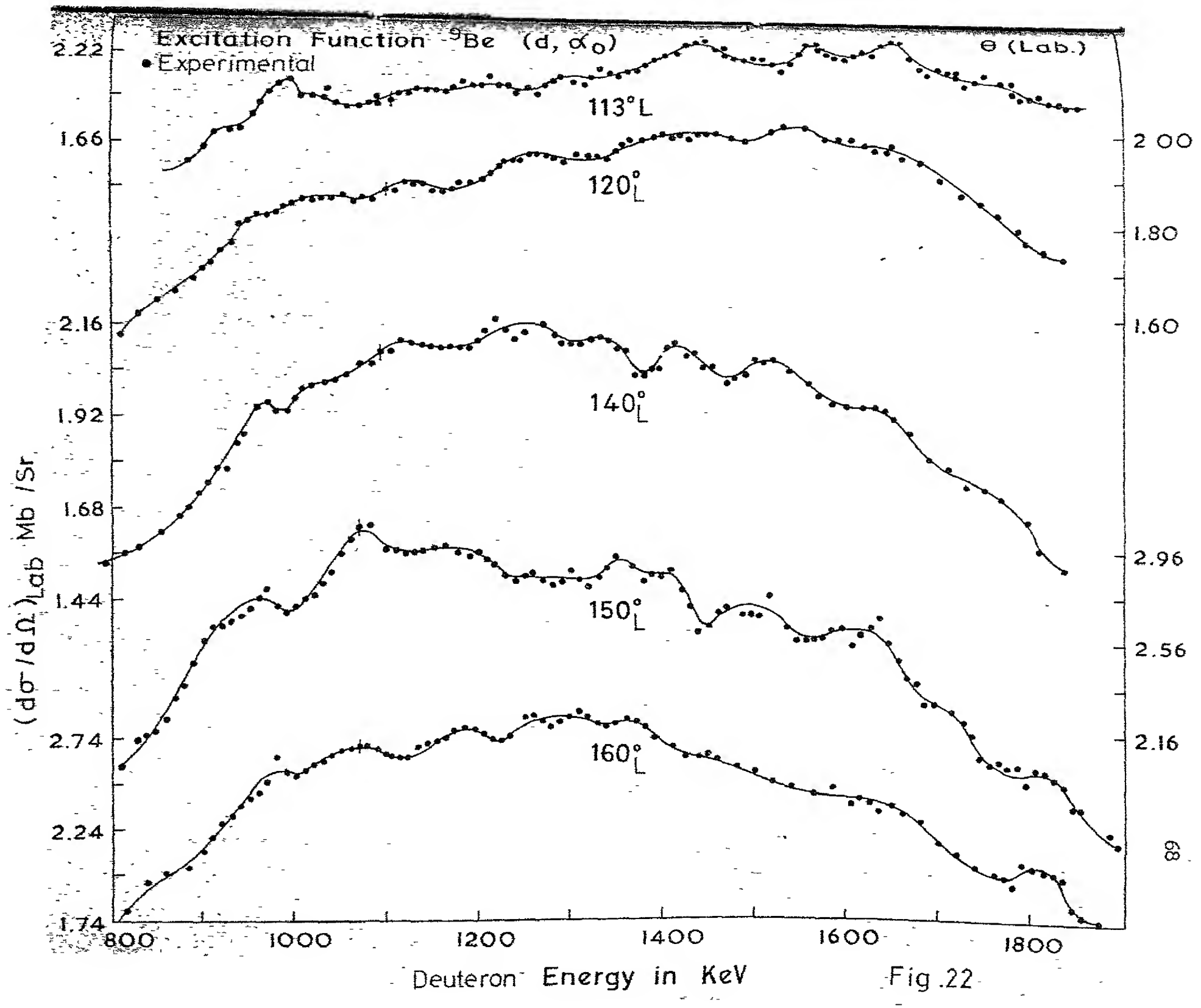
Excitation Function ^{9}Be (d, α_0)
Experimental
θ (Lab.)
113°L
120°L
140°L
150°L
160°L
$(d\sigma/d\Omega)_{Lab}$ Mb /Sr.
2.22
1.66
2.16
1.92
1.68
1.44
2.74
2.24
1.74
2 00
1.80
1.60
2.96
2.56
2.16
68
800
1000
1200
1400
1600
1800
Deuteron Energy in KeV

Fig .22

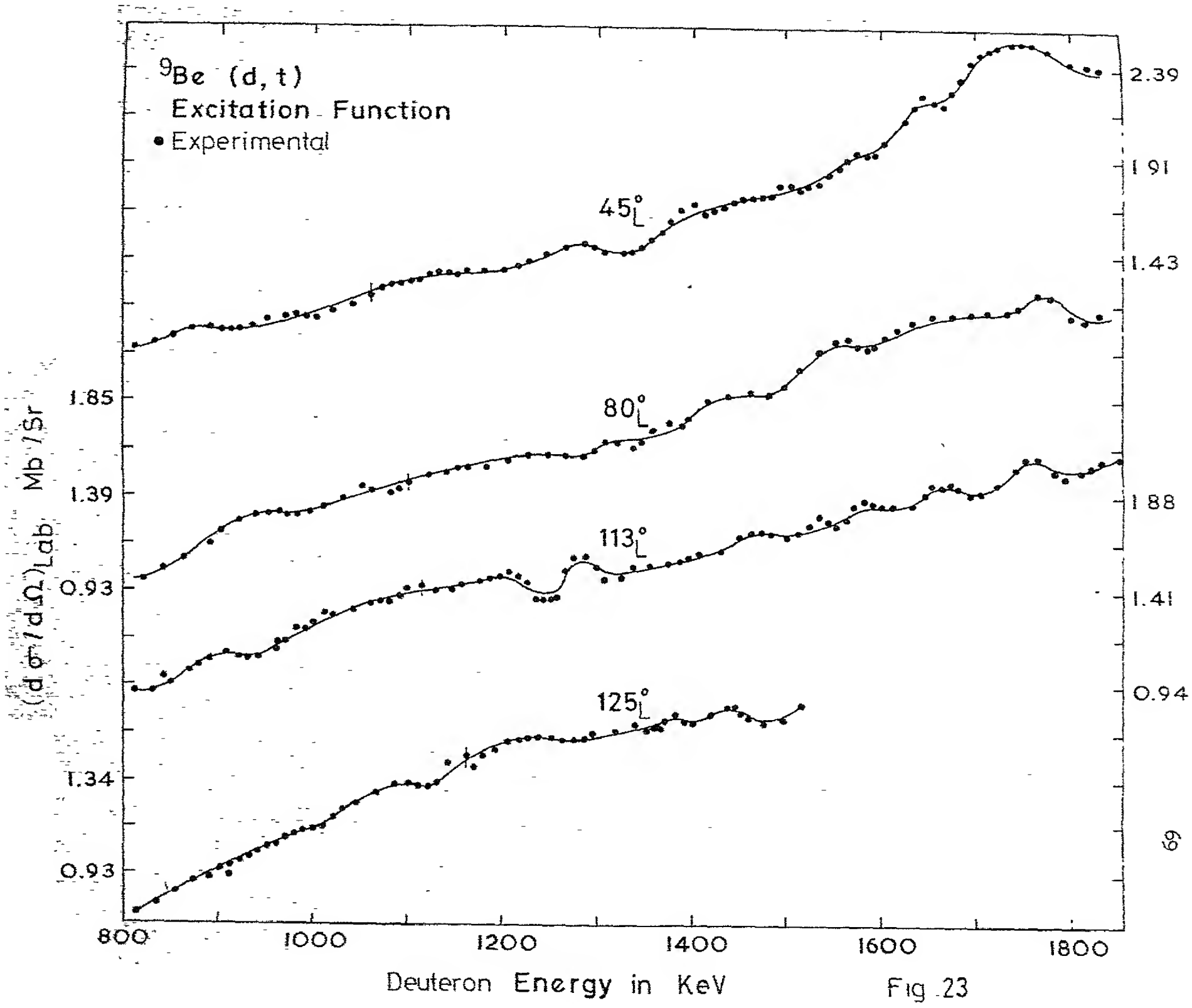
^{9}Be (d, t)
Excitation Function
• Experimental
45°L
80°L
113°L
125°L
2.39
1.91
1.43
1.88
1.41
0.94
69
1.85
1.39
0.93
1.34
0.93
$(d\sigma/d\Omega)_{Lab}$ Mb/Sr
800
1000
1200
1400
1600
1800
Deuteron Energy in KeV

Fig. 23

CHAPTER IV

ANALYSIS OF DATA

The excitation functions of ^{12}C (d,p_o) reaction leading to the ground state of ^{13}C at nine angles is shown in Figures 6 to 9. The excitation function of ^{12}C (d,d) reaction at two backward angles is shown in Figure 10. The striking feature in this data is the appearance of correlated peaks at all angles in (d,p_o) reaction as well as in the (d,d) channel. For example there is a rather well separated peak appearing at about 1450 KeV in all these excitation curves. Interference effects are obviously present and these lead to the difference of details of the excitation curves at different angles. Thus the 1450 KeV resonance is sharpest at 140° in the (d,d) channel and is weak at 80° in the (d,p) channel. Other peaks which are less marked stand out to different extent at different angles. Thus the peaks in the vicinity of 930 KeV, 1310 KeV, 1770 KeV and a broad hump around 1200 KeV can be noticed, which is consistent with the previous data.[17] The data indicates the

presence of a resonant process with a level density which is not too high This is expected for the relatively light compound nucleus ^{14}N at an excitation energy of about 11 5 MeV The data obtained in the past has been analysed by assuming the existence of compound nucleus levels at appropriate excitation energies

The angular distribution of the $^{12}C(d\ p_o)$ reaction in the energy range covered is shown in Figures 11 to 13 The noticeable feature of most of these angular distributions is a maximum at about 35^o and a strong backward peaking The maximum at about 35^o is typical of the direct deuteron stripping reaction while the backwa d peaking is not The angular distributions on and off 1450 KeV resonance are shown in Figure 24 The angular distributions do not change much in their general shape however the backward cross-section is large at the peak energy The dashed curves shown are those predicted on the basis of Plane Wave Butler theory with $l_n = 1$ for the captured neutron The fits obtained for the 35^o maximum are satisfactory However the theory grossly underestimates the relative cross-section at backward angles and at the minimum of the angular distribution The available data at higher energies shows that the backward peaking in the angular distribution decreases until more familiar stripping patterns are observed[16 18] (shown in Figure 25)

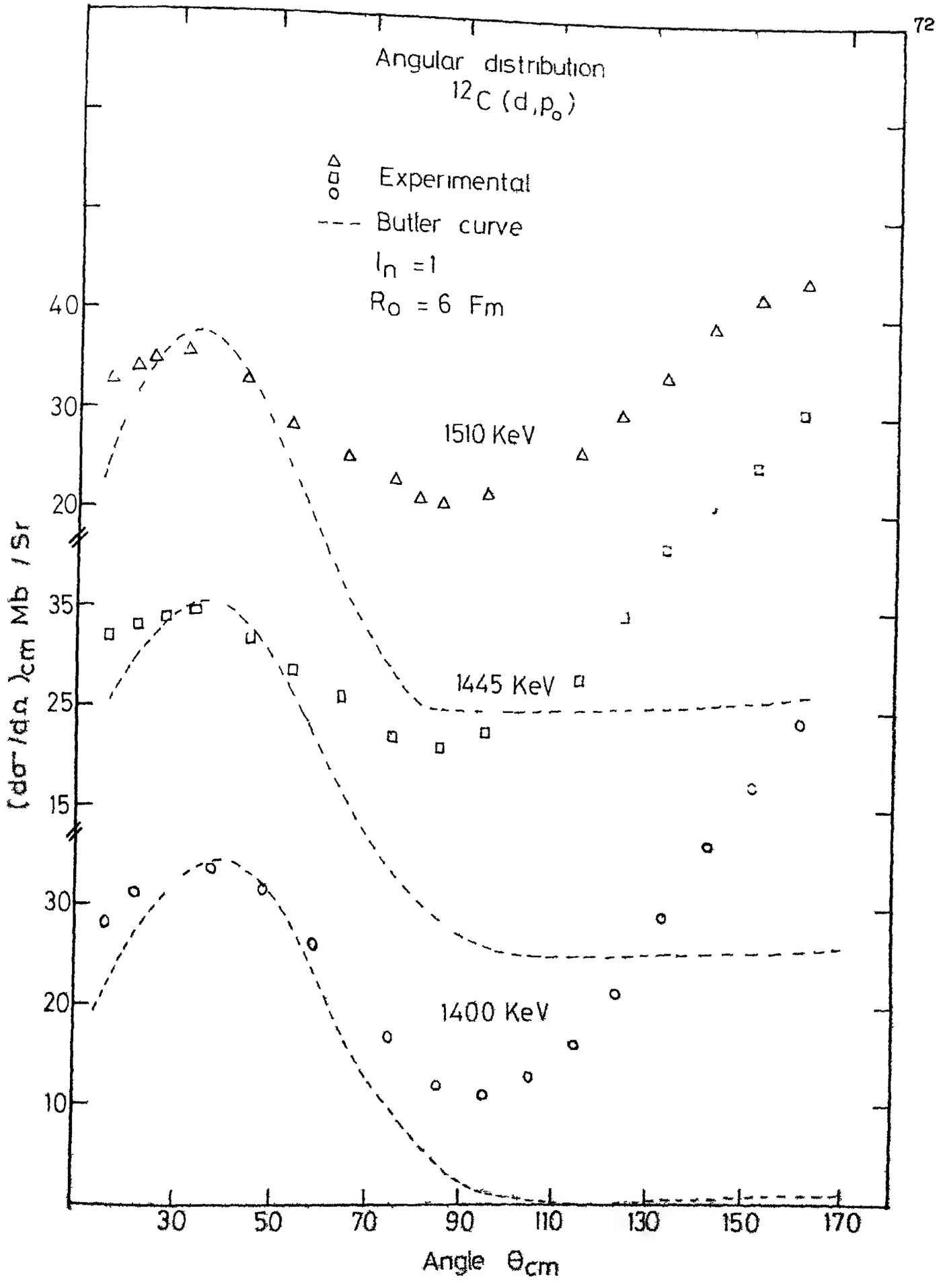
Angular distribution
$^{12}C(d,p_o)$
Experimental
Butler curve
$l_n = 1$
$R_o = 6$ Fm
1510 KeV
1445 KeV
1400 KeV
$(d\sigma/d\Omega)_{cm}$ Mb / Sr
Angle θ_{cm}
40
30
20
35
25
15
30
20
10
30
50
70
90
110
130
150
170

Fig 24

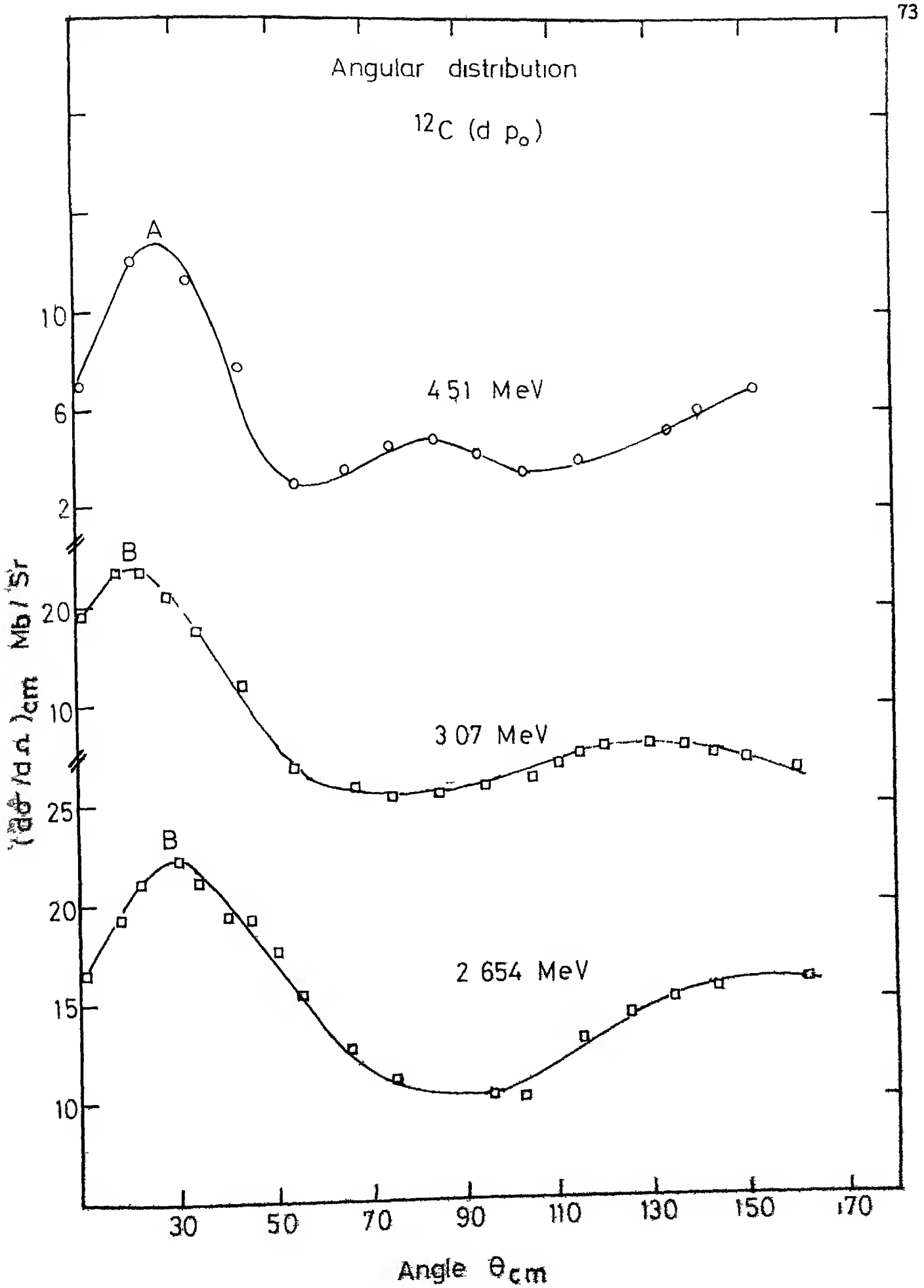
Angular distribution
^{12}C (d p_o)
A
B
B
4.51 MeV
3.07 MeV
2.654 MeV
10
6
2
20
10
25
20
15
10
30
50
70
90
110
130
150
170
Angle θ_{cm}
$(d\sigma/d\Omega)_{cm}$ Mb / Sr

The excitation function of $^{9}Be(d,p_o)$ reaction leading to the ground state of ^{10}Be at nine-angles is shown in Figures 6, 15 and 16 The excitation function of protons from the $^{9}Be(d,p_1)$ reaction leading to the first excited state of ^{10}Be is shown in Figure 21 The excitation functions of $^{9}Be(d\ \alpha_o)$ and $^{9}Be(d\ t)$ leading to the ground state of ^{7}Li and ^{8}Be respectively are shown in Figures 22 and 23 Correlated weak resonances or antiresonances are observed in the excitation curves mentioned above at deuteron energies of 950 KeV, 1080 KeV 1200 KeV, 1300 KeV, 1450 KeV 1620 KeV and 1760 KeV The resonances in all these cases are weak and show that compound nucleus effect is small as compared to those in the case of $^{12}C\ (d,p_o)$ reaction The excitation energy of the compound nucleus $^{9}Be + d = {}^{11}B$ is about 17 MeV which is higher than in the ^{14}N compound state Many channels are open in this case for the decay of the compound nucleus and therefore contribution to any one channel is expected to be small On the other hand stripping process, if present, will contribute predominantly to (d,p) and (d,n) channels Earlier Canavan[19a] has analysed $^{9}Be(d,p_o)$ data in this energy range assuming that compound nucleus process alone is responsible for the reaction mechanism Later groups concluded that the reaction was taking place mainly through direct mechanism and tried to fit data using the stripping theory [20]

The angular distributions of the $^{6}Be(d,p_{o})$ reaction at about 2 MeV is shown in Figures 17 to 20 In the forward angles a maximum at about 35^{o} is observed at most of the energies Also an equally strong backward peaking throughout is observed The peak at 35^{o} is typical of stripping reaction mechanism The angular distribution changes a little as the energy is changed However, the relative forward to backward cross-section increases with the energy A typical angular distribution at 1310 KeV, 1445 KeV, and 1620 KeV is shown in Figure 26 Dashed curves are Plane Wave Butler curves with the neutron captured in the 'p' orbit The fits are good in the forward angle but predictions of relative cross-section remains poor in the backward angles The angular distribution data at higher energies[25,26] (Figure 27) shows considerable decrease in the relative backward cross-section and a pure stripping type of pattern with a small backward cross-section is observed at these energies

In view of these observations it was felt that the possibility of coherent contribution from both the resonant and non-resonant processes should be investigated, although, as was done in the past, it is possible to fit the angular distributions with Legendre polynomials and explain them in terms of contribution from a number of compound nucleus levels excluding apriori the possible non-resonant contribution

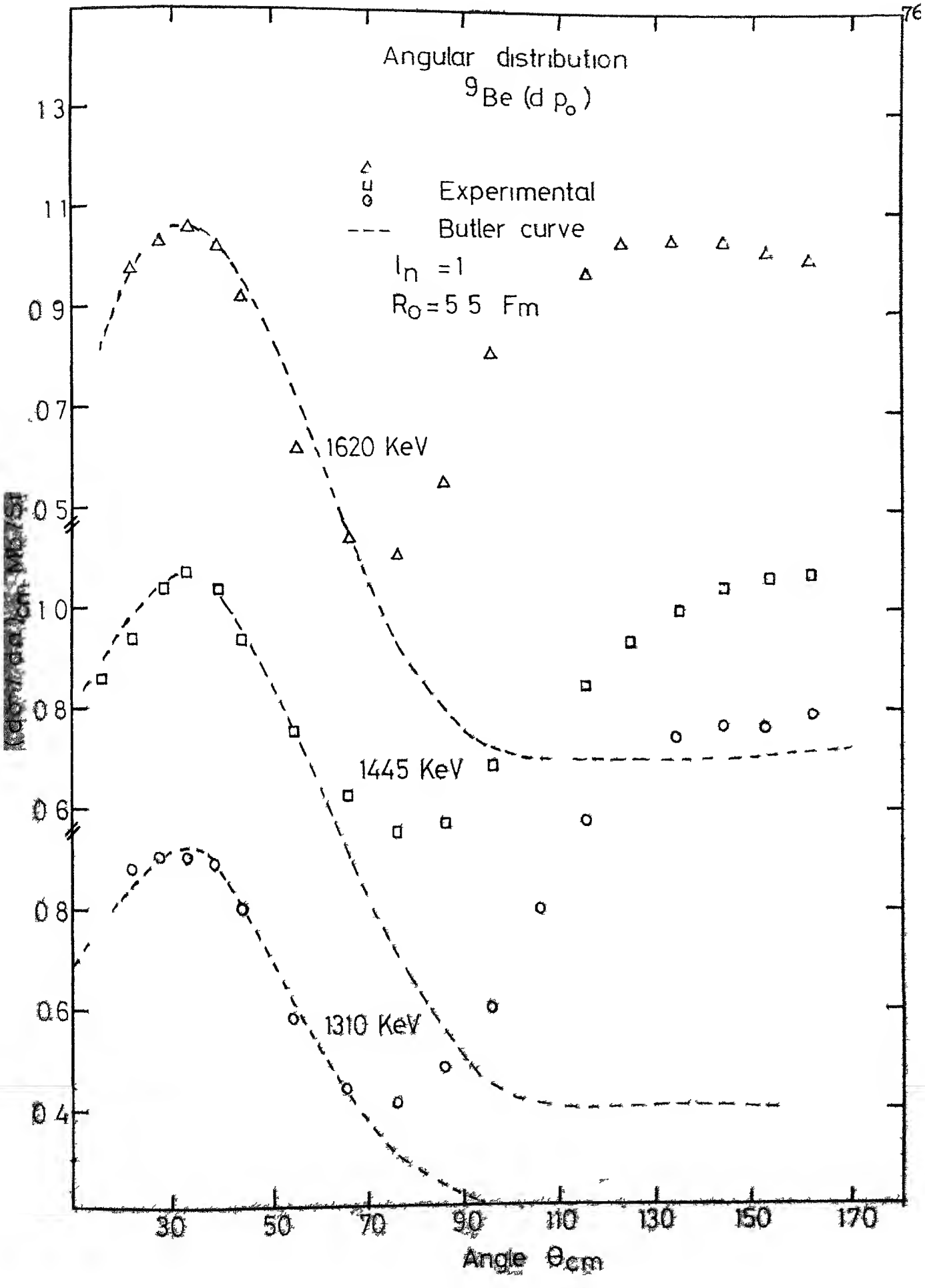
Angular distribution
^{9}Be (d p_o)
Experimental
Butler curve
l_n = 1
R_o = 5 5 Fm
1620 KeV
1445 KeV
1310 KeV
1 3
1 1
0 9
0 7
0 5
1 0
0 8
0 6
0 8
0 6
0 4
30
50
70
90
110
130
150
170
Angle θ_{cm}

Fig 26

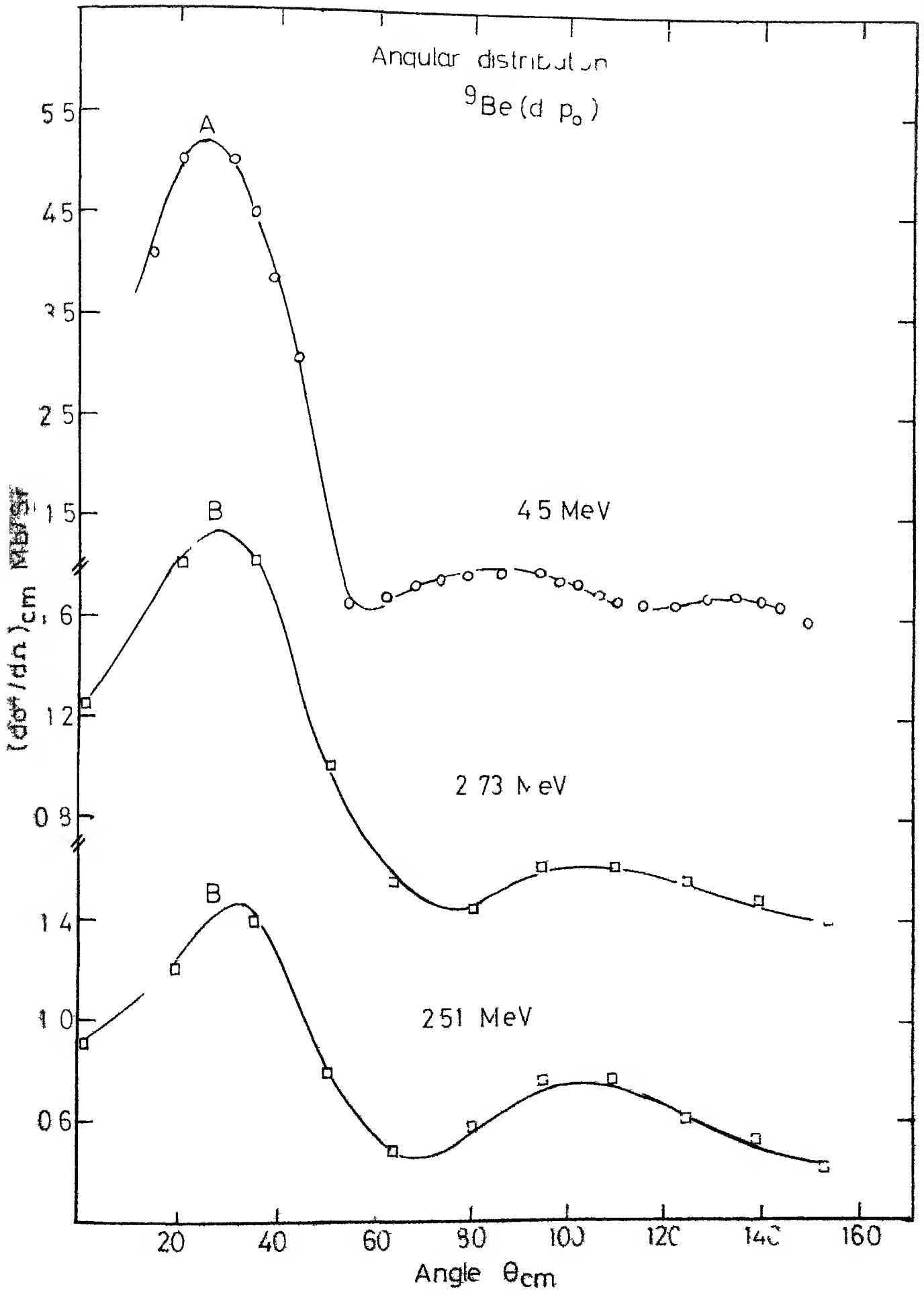
Angular distribution
$^{9}Be(d\ p_0)$
A
B
45 MeV
2 73 MeV
251 MeV
$(d\sigma/d\Omega)_{cm}$ MB/SR
Angle θ_{cm}
55
45
35
25
15
1 6
12
0 8
14
10
0 6
20
40
60
80
100
120
140
160

Fig 27

In this connection the angular distributions obtained were fitted by us in terms of Legendre polynomials. It was found that a satisfactory value of χ^2 in the least square fitting could be obtained by using both even and odd terms upto a maximum order of L, given by $L_{max} = 6$ in the case of $^{12}C\ (d,p_o)$ and $L_{max} = 7$ in the case of $^{9}Be(d,p_o)$ We have

$$L_{max} \leq 2\ l$$

where l is the smaller of the two values l_α and l_β. In the case of ^{12}C we therefore have $l_\alpha \geq 3$ and in the case of ^{9}Be $l_\alpha \geq 4$. To explain the observed distributions on the basis of the compound nucleus theory rather high partial waves in the incident beam have to be invoked. On the other hand it is expected that such high partial waves would lead to stripping mode rather than compound nucleus formation.

Separation of Non-Resonant Amplitude

The separation of compound nucleus part from excitation curve has been earlier suggested by Bonner et al.[16] and Yoshida[27] The separation of non-resonant part from the excitation curves is done on the basis of its smooth energy dependence. The differential cross-section in terms of the amplitudes $q_{sm_s s'm_{s'}}$ is given by the relation

$$\frac{d\sigma}{d\Omega} \Big|_{sm_s s'm_{s'}} = \frac{1}{K_\alpha^2} \left| q_{sm_s s'm_{s'}} \right|^2 \qquad \ldots(4.1)$$

The amplitudes $q_{s\, m_s s'\, m_{s'}}$ is split into a non-resonant (NR) and a resonant (R) part At a given angle θ , we have

$$q(E_\alpha) = q^{NP}(E_\alpha) + q^{R}(E_\alpha) \qquad \ldots(4.2)$$

where the channel quantum numbers have been dropped for the convenience of writing the expressions The resonant amplitude has the following energy dependence

$$q^{R}(E_\alpha) = \sum_n \frac{C_n^{R}\, e^{i\delta_n}}{(E_\alpha - E_n) + i\,\Gamma_n/2} \qquad \ldots(4.3)$$

where the summation is over all the contributing resonances and C_n^{R} is independent of energy E_α The quantity $e^{i\delta_n}$ is the relative phase due to n^{th} resonance.

When only one level of tne compound nucleus is considered and in Eq. (4.3) contribution from single resonance is considered, thc cross-section is given by

$$\frac{d\sigma}{d\Omega}\Big|_{s m_s s' m_{s'}} = \frac{1}{K_\alpha^2}\left| q^{NR} + \frac{e^{i\delta_o}\, C_o^{R}}{(E_\alpha - E_o) + i\Gamma_o/2}\right|^2 \qquad \ldots(4.4)$$

The amplitude q^{NR} is assumed to be constant over the width of the resonance. Equation (4.4) therefore becomes

$$\frac{d\sigma}{d\Omega}\Big|_{s m_s s' m_{s'}} = \frac{1}{K_\alpha^2} \left| q^{NR} \right|^2 \frac{\left| C_o^R \right|^2}{(E_\alpha - E_o)^2 + \Gamma_o^2/4}$$

$$+ \left| q^{NR} C_o^R \right| \frac{2 \cos \delta_o (E_\alpha - E_o) + 2\Gamma_o/2 \sin \delta_o}{(E_\alpha - E_o)^2 + \Gamma_o^2/4} \qquad \ldots(4.5)$$

where factor $\frac{\hbar^2}{m}$ has been absorbed in the amplitudes. To evaluate the cross-section $\frac{d\sigma}{d\Omega}$, the Eq. (4.5) is summed over the final channels and averaged over the initial channels. The relative contribution of each term in Eq (4.5) does not change by this averaging. Carrying out proper summation and re-defining the constants in (4.5) after terms of similar dependence are grouped together, we get,

$$\frac{d\sigma}{d\Omega} = \frac{D}{E_\alpha} + \frac{C_o}{(E_\alpha - E_o)^2 + \Gamma_o^2/4} + \frac{C_1}{E_\alpha ((E_\alpha - E_o)^2 + \Gamma_o^2/4)} \qquad \ldots(4.6)$$

The constants D, C_o, and C_1 are independent of energy E_α. The first term D/E_α gives the value of non-resonant part of the cross-section. The Eq. (4.6) can be re-written as

$$Y = \frac{1}{E} P_1 + P_2 f_2 (E, E_o, \Gamma_o) + P_3 f_3 (E, E_o, \Gamma_o) \qquad \ldots(4.7)$$

The Eq. (4.7) becomes a basis for separation of non-resonant

contribution from total cross-section, when contribution from only one resonance is considered The constants P_1, P_2 and P_3 are treated as parameters in least squaresfitting of this expression (4 7)

If contribution from two levels of the compound nucleus is considered, Eq (4.3) is re-written as,

$$q(E_\alpha) = q^{NR}(E_\alpha) + \frac{C_o^R e^{i\delta_o}}{(E_\alpha - E_o) + i\Gamma_o/2} + \frac{C_1^F e^{i\delta_1}}{(E_\alpha - E_1) + i\Gamma_1/2} \quad \ldots(4.8)$$

The cross-section $\frac{d\sigma}{d\Omega}\Big|_{s\, m_s s'\, m_{s'}}$ is given by

$$\frac{d\sigma}{d\Omega}\Big|_{s\, m_s s'\, m_{s'}} = \frac{1}{K_\alpha^2}\left| q^{NR}(E_\alpha) + \frac{C_1^R e^{i\delta_1}}{(E_\alpha - E_o) + i\Gamma_o/2} + \frac{C_1^R e^{i\delta_1}}{(E_\alpha - E_1) + i\Gamma_1/2}\right|^2$$

$$= \frac{1}{K_\alpha^2}\left[\left|q^{NR}\right|^2 + \frac{|C_o^R|^2}{(E_\alpha - E_o)^2 + \Gamma_o^2/4} + \frac{|C_1^R|^2}{(E_\alpha - E_1)^2 + \Gamma_1^2/4} + q^{NR} C_o^R \times \right.$$

$$\left(\frac{2\cos\delta_o (E_\alpha - E_o) + 2\Gamma_o/2 \sin\delta_o}{(E_\alpha - E_o)^2 + \Gamma_o^2/4}\right) + q^{NR} C_1^R \frac{\{2\cos\delta_1 (E_\alpha - E_1) + 2\Gamma_1/2 \sin\delta_1\}}{(E_\alpha - E_1)^2 + \Gamma_1^2/4}$$

$$\left. + 2C_o^R C_1^R \left[\frac{\{\cos(\delta_o - \delta_1)((E_\alpha - E_o)(E_\alpha - E_1) + \Gamma_1\Gamma_o/4) - \sin(\delta_o - \delta_1)(\Gamma_1/2(E_\alpha - E_o) - \Gamma_o/2(E_\alpha - E_1))\}}{((E_\alpha - E_o)^2 + \Gamma_o^2/4)((E_\alpha - E_1)^2 + \Gamma_1^2/4)}\right]\right] \quad \ldots(4.9)$$

Eq. (4.9) is further simplified by collecting terms of similar energy dependence. After summing over the final channels and averaging over the initial channels, the differential cross-section is given by

$$\frac{d\sigma}{d\Omega} = \frac{D}{E_\alpha} + \frac{C_o}{E_\alpha((E_\alpha-E_o)^2+\Gamma_o^2/4)} + \frac{C_1}{(E_\alpha-E_o)^2+\Gamma_o^2/4} + \frac{C_2}{E_\alpha((E_\alpha-E_1)^2+\Gamma_1^2/4)}$$

$$+ \frac{C_3}{(E_\alpha-E_1)^2+\Gamma_1^2/4} + \frac{C_4}{E_\alpha((E_\alpha-E_o)^2+\Gamma_o^2/4)((E_\alpha-E_1)^2+\Gamma_1^2/4)}$$

$$+ \frac{C_5}{((E_\alpha-E_o)^2+\Gamma_o^2/4)((E_\alpha-E_1)^2+\Gamma_1^2/4)}$$

$$+ \frac{E_\alpha C_6}{((E_\alpha-E_o)^2+\Gamma_o^2/4)((E_\alpha-E_1)^2+\Gamma_1^2/4)} \qquad \ldots(4.10)$$

The constants D, C_o, C_1, C_2, C_3, C_4, C_5, C_6 have been re-defined to include all other constants. The relative phase δ_1, and δ_2 are also treated as constants for a given θ and merged in these constants. The function (4.10) can be rewritten as

$$Y = \frac{D}{E_\alpha} + C_o f_o(E_\alpha, E_o, \Gamma_o) + C_1 f_1(E_\alpha, E_o, \Gamma_o) + C_2 F_2(E_\alpha, E_1, \Gamma_1)$$

$$+ C_3 f_3(E_\alpha, E_1, \Gamma_1) + C_4 f_4(E_\alpha, E_o, E_1, \Gamma_o, \Gamma_1)$$

$$+ C_5 f_5(E_\alpha, E_o, E_1 \Gamma_o, \Gamma_1) + C_6 f_6(E_\alpha, E_o, E_1, \Gamma_o, \Gamma_1)$$

$$\ldots(4.11)$$

Expressions (4.7) and (4.11) could now be used for least squaresfitting to the experimental excitation curves taken at various angles.

While in principle it was possible to fit the excitation curves in the entire energy region studied by considering the contribution of each resonance everywhere, the number of terms in the fitting function and the number of parameters become large. Instead, a few regions of the excitation curve around relatively isolated resonances were studied. In the first step the contributions from the resonance under consideration and the contribution from the non-resonant process were considered The formula (4.7) was therefore used for least squaresfitting in this case. Next the contribution from one neighbouring resonance was added and the least square fitting was done this time with formula (4.11). This was extended to consider the contribution to a single resonance by the non-resonant process and by the two neighbouring resonances The aim at each step was to obtain the value of $\frac{d\sigma}{d\Omega}^{NR}$ given by the first term of the fitting functions at each angle. In the cases studied it was found that the non-resonant cross-section as obtained by using function (4.7) changed when function (4.11) was used instead, but changed little thereafter. Therefore for theextraction of $\frac{d\sigma}{d\Omega}^{NR}$ it was found sufficient to consider the contribution to the main

resonance from the non-resonant process and one neighbouring resonance. The resonant energies and the widths of resonances were varied along with the coefficients in the fitting function, to obtain the best fit. By this method it was found that the excitation function in the neighbourhood of 1450 KeV in the case of $^{12}C(d,p_o)$ could be accounted for by resonance of width 10 KeV located at 1445 KeV, a non-resonant contribution and the contribution from a resonance of width 40 keV located at 1310 KeV. The fits obtained in this region of excitation curve are shown in Figure 28. The non-resonant contribution at 1445 KeV was determined at each angle at which excitation curves were obtained. It was then possible to plot the angular distribution of the non-resonant part alone at 1445 KeV bombarding energy. This extracted non-resonant cross-section was then compared with the DWBA theory of stripping. This procedure was repeated at the 930 KeV resonance whose width was determined as 110 KeV A contribution from neighbour resonance located at 1160 KeV was considered Width of this resonance was determined to be 190 KeV The non-resonant cross-section was also extracted at 1770 KeV with 140 KeV width. The extracted angular distributions due to non-resonant process are shown in Figure 29. The non-resonant contribution accounts for about 20% of the observed cross-section.

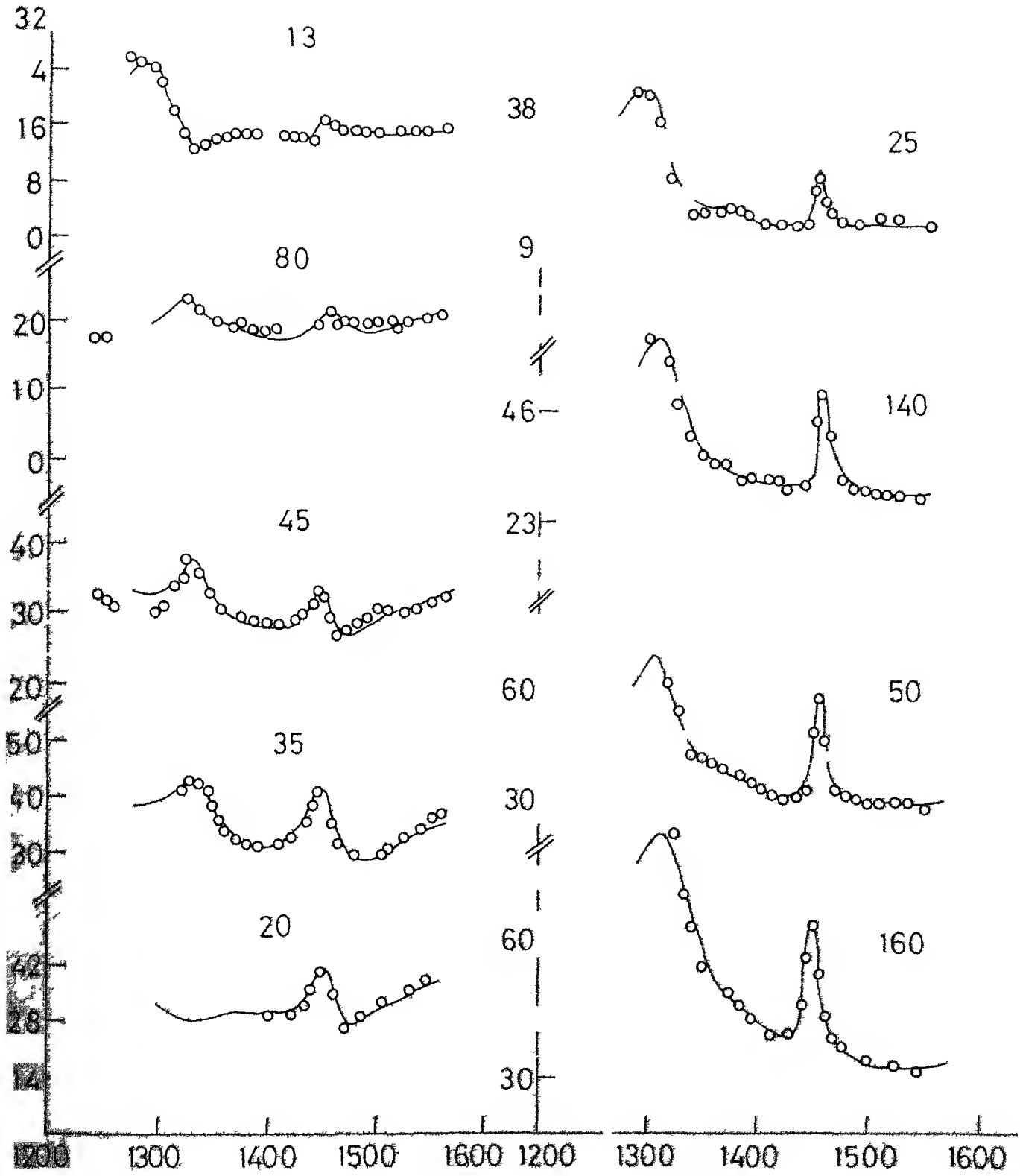
^{2}C d p)
13
80
45
35
20
38
9
46
23
60
30
60
30
25
140
50
160
32
4
16
8
0
20
10
0
40
30
20
50
40
30
42
28
14
200
1300
1400
1500
1600
1200
1300
1400
1500
1600
D t gy
K V

F g 28

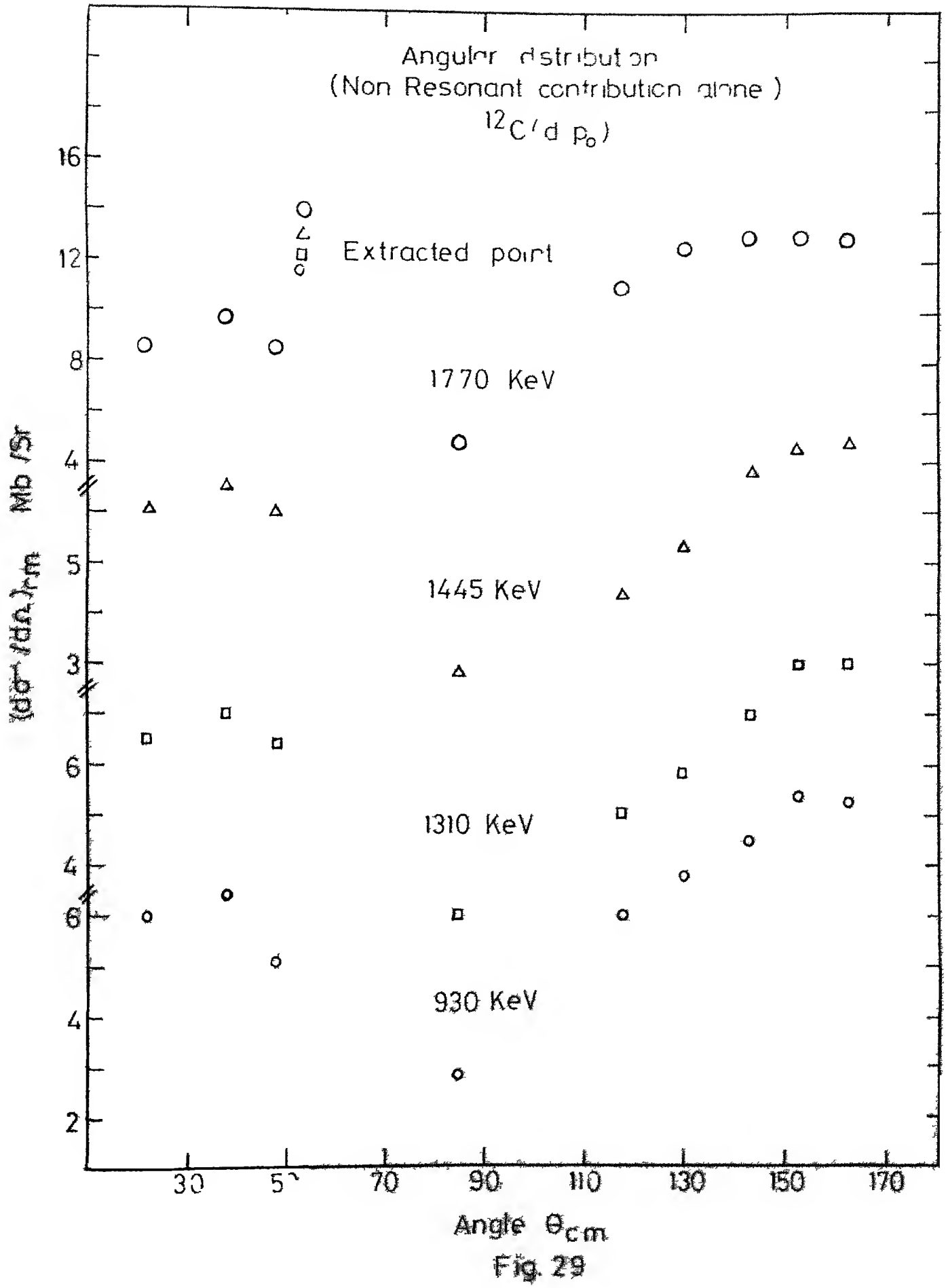
Angular distribution
(Non Resonant contribution alone)
$^{12}C(d,p_0)$
Extracted point
1770 KeV
1445 KeV
1310 KeV
930 KeV
$(d\sigma/d\Omega)_{cm}$ Mb /Sr
Angle θ_{cm}
16
12
8
4
5
3
6
4
6
4
2
30
50
70
90
110
130
150
170

Fig. 29

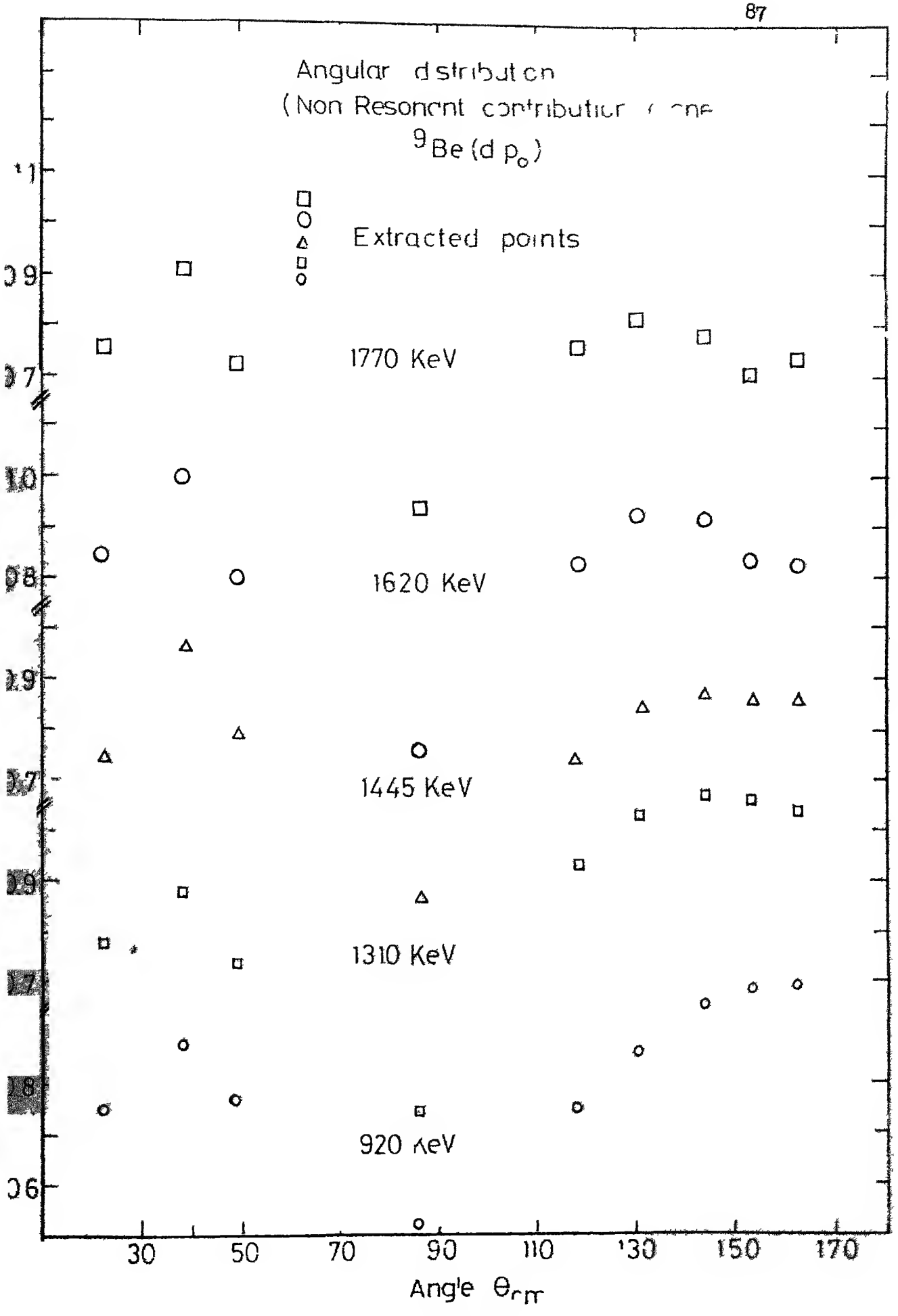
Angular distribution
(Non Resonant contribution) one
$^{9}Be(d\,p_o)$
Extracted points
1770 KeV
1620 KeV
1445 KeV
1310 KeV
920 KeV
30
50
70
90
110
130
150
170
Angle θ_{cm}

Fig 33

In ^{9}Be the non-resonant cross-section contribution was determined at 920 KeV, 1310 KeV, 1450 KeV, 1620 KeV and 1770 KeV, where widths of resonances were identified as 100 KeV, 50 KeV, 80 KeV, 50 KeV and 120 KeV. The angular distributions due to non-resonant contributions are shown in Figure 30. The non-resonant cross-section in this case accounts for about 90% of the observed cross-section

DWBA Calculations

The extracted angular distribution due to the non-resonant process was compared with the direct reaction theory of the stripping process The DWBA calculations were carried out with program DWUCK and the computer BESM-16 at Bhabha Atomic Research Centre, Trombay, Bombay

The distorted wave program DWUCK calculates the differential cross-section as a function of angle θ for a given energy of the incident particle. The quantity σ_{DW}^{lsj} as given by Eq. (2.29b) is calculated for a given value of orbital angular momentum transfer l, spin transfer s and total angular momentum transfer j. The distroted wave χ_L for partial wave L is calculated by solving the following differential equation numerically.

$$\left[\frac{d^2}{dr^2} + k^2 - \frac{L(L+1)}{r^2} + \frac{2\mu_\beta}{\hbar^2}(\bar{V}_\beta)\right] \chi_L(r) = 0 \qquad \ldots(4.12)$$

where

$$\bar{V}_{\beta} = U_N + U_C + U_{SO}$$

and the potential $U_N(r)$ is given by

$$U_N(r) = V_p\, f(X_p) + iW_I \frac{d f(X_I)}{dX_I} \qquad \ldots(4.13)$$

where W_R is real part of the potential and W_I is the imaginary part. The function f(X) is given by

$$f(X) = (1 + e^{X})^{-1}$$

$$X = \left(\frac{r - R_o A^{1/3}}{a}\right)$$

a = Diffuseness parameter

A = Atomic Number of the nucleus.

The potential U_C gives Coulomb interaction due to charged sphere of radius R_c and charge Z_A and is given by

$$U_C = \frac{Z_a Z_A e^2}{r} \qquad r > R_c$$

$$= \frac{Z_a Z_A e^2}{2R_c}\left(3 - \frac{r^2}{R_c^2}\right) \qquad r \leq R_c \qquad \ldots(4.14)$$

The interaction U_{SO} is proportional to spin orbit interaction $\bar{L}.\bar{S}$ and is given by

$$U_{SO} = W_R \frac{VSOR}{45.2} \frac{1}{r} \frac{d f(X_R)}{dr} \bar{L}.\bar{S} \qquad \ldots(4.15)$$

where VSOR comes from the Thomas Spin Orbit term and has a value of 25 for protons and neutrons. The wave function $\chi_L(r)$ satisfies the boundary condition in the asymptotic region where $\bar{V}_\beta \longrightarrow 0$ and also inside the nucleus where $\chi_L(0) \longrightarrow 0$ The $\chi_L(r)$ are computed by numerically integrating the differential equation (4.12) and thus values of $\chi_L(r)$ for a set of discrete values of r is obtained in the entrance and the exit channel with proper choice of potential parameters in the channel concerned. In the case of stripping reaction where a particle is captured in the outer orbit, the form factor is obtained by calculating the bound state wave-function for the captured particle such that it reproduces correct binding energy. Thus for stripping

$$f_{lsj}(r) = R_{Nl}(r)$$

where $R_{Nl}(r)$ is the normalized radial wave-function of the captured particle. After the calculation of form factor $f_{lsj}(r)$, and distorted wave χ_L, integral in Eq. (2.30) is obtained by doing numerical integration. Finally program calculates the quantity σ_{DW}^{lsj} as given by Eq (2.29b) by inserting proper values of Clebsch Gordan Coefficients and spins of the system.

There is more than one choice for the form of potential U(r) in Eq. (4.12) [13a]. The commonly used form is given in

Eq. (4.13). Here real potential is Wood-Saxon type and imaginary potential is derivative of this function.

The calculation of integral in Eq. (2.30) is done using zero-range approximation. The DWUCK program also has facility for taking into account correction due to finite range effect and is calculated in the following way.

The overlap of wave function ϕ_b and ϕ_a is given by

$$\Gamma(X) = \int d\ \tau_o\ \phi_b^*\ V_{ab}\ \phi_a$$

and the fourier transform $G(K^2)$, is defined as

$$G(K^2) = \int e^{i\bar{K}.\bar{X}}\ D(X)\ d\bar{X}$$

The zero range approximation is given by

$$D_o = G(0)$$

and finite range correction parameter FNRNG is evaluated by taking first term in the expansion of $G(K^2)$ about $K^2 = 0$, that is

$$R^2 = \frac{1}{G(K^2)} \left.\frac{\partial G(K^2)}{\partial (K^2)}\right|_{K^2=0}$$

Thus in the reaction where

$$a = b + c \text{ and } B = A + c$$

the finite range correction is computed by the quantity

$$W(r) = \{1 + \frac{2}{\hbar^2} \frac{M_b M_a}{M_a} R^2 (E_b - V_b(r) + E_c - V_c(r) - E_a - V_a(r))\}^{-1} \quad .(4.16)$$

Potential $U_N(r)$ in differential Eq. (4 12) is a local potential. The program DWUCK takes into account correction due to non-locality. The effect of the non-locality is taken into account by multiplying a wave function for an equivalent local potential $U_N(r)$ by the factor[28]

$$f(r) = \frac{1}{(1 - \frac{\beta^2}{4} \frac{2M}{\hbar^2} U_N(r))^{\frac{1}{2}}} \quad . .(4.17)$$

in the channel under consideration. Here β is range of non-locality and is 0.85 for protons, 0.54 for deuteron and 0.2 to 0.3 for ^{3}He.

The effect of finite-range correction and non-locality in general results in reduction of the cross-section, but the over all change in the shape of angular distribution is not expected.

In calculating the DWBA cross-sections with DWUCK, the principal input consists of the optical model parameters in both the incoming and outgoing channels. The values of optical

parameters which provides satisfactory fit at high energy of about 5 MeV[25,29,30] were used as intial values in fitting the extracted curve. These values are given in Table 1.

Table 1

Target	Incident Particle	Real Potential			Imaginary Potential (Derivative type)		
		W_R	r_R	a_R	W_I	r_I	a_I
^{9}Be	D	-160	0.9	0.9	-12	2.1	0.5
$r_c = 1.3$	P	-49	1.25	0.65	-7	1.25	0.47
^{12}C	D	-69	1.60	0.61	-4.0	1.41	0.65
$r_c = 1.3$	P	-51	1.25	0.65	-7.0	1.25	0.47

In the first place, since the deuteron bombarding energy is lower than the Coulomb barrier, it was thought that the nuclear interaction of the optical potential may not be necessary and Coulomb distortions alone would be sufficient for the calculations. In this case it may be noted that according to Eq (2.18) the fully distorted waves, including nuclear distortions, must be used in the final channel β although the wave function Ψ^+ could be tried as the incident wave with the Coulomb distortion alone. This is necessary if $V_\beta - \bar{V}_\beta$ is to be equated to V_{pn}. Preliminary DWBA calculations

with only the Coulomb interaction in the incident channel were carried out. The calculated angular distributions were somewhat similar to the Butler curves with higher cross-sections predicted at backward angles. One such curve for $^{9}Be(d,p_o)$ at 1445 KeV is shown in Figure 31 The fit for the backward angles is poor. A more serious discrepency is however in the absolute cross-section where the predicted value is about 15 times the observed value It was therefore concluded that a nuclear distortion of the incident wave can not be neglected.

In the DWBA calculations for ^{12}C (d,p_o) the optical parameters were varied about their initial values. Further calculations were made with and without spin orbit term with finite range correction and possible correction due to non-local effects were also investigated. The inclusion of spin-orbit term in the optical potential increased the predicted back angle cross-section. The inclusion of corrections due to finite range and non-local effect did not alter the shape of the angular distribution significantly but reduced the overall cross-section (Figure 32). For $^{9}Be(d,p_o)$ reactions only finite range correction was included. Figures 33 to 36 show DWBA fits to $^{12}C(d,p_o)$ with only spin orbit term. Figures 37 to 41 show DWBA fits to $^{9}Be(d,p_o)$ The optical parameters which gave the best fit in the case of ^{12}C and ^{9}Be are given

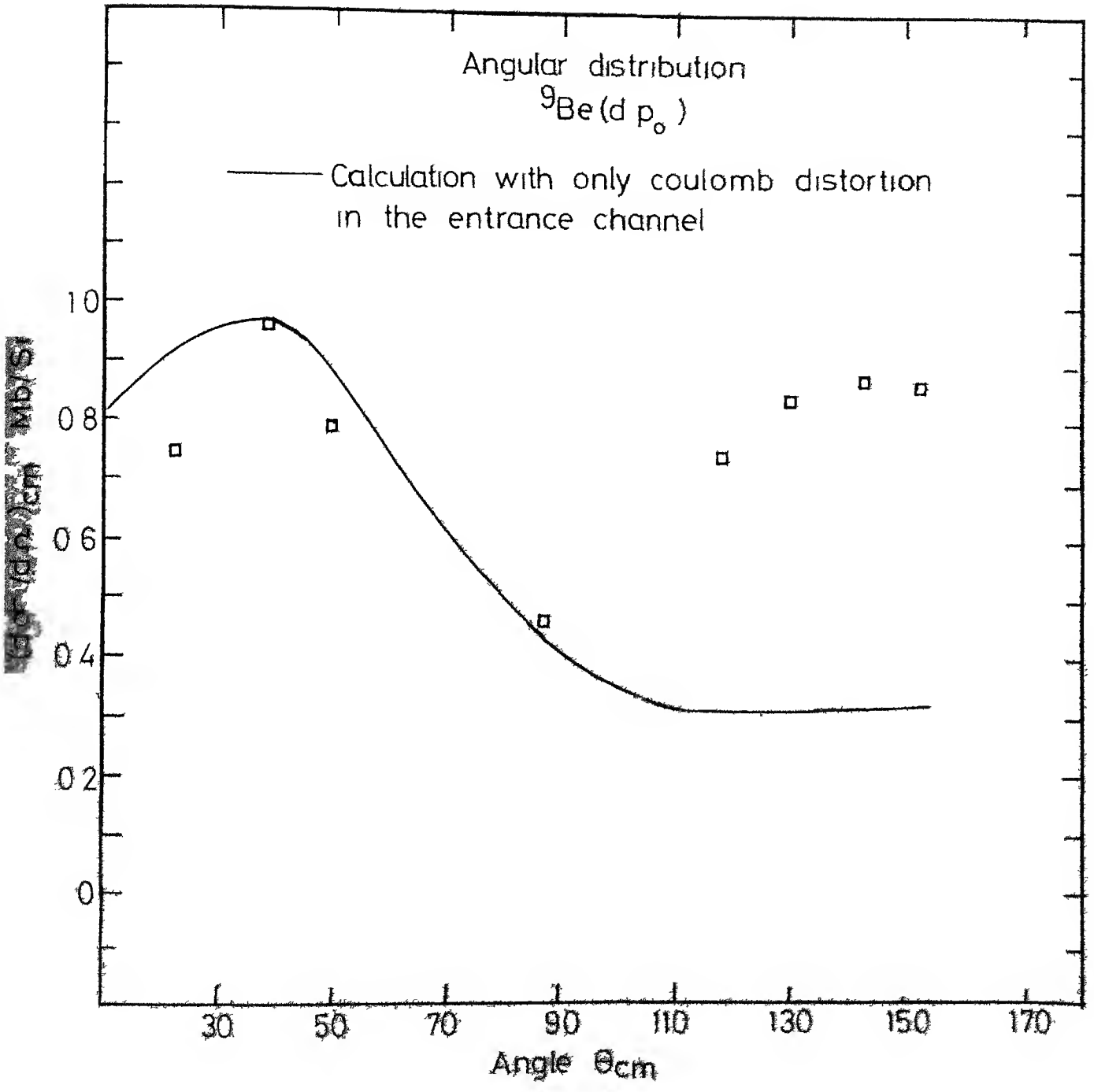
Angular distribution
$^{9}Be(d\ p_o)$
Calculation with only coulomb distortion in the entrance channel
10
0 8
0 6
0 4
0 2
0
30
50
70
90
110
130
150
170
Angle θ_{cm}

Fig 31

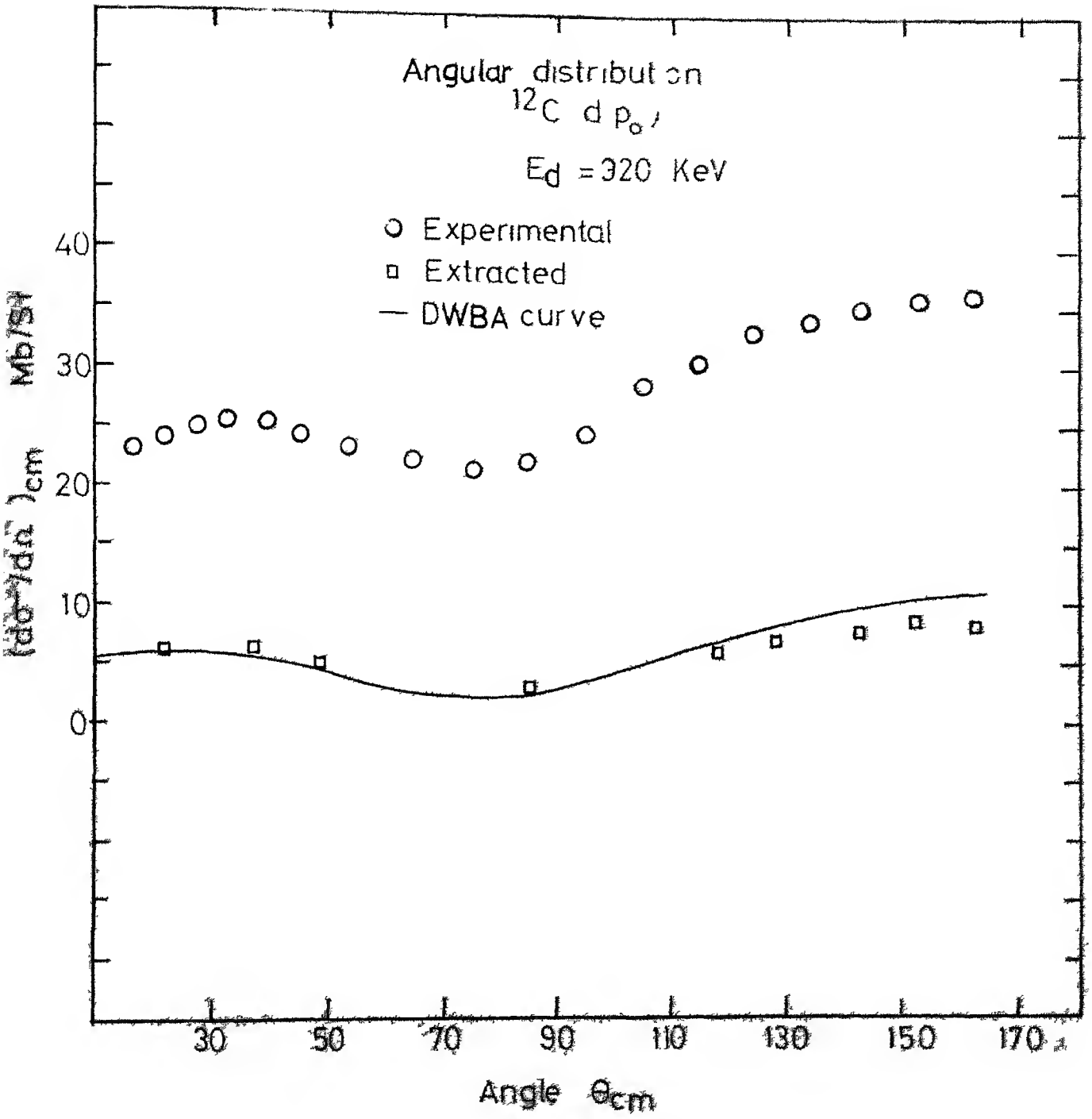
Angular distribution
^{12}C d p_0
E_d = 920 KeV
Experimental
Extracted
DWBA curve
40
30
20
10
0
30
50
70
90
110
130
150
170
Angle θ_{cm}

Fig 3.3

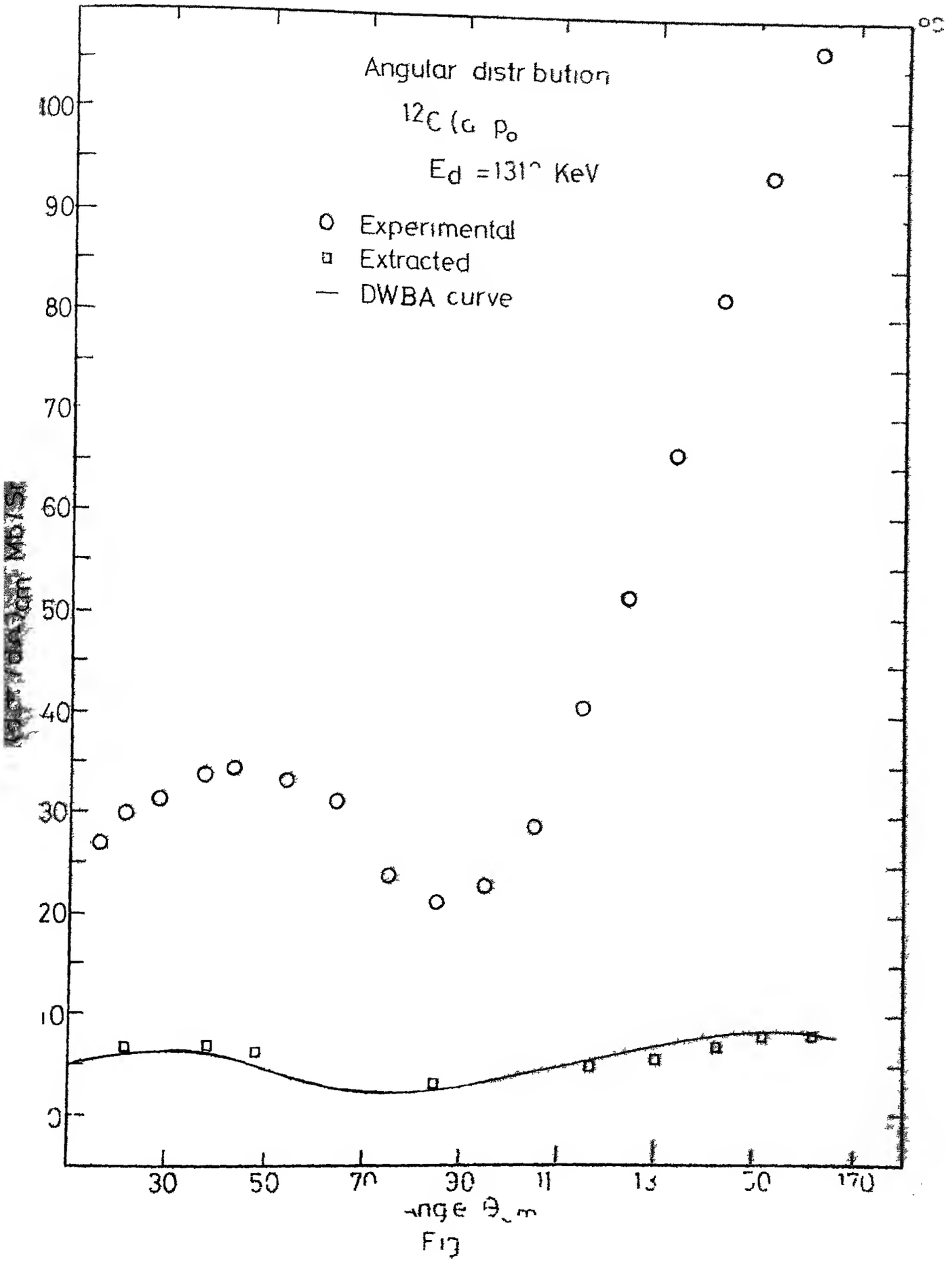
Angular distribution
^{12}C (α p_0
E_d = 131^ KeV
Experimental
Extracted
DWBA curve
100
90
80
70
60
50
40
30
20
10
0
30
50
70
90
11
13
50
170
mb/sr

Fig

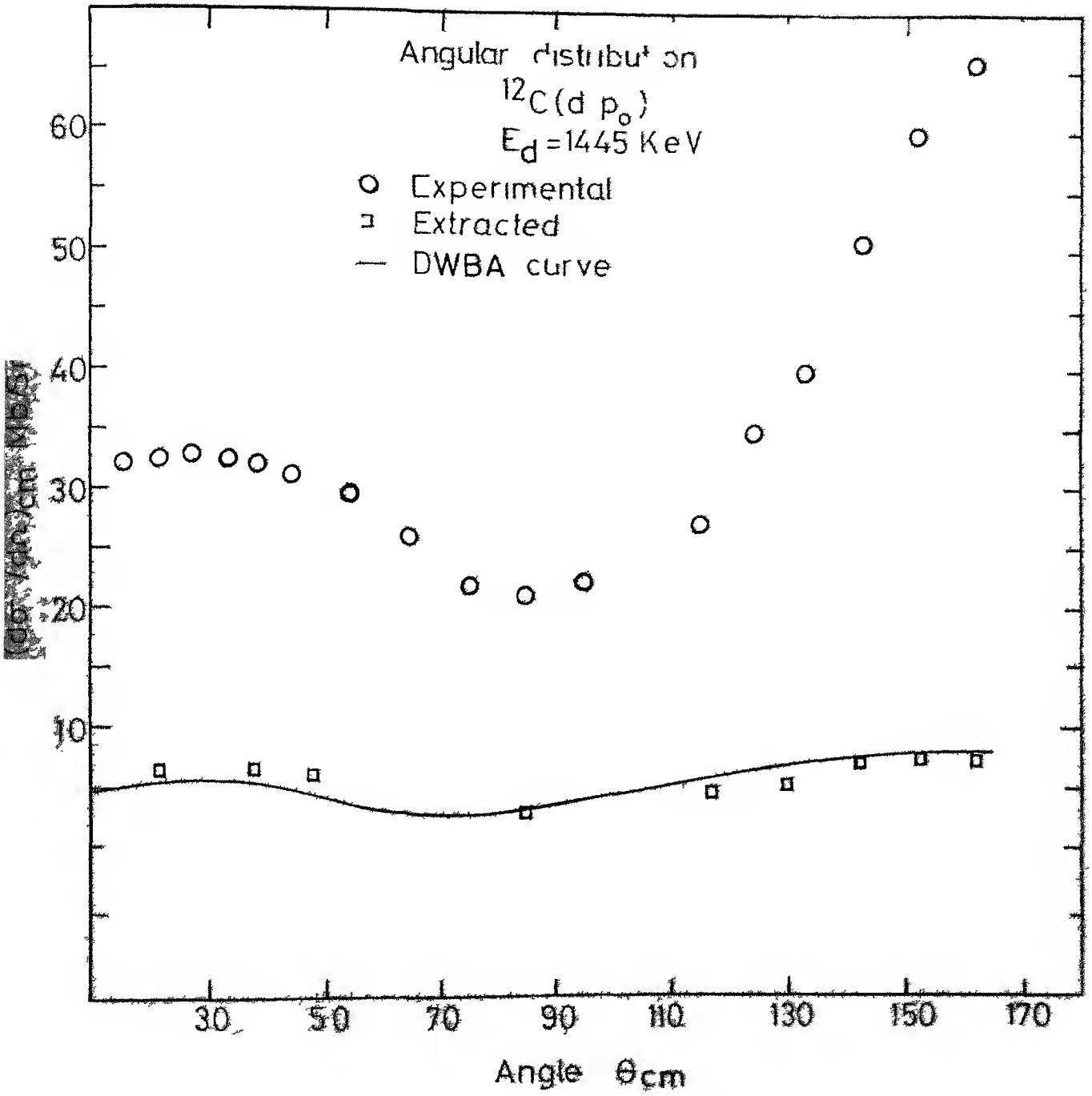
Angular distribution
$^{12}C(d\ p_o)$
E_d = 1445 KeV
Experimental
Extracted
DWBA curve
60
50
40
30
20
10
30
50
70
90
110
130
150
170
Angle θ_{cm}

Fig 35

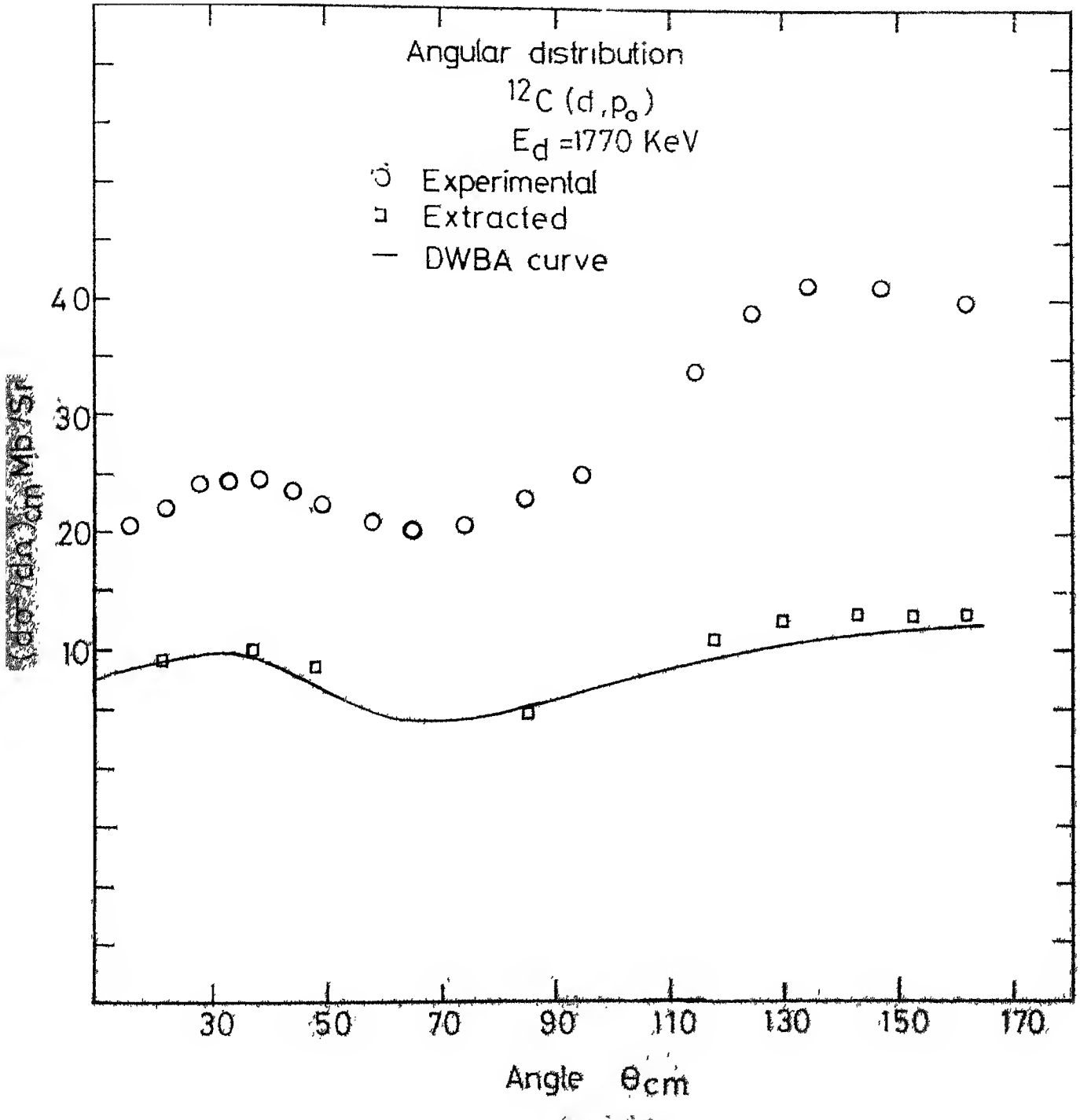
Angular distribution
12C (d, p0)
Ed =1770 KeV
Experimental
Extracted
DWBA curve
40
30
20
10
30
50
70
90
110
130
150
170
Angle θcm

Fig.36

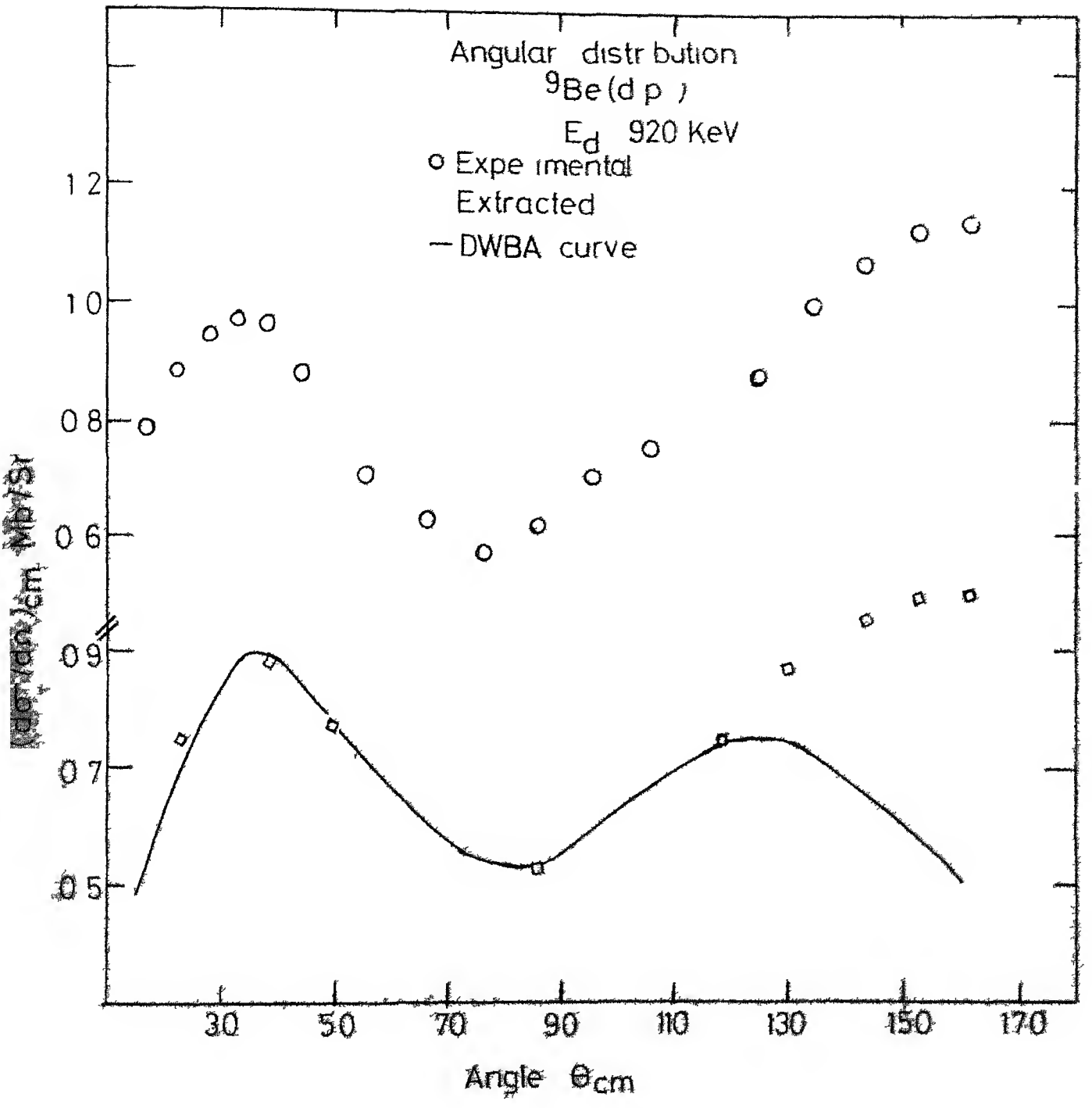
Angular distribution
$^{9}Be(d,p)$
E_d 920 KeV
o Experimental
Extracted
— DWBA curve
1 2
1 0
0 8
0 6
0 9
0 7
0 5
dσ/dΩ)cm Mb/Sr
30
50
70
90
110
130
150
170
Angle θ_{cm}

Fig 37

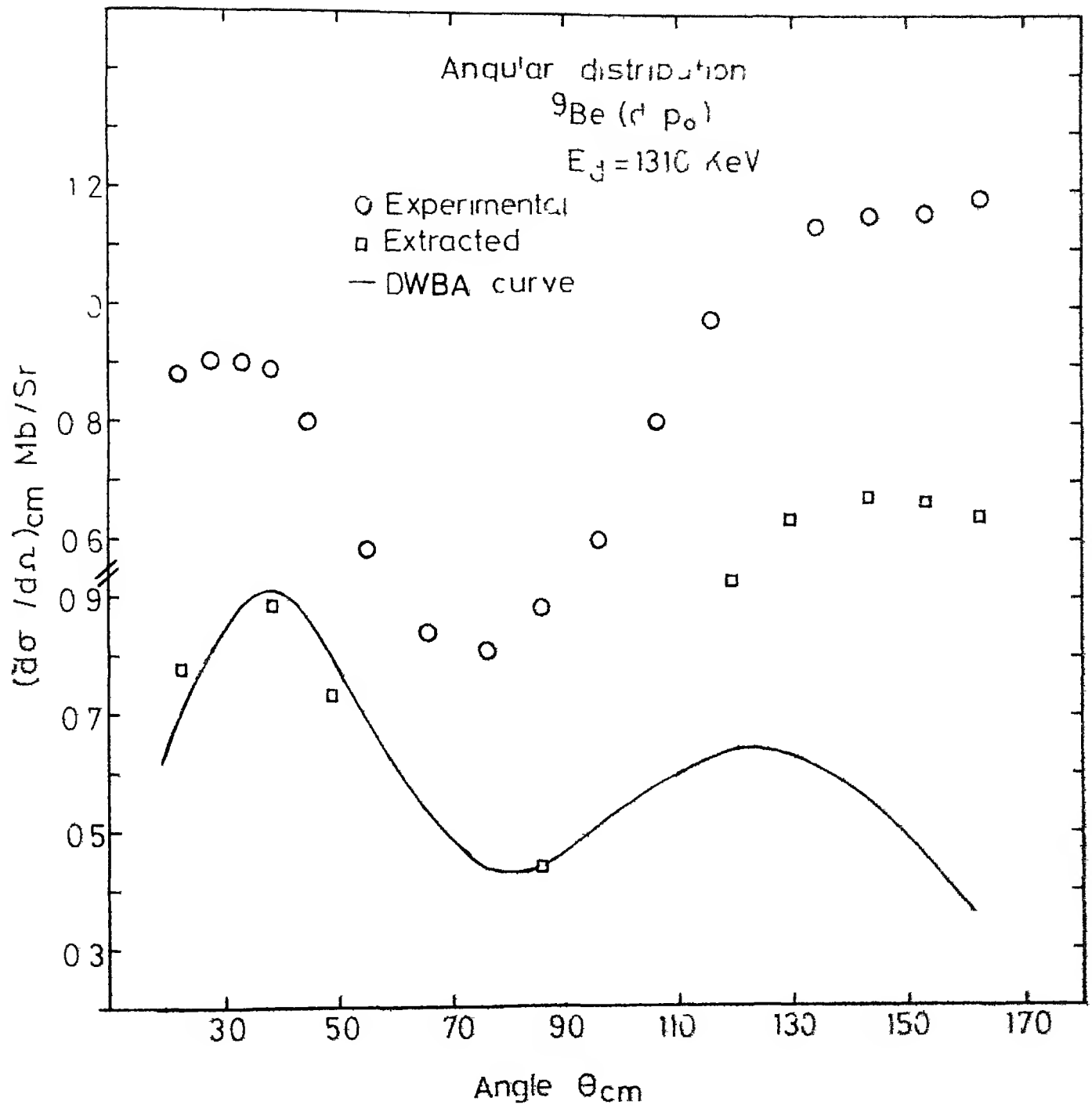
Angular distribution
^{9}Be (d p$_0$)
E$_d$ = 1310 KeV
O Experimental
□ Extracted
— DWBA curve
(dσ /dΩ)cm Mb/Sr
1 2
1 0
0 8
0 6
0 9
0 7
0 5
0 3
30
50
70
90
110
130
150
170
Angle θcm

Fig 38

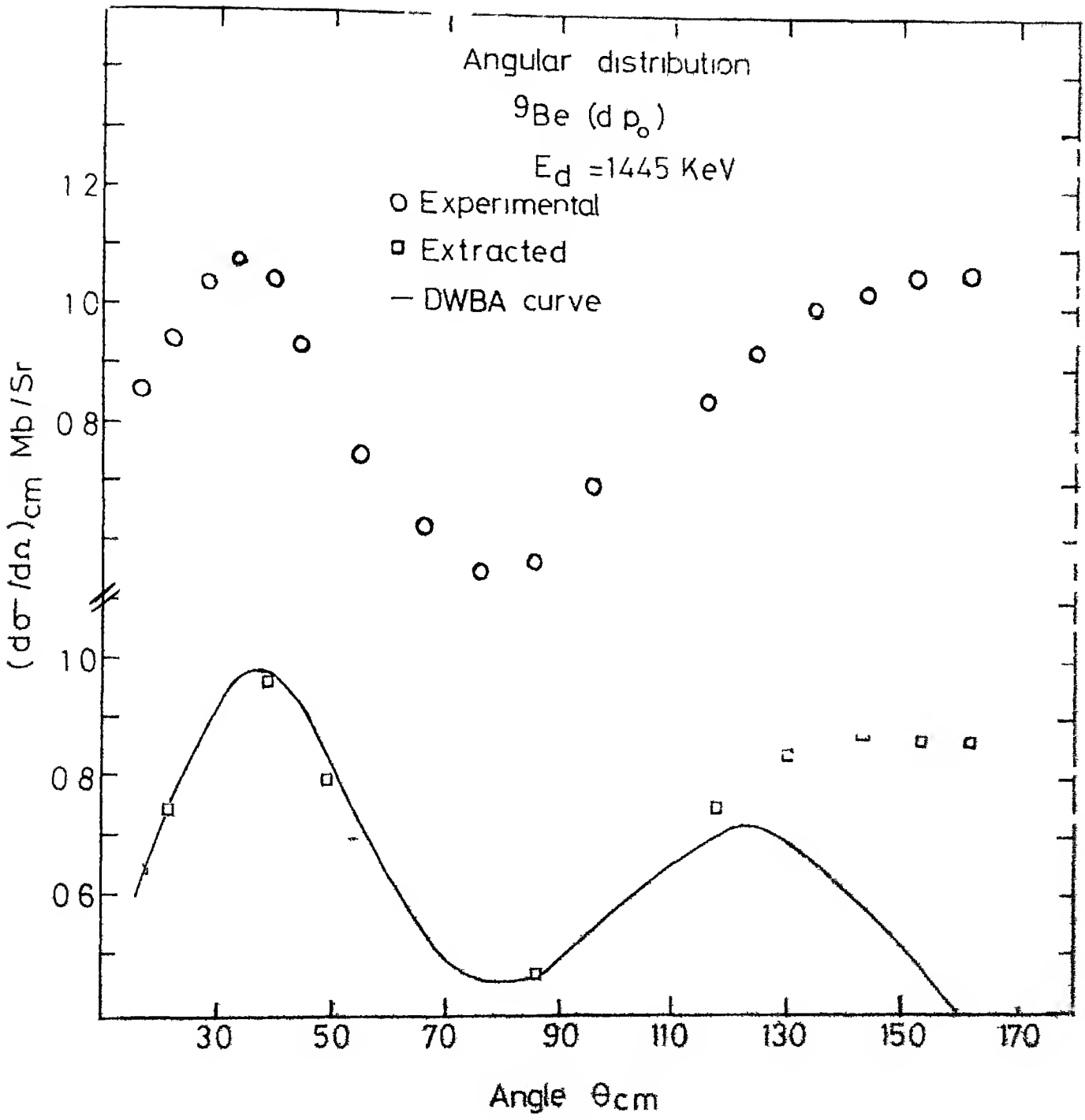
Angular distribution
^{9}Be (d p_o)
E_d =1445 KeV
o Experimental
□ Extracted
— DWBA curve
$(d\sigma/d\Omega)_{cm}$ Mb/Sr
12
10
08
10
08
06
30
50
70
90
110
130
150
170
Angle θ_{cm}

Fig 39

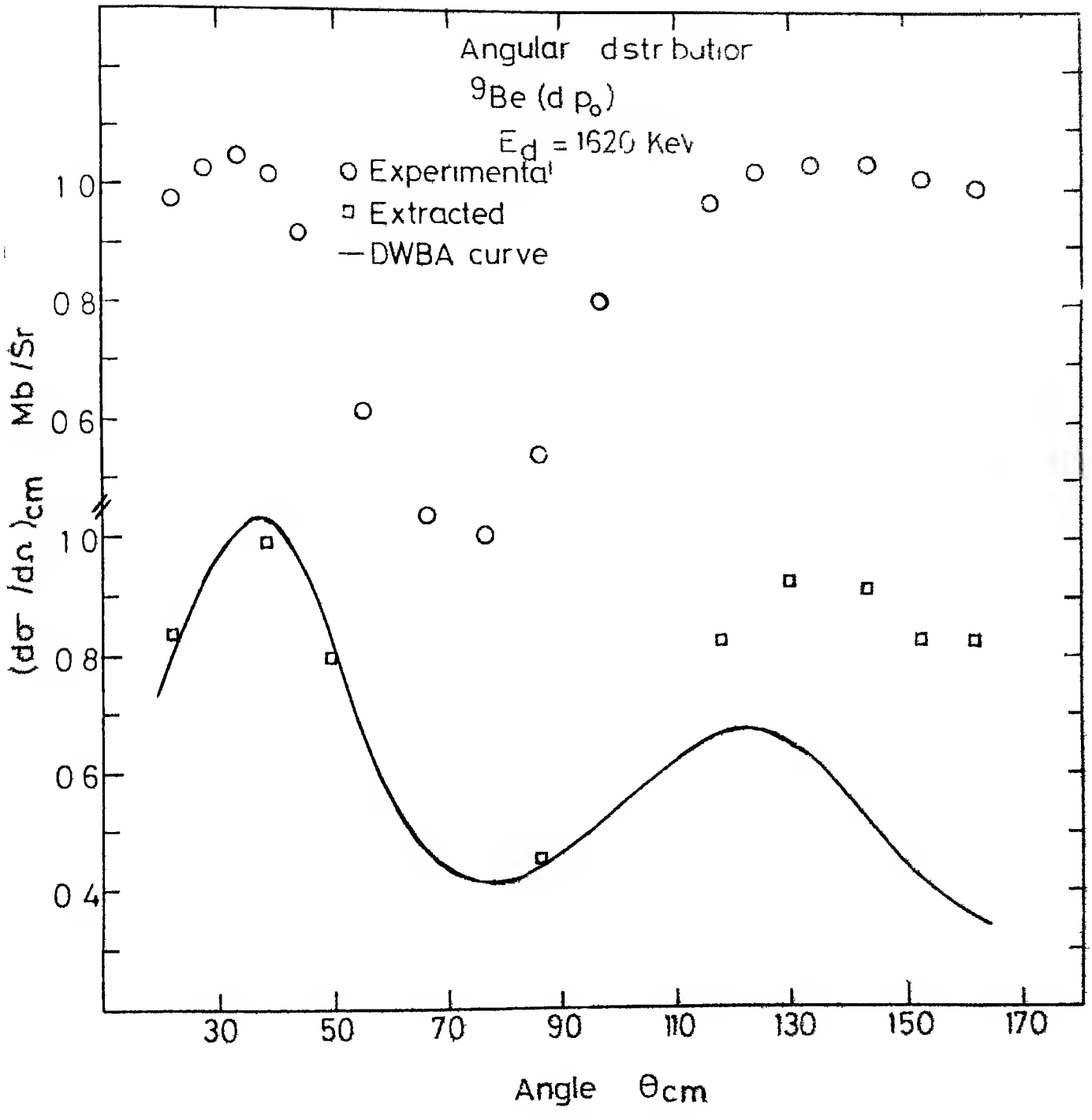
Angular distribution
^{9}Be (d p_0)
E_d = 1620 Kev
Experimental
Extracted
DWBA curve
$(d\sigma/d\Omega)_{cm}$ Mb/Sr
1 0
0 8
0 6
1 0
0 8
0 6
0 4
30
50
70
90
110
130
150
170
Angle θ_{cm}

Fig 40

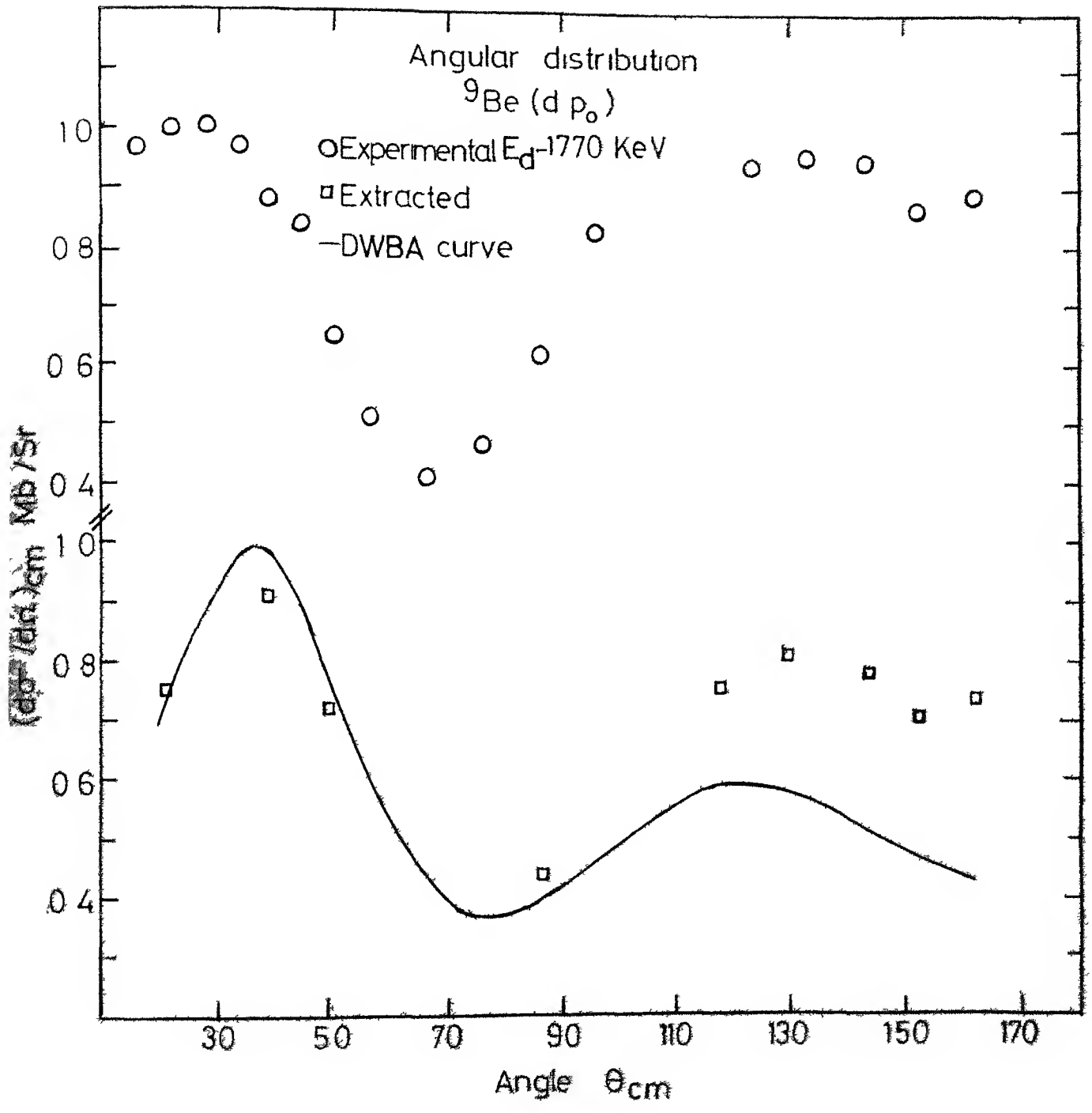
Angular distribution
^{9}Be (d p_o)
OExperimental E_d-1770 KeV
Extracted
—DWBA curve
10
0 8
0 6
0 4
1 0
0 8
0 6
0 4
Mb /Sr
30
50
70
90
110
130
150
170
Angle θ_{cm}

Fig 4)

in Table 2.

Table 2

Target	Incident Particle	Real Potential			Imaginary Potential (Derivative type)		
		W_R	r_R	a_R	W_I	r_I	a_I
^{9}Be	D	-160	0.9	0.9	-12	2 1	0.47
r_c= 1.3	P	-49.5	1.25	0.65	-7.0	1.25	0.65
^{12}C	D	-69	1.6	0.61	-4.0	1.41	0.65
r_c= 1.3	P	-52.4	1.45	0.65	-5.4	1.22	0.65

It may be noted that the optical parameters given in Table 2 are close to those given in Table 1 for higher energy data.

Expression (2.31) for the direct cross-section for (d,p_o) reaction involves the spectroscopic factor s^{lsj}. A comparison of the DWBA calculation with the experimental results provides a value of spectroscopic factor s^{lsj} which is to be compared with that obtained from nuclear structure calculations.[31] The values obtained from the DWBA analysis of the data and those obtained from nuclear structure calculations are shown in Table 3.

Table 3

Energy (KeV)	Experimental					Calcd.
	920	1310	1445	1620	1770	
$^{9}Be(d,p_o)$	2.2	1.9	2.0	1.9	1.7	2.36
$^{12}C(d,p_o)$	3.0	1.2	1.1		1.2	0 613

It may be noted that the DWBA analysis of the unextracted experimental curve would have led to a spectroscopic factor which would be larger than the theoretically expected values by a factor of about 8 for the case of $^{12}C(d,p_o)$.

We may summarise the results of the analysis as follows The excitation functions in $^{12}C(d,p_o)$ reaction show resonances which appear at various angles and also in the (d,d) channel. The angular distributions indicate the possible existence of a non-resonant process also. It is possible to extract the non-resonant cross-section from the observed excitation curve on the basis of known energy variations of the resonant amplitude (Breit-Wigner formula) and the slow energy variation of the non-resonant amplitude. The non-resonant contribution is about 20%. The extracted angular distributions have been compared with the DWBA calculations made with optical parameters close to those used at higher energies. The agreement

in the shape and absolute value is satisfactory. The results on $^{9}Be(d,p_{o})$ are similar The resonances are, however, weaker and the direct cortribution is found to be about 90%. This is understandable since due to higher excitation of the compound nucleus ^{11}B, more channels are open and a corresponding smaller percentage of the compound nucleus contribution is in the proton channel Although the fit in the backward direction in the case of ^{9}Be is not satisfactory, the forward cross-section in the angular dependence and magnitude is well reproduced.

CHAPTER V

CONCLUSION

The aim of this work was to understand the reaction mechanism of (d,p) reactions on light targets at sub-Coulomb bombarding energies in the range of 0.8-2 0 MeV. The targets used were ^{9}Be and ^{12}C The features of the stripping mechanism such as the small angle peak for l=l capture, which are easily identified at about 4 MeV bombarding energies, were still present though not as distinct as in the high energy data, indicating the possible presence of the stripping mode at low energies The excitation functions however, showed resonances typical of compound-nucleus-formation mode.Assuming a coherent resonant and non-resonant contribution it was possible to separate the non-resonant cross-section and compare it with that predicted on the basis of DWBA calculations of the stripping mode. From the analysis the following conclusions could be drawn

(1) The approach of accounting for the asymptotic behaviour of the unbound wave-functions, which are coupled to the bound wave functions, in terms of coherent contributions obtained from direct reaction model and compound-nucleus model (based on physical considerations) leads to satisfactory agreement with the data in the reactions studied.

(2) The contribution of direct reactions to the cross-section in ^{12}C (d,p_o) reaction is about 20% and in ^{9}Be (d,p_o) it is about 90% in the energy range studied.

(3) Even at sub-Coulomb bombarding energies used, it was found that the distortion of the incident wave is important and the Coulomb distortion alone does not lead to satisfactory results.

(4) At higher bombarding energies of about 4 MeV the stripping mode predominates and the optical model parameters for the DWBA calculations have been well determined. Essentially the same parameters can be used to fit the angular distributions at the energies studied provided that the resonant part is extracted out.

The effect of finite-range correction and non-local correction in the ^{12}C (d,p_o) reaction is to reduce the cross-section in magnitude by about 10% without much change in the shape of the angular distribution.

(6) Resonances were located in the compound nucleus ^{14}N at excitation energies consistent with earlier results.[17a] The widths of the resonances which we obtained are however somewhat on the lower side in most cases. This difference is to be expected since we have included non-resonant contribution in the analysis. The spin and parity assignment made previously by neglecting the non-resonant contribution needs re-examination.

BIBLIOGRAPHY

1. N. Bohr, Nature, 137, 344 (1936)

2. (a) J M Blatt and L.C. Biedenharn, Rev. Mod. Phys., 24, 258 (1952).

   (b) W. Hauser and H. Feschbach, Phys. Rev., 87, 366 (1952).

   (c) P.M. Endt and M. Demeur, Nuclear Reactions, Vol 1, Amsterdam (North-Holland Publishing Co. 1959).

   (d) A.M Lane and R.G. Thomas, Phys. Rev. 48, 500 (1935)

   (e) G. Breit and E.P Wigner, Phys. Rev , 49, 519 (1936).

3. J.R. Oppenheimer and M. Philips, Phys. Rev , 48, 500 (1935).

4. R. Serber, Phys. Rev., 72, 1008 (1947)

5. (a) S.T. Butler, Phys. Rev., 80, 1095 (1950).

   (b) S.T. Butler, Nature, 166, 709 (1950).

6 H Margenau and G.M Murphy, The Mathematics of Physics and Chemistry, (Van Nostrand, East-West Press), 1956.

7. M.K Bannerjee, The Theory of Stripping and Pickup Reactions, Nuclear Spectroscopy Part B, Edited by Fay Ajzenberg-Selov,(Academic Press, New York and London), 1960.

8. (a) S.T. Butler, Nuclear Stripping Reactions (John Wiley and Sons, New York, 1957)

   (b) A. Bhatia, K. Huang, R. Huby and H. Newns, Phil. Mag., 43, 485 (1952).

9. J.R. Erskine, W.W. Buechner and H.A. Enge, Phys. Rev., 128, 720 (1962).

10 H.W. Fulbright, J.A. Bruner, D.A. Bromley, Phys Rev., 88, 700 (1952).

11 W. Tobocman, Theory of Direct Nuclear Reactions, New York, Oxford University Press, 1961.

12 P.P Jones, The Optical Model in Nuclear and Particle Physics (Interscience Publishers), 1963.

13. (a) P.D. Kunz, Univ of Colarado (Unpublished), DWUCK program, Report No. COO-535-606, 1970.

(b) R.H. Bassel, R.M. Drisko and G R. Satchler, Oak Ridge National Laboratory, ORNL-3240 (Code SALLY).

14. J. Rapaport, - A Sperduto and M Salomaa, Nucl. Phys., A197, 337 (1972).

15. (a) D.H. Wilkinson, Phil Mag , 3, 1105 (1958).

(b) R.H. Siemssen, M Cosack and P. Felst, Nucl. Phys., 69, 209 (1965)

(c) R.H Siemssen, M Cosack and R. Felst, Nucl. Phys., 227 (1965)

16. T.W. Bonner, J.T. Eisinger, Alfred A., Kraus J.R. and J.B Marion, Phys Rev., 101, 209 (1956).

17. (a) E. Kashy, P.R. Perry, J.R. Risser, Phys. Rev., 117, 1289 (1960).

(b) N Sharma, M. Govindjee and H.R. Allan, Proc. of Phys. Soc. (London), A70 , 68 (1957).

18. M.T. McEllistrem, K W. Jones, Ren Chiba, R.A. Douglas, D.F. Herring and E.A.Silverstein, Phys. Rev., 104-2, 1008 (1956).

19. (a) Fredrick L. Canvan, Phys. Rev., 87, 136 (1952).

(b) R.K. Smither, Phys. Rev., 107, 197 (1957).

20. (a) Mira K. Juric, Phys. Rev., 98, 85 (1955).

(b) E. Friedland, H W. Alberts and C.C. Van Staden, Z. Physik, 267, 97 (1974).

21. Norman Austem- Direct Nuclear Reaction Theories, (Wiley-Interscience, John Wiley & Sons), 1970.

22. G.R. Satchler, Nucl. Phys., 55, 1 (1964).

23. Shiro Yoshida, Lectures on 'Stripping and Pick-up Reactions and Their Application to Nuclear Spectroscopy,' 1966, (Lectures delivered at Tata Institute of Fundamental Research, Bombay)

24. J.M. Blatt and V F. Weisskopf, Theoretical Nuclear Physics (John Wiley & Sons, New York, 1952).

25. D.L. Powel, G.M. Crawley, B.V.N. Rao and B A. Robson, Nucl Phys., A147, 65 (1970).

26. Toshiyuki Ishimatsu, Naoyuki Takano, Yuki Hachiya and Takao Nakashima, J. Phys. Soc. Jap., No. 16, 367 (1961).

27. S. Yashida,Competition Between Direct Interactions and Compound Nucleus Process, page 336, Proc. of the Int. Conf. on Nuclear Structure, Kingston, Canada, 1960 (North Halland Publishing Company).

28 S.A. Hjorth, J.X. Saladin and G.R. Satchler, Phys. Rev., 138B, 1425 (1965).

29. P.M Chudleigh, C.K. Gowers and E.G Muirhead, Nucl. Phys., A123, 114 (1969).

30. H. Cords, G.U. Din and B.A. Robson, Nucl. Phys., A127, 95 (1969).

31. S. Cohen and D. Kurath, Nucl. Phys. A101, 1 (1967).

PHY-1975-D-BAH-STU